AD_____

Award Number: DAMD17-98-1-8587

TITLE: Prostate Carcinoma Metastasis Tracked with Histochemical Marker Genes

PRINCIPAL INVESTIGATOR: Lloyd A. Culp, Ph.D.

CONTRACTING ORGANIZATION: Case Western Reserve University
Cleveland, Ohio 44106-4919

REPORT DATE: January 2001

TYPE OF REPORT: Final

PREPARED FOR: U.S. Army Medical Research and Materiel Command
Fort Detrick, Maryland 21702-5012

REPORT DOCUMENTATION PAGE

Form Approved
OMB No. 074-0188

1. AGENCY USE ONLY (Leave blank)	2. REPORT DATE	3. REPORT TYPE AND DATES COVERED
	January 2001	Final (1 Jul 98 - 31 Dec 00)

4. TITLE AND SUBTITLE
Prostate Carcinoma Metastasis Tracked with Histochemical Marker Genes

5. FUNDING NUMBERS
DAMD17-98-1-8587

6. AUTHOR(S)
Lloyd A. Culp, Ph.D.

7. PERFORMING ORGANIZATION NAME(S) AND ADDRESS(ES)
Case Western Reserve University
Cleveland, Ohio 44106-4919

E-Mail: lac7@po.cwru.edu

8. PERFORMING ORGANIZATION REPORT NUMBER

9. SPONSORING / MONITORING AGENCY NAME(S) AND ADDRESS(ES)
U.S. Army Medical Research and Materiel Command
Fort Detrick, Maryland 21702-5012

10. SPONSORING / MONITORING AGENCY REPORT NUMBER

11. SUPPLEMENTARY NOTES
This report contains colored photos

12a. DISTRIBUTION / AVAILABILITY STATEMENT
Approved for Public Release; Distribution Unlimited

12b. DISTRIBUTION CODE

13. ABSTRACT *(Maximum 200 Words)*

This project examines mechanisms by which human prostate carcinoma (PCA) cells undergo metastasis in an athymic nude mouse(male) model system since little attention has been devoted to these events for PCA. This includes PCA CWR22, CWR22R, and CWR21 xenografts adapted to tissue culture. To track tumor cells at the single-cell level and quantitatively, histochemical marker genes have been transfected for resolution as blue-, red-, or black-staining cells. Specific aim I examines the organ specificity of metastatic spread (particularly to bone and liver wich escape detection in most animal models). LacZ-tagged CWR22R cells have been isolated and s.c. injected. We routinely observe micrometastases in lung, liver, and bone and specificity of these events further evaluated in an experimental metastasis model. Aim II examines any significance for androgen for metastatic spread; with CWR22R, androgen-relatedness has been observed for both initiation of primary tumors and specificity of metastasis. Aim III evaluates possible interclonal cooperativity by injecting two different PCA cell types tagged with different marker genes. These experiments identify a new model for human prostate carcinoma derived from a primary tumor (therefore, not an already-metatastically selected population from the patient) that mimicks the progression characteristics of the human disease

14. SUBJECT TERMS	15. NUMBER OF PAGES
Prostate cancer, metastasis, histochemical marker gene, androgen	142
	16. PRICE CODE

17. SECURITY CLASSIFICATION OF REPORT	18. SECURITY CLASSIFICATION OF THIS PAGE	19. SECURITY CLASSIFICATION OF ABSTRACT	20. LIMITATION OF ABSTRACT
Unclassified	Unclassified	Unclassified	Unlimited

Table of Contents

REPORT BODY--Title: Prostate Carcinoma Metastasis Tracked with Histochemical Marker Genes; P.I., Lloyd A. Culp

Introduction:

Prostate carcinoma (PCA) in humans is most devastating because of its metastatic capability, particularly to lung, bone, and liver. Unfortunately, little experimental study has been dedicated to the mechanisms by which PCA undergoes its progression from the primary tumor in the prostate gland into these and possibly other organ sites. This project will examine these mechanisms more carefully by inserting a genetic tag into PCA cell types that light these cells up as specific colors (thereby readily distinguishing them under the microscope as blue, red, or black cells in a background of colorless tissue)[1-3]. These genetic tagging experiments with histochemical marker genes are powerful by permitting us to detect single tumor cells in virtualy any organ and for quantitating micrometastasis to any target organ. By these means, androgen-dependent PCA cells will be tagged with one marker gene and androgen-independent PCA cells with another marker gene. Metastatic capabilities will be compared individually and when two cell types are mixed. In addition, metastatic-competent cells will be compared with nonmetastatic cells individually and when mixed to determine if metastatic cells can convey some metastatic potential to the other cell type. These experiments will be conducted in athymic nude mice which lack cell-mediated immunity and to verify the accuracy of this animal model system to the human disease process. They will also include injecting the PCA tumor cells into different sites of the animal to determine which site leads to the most accurate model of human disease. Overall, these studies will shed considerable light on the mechanims by which prostate carcinoma develops the capacity to progress from the primary tumor into multiple target organs during metastasis.

Body:

[1] We have isolated two tissue culture cell lines from the CWR21 xenograft (human PCA) provided to us by Dr. Thomas Pretlow and described in the literature [4,5)]. They are referred to as CWR21A and B, are the first lines generated from this xenograft, and are being characterized by several approaches. (a) Dr. James Mohler (Univ. of North Carolina) is characterizing the androgen receptor gene in these cells to determine if it is wild-type or harbors the mutation characteristic of certain xenografts. (b) Dr. Stuart Schwartz of this institution is performing cytogenetic analyses to verify their origin--average number of chromosomes per cell, translocation of specific chromosome segments, deletion of specific chromosomes, and analyses of several chromosomal markers of the Pretlow xenografts. (c) These cells have been injected into the subcutis of athymic nude mice by our laboratory to test tumorigenicity and possible metastasis. Both lines are incredibly tumorigenic, generating large primary tumors at 2-3 weeks without Matrigel co-injection; many other PCA cell lines require 10-15 weeks to generate such tumors. CWR21A and B cells generate large lung metastases in all animals bearing primary tumors and metastases in other organs as well. These may be very

important cell models of highly-metastatic PCA in the nude mouse model system. *Under "Statement of Work", these experiments address Aim I b.*

[2] CWR21A and B cell lines described above are being transfected with the human placental alkaline phosphatase marker gene (*PAP*) to provide a histochemical marker that stains these cells differently from the *lacZ* marker gene in CWR22R cells (see below)-- see ref. 6-8. Transient transfections have optimized transfection conditions for lipofectamine as delivery agent [1,3]. *Under "Statement of Work", these experiments address Aim I a.*

[3] To test for androgen-dependence or independence of tumor formation and metastasis, CWR21A and B cells are being injected into mice with or without testosterone pellets implanted s.c. (since young nude male mice have very low levels of endogeneous testosterone). Castrated mice are also being tested for their responsiveness to these cells (with or without testosterone pellets). These experiments have just been undertaken to test whether testosterone modulates the rapid rate of primary tumorigenesis and/or the metastatic behavior of these cells. *Under "Statement of Work", these experiments address Aims II b and c.*

[4] The *lacZ* marker gene has been successfully transfected into CWR22R cells grown in culture, using our previously-described methods (references in **[1,2]**). Several stable transfectants have been isolated and are being characterized. These cells are referred to as LZ-CWR22R clone H, clone D, etc. These initial experiments are described in Appendix-references A-D. In brief, a wide spectrum of genetic and epigenetic stability of *lacZ* expression has been observed. Clone H is extremely stable with >90% of the cells staining blue with X-gal after 25 passages in culture. In contrast, clone D is very unstable with <15% of the cells staining after 7 passages and by 10 passages only a few cells stain. Clone B is intermediate-- by 10 passages, approx. 50% of the cells stain. The turn-off in expression of this marker gene is apparently not under control of hypermethylation of its promoter since addition of aza-deoxycytidine to these cells (a methylation inhibitor) has no effect on expression. *Under "Statement of Work", these experiments address Aim I a.*

[5] LZ-CWR22R-clone H cells have been injected into the subcutis of nude mice in PBS or Matrigel vehicles (reported in Appendix-reference C). They form tumors slowly over a period of 8-10 weeks that stain very blue, indicating the stability of the histochemical marker gene in vivo. With PBS, approx. 40% of the animals form primary tumors; with Matrigel, all animals form s.c. tumors. All tumor-bearing animals demonstrate blue-staining micrometastases in the lung (App.-ref. C). Approximately, one-half these animals also have micrometastases in liver and bone upon PBS injection; a subset of the liver micrometastases grow into excellent blue-staining overt metastases. These latter results are very important because there has been great difficulty in other PCA model systems for identifying consistent metastasis to liver and bone which are major sites of the human disease. Therefore, we have a much more reliable model of the human PCA disease with these cells. In addition, a few animals display micrometastases in the brain; the significance of this finding remains to be determined. These results are reported in App.-ref.

C. *Under "Statement of Work", these experiments address Aims I b and d and II b.*

[6] LZ-CWR22R-clone H cells have been injected with or without Matrigel to determine if this exogenous extracellular matrix alters the tumorigenicity and/or metastatic behavior of these cells (App.-ref. C). All animals form primary tumors with Matrigel, all of which develop lung micrometastases. A higher proportion of these animals form bone micrometastases (>60%) than PBS-injected animals but a lower proportion of liver micrometastases (20%). Therefore, Matrigel may permit more facile selection and expansion of variants that are effective colonizers of bone than the liver.*Under "Statement of Work", these experiments address Aims I d and II c.*

[7] LZ-CWR22R-clone H cells have been injected into tail veins to test which organs may be colonized by the latter steps of the metastatic cascade (App.-ref. D). All animals developed transient micrometastases in their lung, some of which survived >24hours. Of particular importance, micrometastases were also numerous in the liver and bone with the kinetics of clearance and stabilization quite different from those of lung. *LacZ*-tagged fibrosarcoma or neuroblastoma cells injected identically colonized the lung but never the liver or bone, demonstrating tumor-type specificity for these events. Orthotopic injection of these cells into the prostate gland is now being undertaken. *Under "Statement of Work", these experiments address Aims I b, I c, and II a.*

[8] In Appendix-reference D, we also quantitate the number of cells in the earliest experimental micrometastases formed in the lung and liver (bone is currently under investigation). This has been performed by careful serial sections of many individual micrometastases in these key organs. Twenty-two separate micrometastases in the lung revealed from 1 to as many as 19 cells per site, indicating considerable heterogeneity in formation of these sites. In contrast, 8 separate liver micrometastases only revealed 1 or 2 cells per site, indicating much simpler cellular complexity to these sites. The relative size of bone sites is also consistent with only 1 or 2 cells per site. In rare instances, tumor cells could be detected in the small blood vessels of the lung within minutes after their injection. *Under "Statement of Work", these experiments address Aims I b, I c, and II a.*

[9] Several primary tumors derived from CWR21A and B cells, as well as from LZ-CWR22R-clone H cells, have been isolated back into culture and cell lines established. These tumor lines will be particularly valuable for testing clonal dominance in Aim III of this project. In addition, several overt metastases in lung or liver (also micrometastatic cells from these organs) have been isolated into tissue culture using the drug-resistance marker for their selection; this will permit us to test for organ specificity of metastasis during a second round. *Under "Statement of Work", these experiments address issues in Aims III a,b, and c.*

Some of the experiments of Aim III cannot be undertaken until we obtain a PAP-transfected population of CWR21 A or B cells, as well as PAP-transfected tumor cells isolated back into culture as described in item 8 above. A notable failure of this project has been our inability to obtain a PCA cell line from the

CWR22 xenograft of Pretlow [4,5]. A number of new initiatives and selective environments will be used in further attempts to obtain this important cell line (completing the series of all three xenografts with their unique biological and tumorigenic properties).

Key Research Accomplishments:

- Isolation and characterization of CWR21 A and B cell lines from the CWR21 xenograft
- Androgen receptor status in these cells
- Cytogenetic analyses of these cell lines
- Aggressive formation of primary tumors and metastases to multiple organs
- Transfection with the PAP histochemical marker gene
- Androgen-dependence or independence in formation of primary tumors and metastasis
- *LacZ* transfection of tissue cultured CWR22R PCA cells
- Genetic stability of the marker gene in various stable transfectants
- Testing hypermethylation regulation of marker gene expression
- Tumorigenicity and metastatic competence of *lacZ* transfectants of CWR22R cells
- Kinetics of primary tumor formation and X-gal stainability
- Micrometastasis to lung, liver, bone, and brain
- Overt metastasis in lung and liver
- Tumorigenicity/metastasis with or without Matrigel co-injection
- Re-isolation into tissue culture of primary tumor cells from CWR21A and B and LZ-CWR22R clone H tumors
- Experimental metastasis analyses of LZ-CWR22R clone H
- Kinetics of formation of lung, liver, and bone micrometastases
- Serial sectioning to determine cellular composition of many individual lung and liver micrometastases (currently underway for bone as well)

Reportable Outcomes (Reprint/preprint Copies in Appendix):

Development of new PCA cell and tumor systems with genetic tags;

Isolation of CWR21A and B cell lines from the CWR21 xenograft of human PCA;

Generation of tissue cultured cell lines from primary tumors and overt metastases of LZ-CWR22R-clone H;

(A) Reprint: Culp, L.A., Lin, W.-c., Kleinman, N.R., Campero, N.M., Miller, C.J., and Holleran, J.L. Tumor Progression, micrometastasis, and genetic instability tracked with histochemical marker genes. Progress Histochemistry and Cytochemistry, **33**, No.3-4, 329-350 (1998).

(B) Preprint: Culp, L.A., Lin, W.-c., Kleinman, N.R., Kogerman, P., Judware, R., Miller, C.J., and Holleran, J.L. Targeting the metastatic process. In

Targeted Therapy for Cancer, ed. Konstantinos N. Syrigos and Kevin J. Harrington, Oxford University Press, London, UK, 2000, in press.

(C) Reprint: Holleran, J.L., Miller, C.J., and Culp, L.A. Tracking micrometastasis to multiple organs with *lacZ*-tagged CWR22R prostate carcinoma cells. J. Histochem. & Cytochem., 48: 643-651 (2000).

(D) Preprint: Holleran, J.L., Miller, C.J., Edgehouse, N.L., Pretlow, T.P., and Culp, L.A. Differential experimental micrometastasis to lung, liver, and bone with *lacZ*-tagged CWR22R prostate carcinoma cells. J. Histochem. & Cytochem., submitted (2001).

Conclusions: These experiments have successfully generated new tissue culture human PCA cell lines from previously-characterized xenograft models of the disease in athymic nude mice. Furthermore, these cell lines are very aggressive in forming tumors and in metastasizing to multiple organs. The histochemical marker gene, *lacZ*, has been successfully transfected into CWR22R cells and the genetic stability of this gene evaluated. These cells generate excellent blue-staining primary tumors, micrometastases to multiple organs (including lung, liver, bone), and overt metastases in some organs. Primary and metastatic tumors have been re-isolated into culture to provide highly-selected subsets to test organ specificity of metastasis and clonal dominance during metastasis. Genetically-tagged PCA tumor cells generated in this project provide an extremely sensitive system for tracking progression and metastasis. Overall, considerable progress has been made to generate a more accurate model of the human disease in the nude mouse model system and the mechanisms of metastatic progression of the disease. In addition, other PCA cell lines generated in this project will be highly valuable reagents for other investigators of this important disease in animal model systems.

References:

(1) Culp, L.A., Lin, W.-c., Kleinman, N.R., Campero, N.M., Miller, C.J., and Holleran, J.L. Tumor Progression, micrometastasis, and genetic instability tracked with histochemical marker genes. Progress Histochemistry and Cytochemistry, **33**, No.3-4, 329-350 (1998).

(2) Culp, L.A., Lin, W.-c., Kleinman, N.R., Kogerman, P., Judware, R., Miller, C.J., and Holleran, J.L. Targeting the metastatic process. In Targeted Therapy for Cancer, ed. Konstantinos N. Syrigos and Kevin J. Harrington, Oxford University Press, London, UK, 2001, in press.

(3) Holleran, J.L., Miller, C.J., and Culp, L.A. Tracking micrometastasis to multiple organs with *lacZ*-tagged CWR22R prostate carcinoma cells. J. Histochem. & Cytochem., **48**: 643-651 (2000).

(4) Cheng, L., Sun, J., Pretlow, T.G., Culp, J., and Yang, N.-S. CWR22 xenograft as an ex vivo human tumor model for prostate cancer gene therapy. J. Natl. Cancer Inst. **88**: 607-611(1996).

(5) Nagabhushan, M., Miller, C.M., Pretlow, T.P., Giaconia, J.M., Edgehouse, N.L., Schwartz, S., Kung, H.-J., de Vere White, R.W., Gumerlock, P.H., Resnick, M.I., Amini, S.B., and Pretlow, T.G. CWR22: the first human prostate cancer xenograft with strongly androgen-dependent and relapsed strains both in vivo and in soft agar. Cancer Res. **56**: 3042-3046 (1996).

(6) Lin, W.-c., Pretlow, T.P., Pretlow, T.G., and Culp, L.A. Bacterial lacZ gene as a highly sensitive marker to detect micrometastasis formation during tumor progression. Cancer Res. **50**: 2808-2817 (1990).

(7) Lin, W.-c., Pretlow, T.P., Pretlow, T.G., and Culp, L.A. Development of micrometastases: earliest events detected with bacterial lacZ gene-tagged tumor cells. J. Natl. Cancer Inst. **82**: 1497-1503 (1990).

(8) Lin, W.-c., Pretlow, T.P., Pretlow, T.G., and Culp, L.A. High resolution analysis of two different classes of tumor cells in situ tagged with alternative marker genes. Am. J. Pathol. **141**: 1331-1342 (1992).

PROGRESS IN HISTOCHEMISTRY AND CYTOCHEMISTRY

Volume 33/1998 Number 3-4

Ann M. Dvorak

Histamine Content and Secretion in Basophils and Mast Cells

Lloyd A. Culp et al.

Tumor Progression, Micrometastasis, and Genetic Instability Tracked with Histochemical Marker Genes

GUSTAV FISCHER

ISSN 0079-6336
Progr. Histochem. Cytochem.
Jena · 33(1998)3-4 · pp. 169-350

Progr. Histochem. Cytochem.
Vol. 33 · No 3-4(1998) · pp. XI-XVI, 329-350

Tumor Progression, Micrometastasis, and Genetic Instability Tracked with Histochemical Marker Genes

Lloyd A. Culp, Wen-chang Lin, Nanette R. Kleinman, Nicolas M. Campero, Carson J. Miller, Julianne L. Holleran

With 6 Figures and 1 Table

GUSTAV **FISCHER** Jena Stuttgart Lübeck Ulm

Contents

LLOYD A. CULP, Ph.D., Professor of Molecular Biology/Microbiology, Professor of Oncology/General Medical Science
WEN-CHANG LIN[1], Ph.D.,
NANETTE R. KLEINMAN[2], D.V.M.,
NICOLAS M. CAMPERO, B.S.
CARSON J. MILLER*, B.A.
JULIANNE L. HOLLERAN*, B.S.
Department of Molecular Biology and Microbiology,
Case Western Reserve University, School of Medicine
Cleveland, OH 44106 (USA)

[1] Current address: Institute of Biomedical Science
Academia Sinica and Clinical Cancer Center
National Health Research Institutes
Taipei, Taiwan, Republic of China

[2] Current address: Animal Resource Center
Case Western Reserve University, School of Medicine
Cleveland, OH 44106 (USA)

* These authors contributed equally to the prostate carcinoma studies

Acknowledgement
The authors acknowledge partial support from NIH grants to LAC (CA27755 and NS17139) and from the Comprehensive Cancer Center of the Ireland Cancer Center at Case Western Reserve University (NCI P30-CA43703). Prostate carcinoma studies were performed under auspices of U.S. Army grant PC970068 (LAC). Athymic nude mouse experiments were conducted in the Athymic Animal Facility (AAALAC-I-approved) of the Case Western Reserve University/Ireland Cancer Center, assisted by Jose Mariappuram, and approved by the Animal Care and Use Committee. One of the authors (NK) was supported by the Animal Resource Center of Case Western Reserve University. The authors thank Drs. THOMAS and THERESA PRETLOW of the Department of Pathology with tumor and organ tissue sectioning, immunohistochemistry protocols, and pathology consultation. Special appreciation is extended to Dr. JAMES JACOBBERGER of the Ireland Cancer Center at Case Western Reserve University for the donation of tissue culture-adapted CWR22R human prostate carcinoma cells.

✉ Correspondence to: Dr. Lloyd A. Culp, Department of Molecular Biology and Microbiology, Case Western Reserve University, School of Medicine, 10900 Euclid Avenue, Cleveland, OH 44106 (USA), Fax: 216-368-3055

1 Introduction and background

1.1 Rationale for histochemical markers

The tracking of tumor cells during their many stages of progression and metastasis has been an elusive goal in animal model systems. One exception to this problem has been melanoma studies in which the black pigmentation produced in the cytoplasm of these cells facilitated their identity as small clusters of cells, although single tumor cells were virtually unidentifiable (FIDLER et al., 1978; HEPPNER and MILLER 1983; MILLER et al., 1987; FIDLER and ELLIS 1994). This handicap of single-cell tracking was overcome by developmental biologists who sought to track the lineage of single or select cells in the embryo during the complex processes of differention. SANES et al. (1986) used the bacterial *lacZ* gene to track embryonic cell pathways virtually at the single cell level in the developing embryo. This use of the histochemical marker gene was followed by many similar analyses in developmental systems.

The pioneering studies of SANES et al. (1986) prompted us to implement the "nontoxic" *E. coli lacZ* gene in our own tumor progression studies since we had considerable difficulty tracking progression and metastasis of fibrosarcoma or neuroblastoma systems at their earliest stages (RADINSKY et al., 1987; CULP and BARLETTA 1990). Histochemical marker genes, such as *lacZ*, were advantageous to us over fluorescing markers, such as luciferase or green-fluorescent protein, because we sought to distinguish tumor cells in the normal tissue architecture; fluorescence analyses would have made this impossible. For H-*ras* transformed Balb/c 3T3 cells (LZEJ cells) injected into athymic nude mice, LIN et al. (1990a, b) showed the ultrasensitive detection of *lacZ*-tagged tumor cells in virtually any organ, both during spontaneous metastasis from the subcutaneous site and after experimental metastasis via injection into the tail vein. These studies identified micrometastasis not only to the lung but also to the brain and the kidney for the first time (LIN et al. 1990a, b; LIN and CULP 1992a). Using methyacrylate-embedded serial sections of lung or other organs, they also showed that single tumor cells could be readily identified in any organ (LIN et al. 1990b; LIN and CULP 1992b). Facile identification of single tumor cells also applied to the earliest primary tumors developing at the subcutaneous site (O'CONNOR and CULP 1994).

These methods were then extended to analysis of human neuroblastoma in an athymic nude mouse model system. Primary tumor development at intradermal or subcutaneous sites could be readily tracked with *lacZ*-tagged Platt neuroblastoma cells (KLEINMAN et al. 1994). They revealed the tissue-restrictive growth pattern of tumors and the neovascularization of expanding tumors. Histochemical marker gene tracking also permitted development of an orthotopic model of neuroblastoma. Injection of neuroblastoma cells into the adrenal gland resulted in subsequent metastasis to target organs not observed with intradermal or subcutaneous tumors (FLICKINGER et al. 1994; JUDWARE et al. 1995).

1.2 Alternative marker genes for tagging multiple tumor cell classes

The use of the *lacZ* gene proved so effective in our tumor analysis that we sought to use other marker genes, lighting cells up with different colored products, so that two or more tumor cell classes could be tracked simultaneously. For these reasons, human placental alkaline phosphatase gene (PAP) was developed as a marker gene since (a) background alkaline phosphatase staining could be eliminated with a 60° heat step without affecting activity of the transfected gene enzyme, (b) different histochemical substrates could be used to generate reddish-brown, black, or other colors readily distinguished from the blue staining of the *lacZ* β-galactosidase enzyme, and (c) the enzyme intercalated into the intracellular membranes of cells leaving the histochemical product bound within the cytoplasm (Lin et al. 1992). In a similar vein, the *Drosophila* alcohol dehydrogenase gene (ADH) was also developed since its histochemical products could be readily distinguished from the other two. Both ADH and PAP enzyme activities are nontoxic to animals cells and provide nonselective activities with which to study progression and metastasis.

All three genes were inserted into two different sets of integrating plasmids-one set regulated by the RSV LTR promoter while the second set was regulated by the cytomegalovirus late-gene promoter, providing options in terms of promoter regulation in our tumor systems. *Sis*-transformed Balb/c 3T3 cells (tumorigenic but not metastatic from the subcutaneous site) were then transfected with the PAP gene to yield the APSI cell line (Lin et al. 1992, 1993). When LZEJ and APSI cells were mixed and the mixture then injected into tail veins of animals, individual micrometastases could be identified and enumerated containing only one of the cell types. Moreover, a significant fraction contained both cell types, an indication of the multi-cell nature of the earliest experimental micrometastases. These studies also demonstrated that the high-metastatic LZEJ cells could facilitate the metastatic competence of the normally-nonmetastatic APSI cells (Lin et al. 1992, 1993).

1.3 Topology of two tumor cell classes as primary tumors develop

Development of the two-marker-gene system (Lin et al. 1992) permitted us to examine the development of primary tumors when mixtures of LZEJ and APSI cells were injected subcutaneously (Lin et al. 1993). We might have expected that both tumorigenic cell classes would be completely intermixed in the primary tumor. As shown in Fig. 1, a surprising finding emanated from these studies. Staining yielded a pattern of homogeneously-staining regions of each tumor class in an overall multi-regional pattern (Fig. 1). Each cell class was dominant in specific regions of the primary tumor with only limited intermixing of the two cell classes at their interfaces. This was the case in more than 20 primary tumors examined, indicating that this regional growth pattern of each tumor cell class was the general rule for these two very related classes (the difference being whether the human EJ-*ras* or c-*sis* oncogenes were the transforming principal).

Fig. 1. Topology of two tumor cell classes in a primary tumor. LZEJ (*lac*Z-transfected, H-*ras*-transformed 3T3) and APSI (PAP-transfected, c- *sis*-transformed 3T3) were suspended from separate tissue cultures, mixed in suspension, and then injected into the subcutis of an athymic nude mouse (Lin et al. 1992, 1993). When a 5 mm-diameter tumor had developed, the animal was euthanized and the tumor excised. The intact tumor was then fixed with a formaldehyde/glutaraldehyde solution and then sequentially stained-first, for PAP enzyme activity and then for β-galactosidase activity. APSI cells stain reddish-brown while LZEJ cells stain blue. It is apparent that the two tumor cell classes concentrate into regions of homogeneity in the primary tumor and are not completely intermixed.

Two possibilities for the regional dominance in these primary tumors come to mind. First, each cell class may migrate in the earliest primary tumor to form homogeneous aggregates in each region. Thus, each aggregate would give rise to a relatively homogeneous population of only LZEJ or APSI cells. Alternatively, there may be clonal dominance of one cell type over another based on competitive advantage of the tissue architecture in that location. In others words, LZEJ cells would outgrow APSI cells in some regions because they have an extracellular matrix or growth factor advantage while the reverse would be true in other regions. Clearly, this is an important finding since it indicates that tumor cells are highly discriminatory in their growth patterns. It also offers a model system as to how minor subpopulations could develop in specific regions of a large primary tumor.

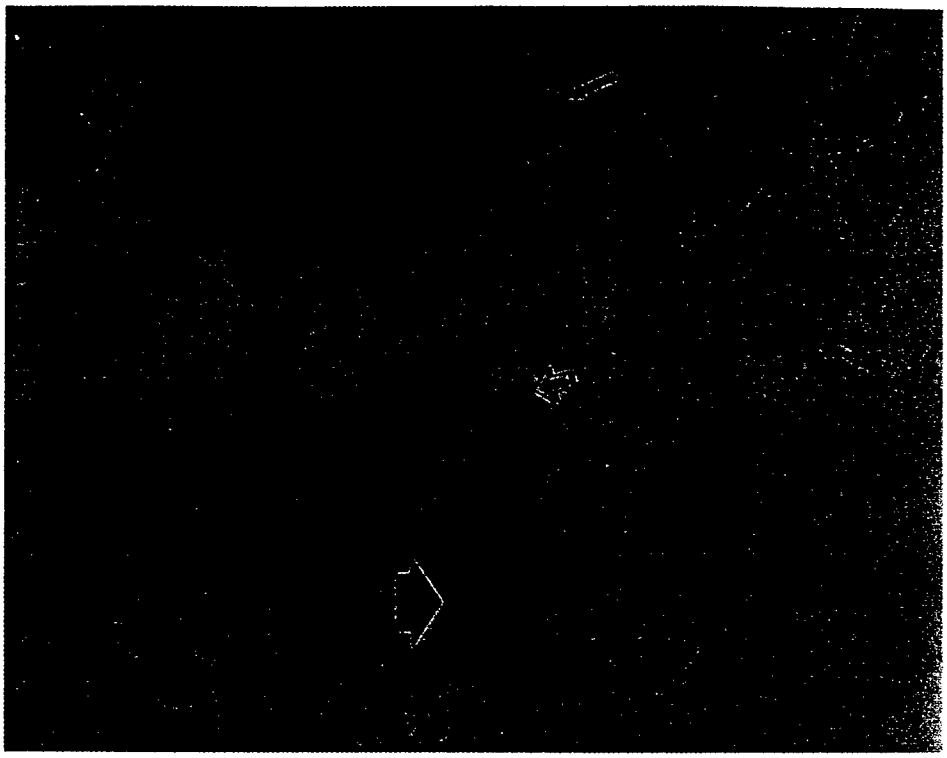

Fig. 2. Tumor cells adhering to the endothelium of a blood vessel. *Ras*-transformed, *lacZ*-tagged Balb/c 3T3 cells (LZEJ) (LIN et al. 1990a, b) were injected into the tail veins of athymic nude mice. At 30 minutes post-injection, animals were sacrificed; the lungs were then excised, fixed, and embedded in methacrylate at −20 °C and cut into 4 μm sections for X-gal staining (LIN et al. 1990b). Blood vessels were detected with alkaline phosphatase staining (red-staining; broad solid arrow) while tumor cells stained blue with X-gal (small, open arrows). Note that there are tumor cells adhering to the endothelium within the blood vessel, possibly in the process of extravasation, while other tumor cells have already escaped into the tissue space. × 400.

2 Micrometastasis development

2.1 Tumor cell binding to endothelium of lung blood vessels

A major motivation for using histochemical marker genes was the ultrasensitivity for detecting micrometastases at their earliest time points. Figure 2 shows the power of this methodology. LZEJ cells were injected into the tail veins of nude mice and then animals sacrificed at various times from 5 minutes to >24 hours later. At the very early time points (e.g., 30 minutes in Fig. 2), serial sectioning of the lungs revealed some tumor cells

which had escaped from blood vessels into tissue sites and, in some exceptional cases as shown, tumor cells could be shown binding to the endothelium of the small blood vessels of the lung.

This ability to detect single tumor cells at the endothelium will permit us to ask some very specific questions about gene regulation at the earliest time points of micrometastasis initiation. As an example, laser-capture microdissection has recently been developed to permit investigators to evaluate, by RT-PCR, gene activities in single tumor cells in fixed sections of tissues (EMMERT-BUCK et al. 1996). Histochemical tagging of tumor cells permits us to carefully identify their location and number. In combination with laser-capture microdissection, a vast array of very important questions can now be addressed directly with *in vivo* analyses (see section 5.2 for expansion of this issue).

2.2 Multiple tumor-cell foci – possible mechanisms of formation

In our early studies of micrometastasis to the lung using LZEJ cells (LIN et al. 1990a, b, 1992, 1993), it became clear that single tumor cells were not populating the blood vessels of the lung but rather collections of seveal tumor cells, frequently 2–6 at each locus. Serial sections of one of these micrometastases are shown in Fig. 3 where 6 cells can be identified in one focus. Furthermore, the clearing of approximately 97–8% of micrometastases within 24 hours was an all-or-none phenomenon – i. e., all cells of these multiple-cell foci were cleared rather than the average number of cells per focus decreasing from 5 or 6 down to 1 or 2 cells. This indicated that NK cells were completely competent for clearing all cells in a multiple-cell focus, not just a few cells. While the micrometastasis shown in Fig. 3 is captured at the 1 hour time point, virtually the same results would be obtained at the 24 hour time point when "clearing" of selected micrometastases had been completed.

These results raise the intriguing issue as to what makes the persistent micrometastases resistant to the animal's clearance mechanisms. This question was first raised by the studies of Fidler, Nicolson, and their colleagues and remains unanswered today (FIDLER et al. 1978; NICOLSON 1993; FIDLER and ELLIS 1994). There are at least three different mechanisms that would explain the persistence and stabilization of the few percent of all early micrometastases. First, these micrometastases may colonize the lung at special sites that are not amenable to NK cell or other immune effector cell action. Second, these persistent micrometastases may penetrate the endothelium most effectively and thereby evade NK cell action. Finally, the cell surface properties of this select subset of tumor cells may be different from the majority and somehow make them tolerant of any killing mechanism mediated by NK and other immune effector cells. Again, this is an area of tumor biology that is clearly understudied, requiring greater molecular and mechanistic analysis.

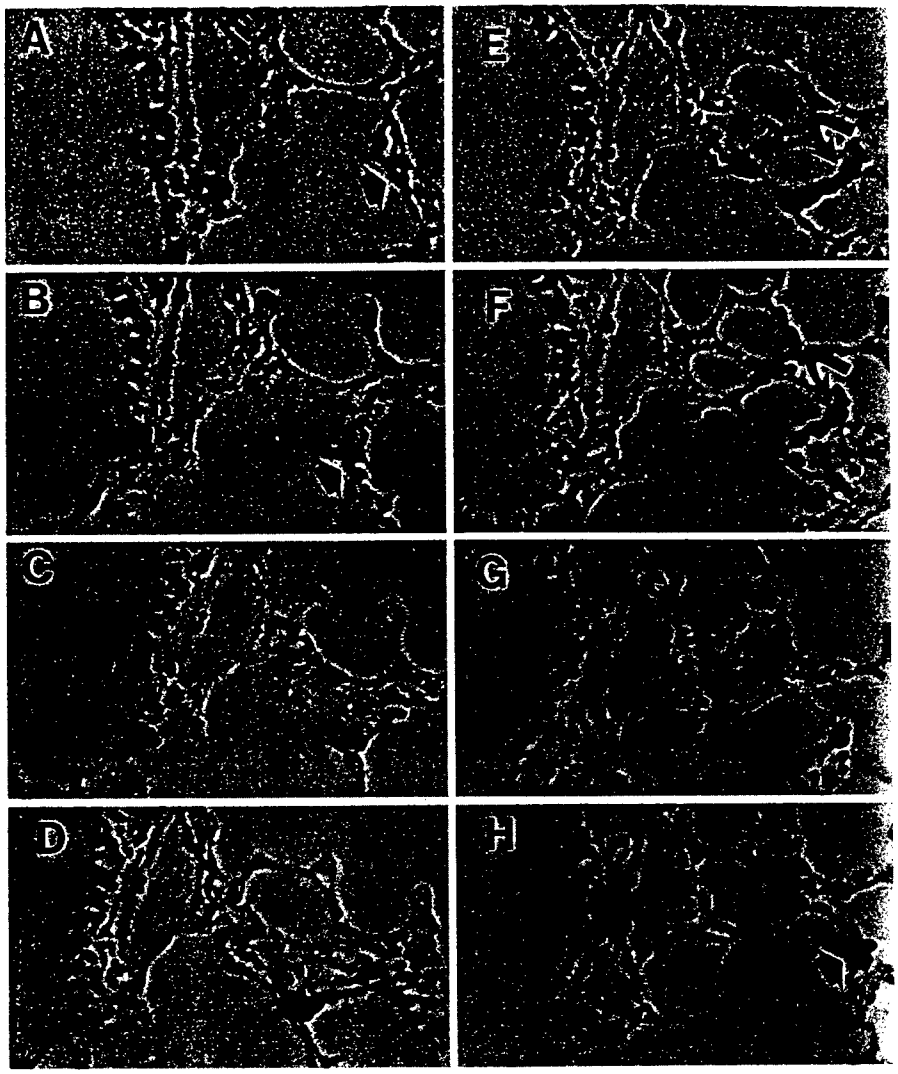

Fig. 3. Serial sections of a single micrometastasis. LZEJ tumor cells were injected into the tail vein of an athymic nude mouse. At 1 hour postinjection, the mouse was sacrificed; the lungs were excised, fixed, and X-gal-stained. One micrometastasis was carefully cut out of the tissue which was serially sectioned to give the sections [A]–[H] shown here. Note that this micrometastasis is comprised of 6 or 7 cells (the broad solid arrows). The bent arrows indicate a tangential turning point of this micrometastasis along a lung air sac structure. ×360. (Taken from LIN and CULP 1992b, with permission.)

2.3 Differential expansion into overt metastases

The questions raised above led us to investigate the fate of micrometastases in the lung and other organs. In the brain, micrometastases of LZEJ survived for 1–3 weeks and then competely disappeared, possibly because they encountered an environment hostile to their survival (LIN and CULP 1992a). Such environmental factors may include an inappropriate extracellular matrix with which to interact and/or inadequate supplies of growth factors because of the blood:brain barrier.

In contrast, the fates of micrometastases in the lung were far more complex (LIN et al. 1992, 1993). When APSI cells were injected alone into tail veins, they generated micrometastases in the lung that rarely developed into overt metastases. In most cases, these micrometastases disappeared with time. In contrast, when LZEJ and APSI cells were coinjected, micrometastases of both tumor classes persisted and many more APSI foci developed into overt metastases, as did LZEJ foci as expected. This suggested that the LZEJ cells potentiated outgrowth of APSI micrometastases in this "foreign" tissue.

When LZEJ cells were injected alone into tail veins, the fates of micrometastases in the lung were varied over a 2–4 week period (LIN et al. 1990b, 1993). Some micrometastases failed to expand into overt metastases while others did expand. Whether micrometastasis expansion occurs or not is an important issue in mechanistic studies of these events. Using nonfixed lungs from euthanized animals and FDG substrate for *lacZ*-coded β-galactosidase (fluorescein-digalactoside which penetrates living cells without killing them and generates a fluorescing product with the bacterial enzyme), it will be possible to identify "live" micrometastases and distinguish them from overt metastases. These two cell classes can then be recovered from lungs, grown out in culture, analyzed for their gene regulation patterns, and reinjected into a second group of animals to determine if these patterns breed true.

2.4 Earliest detection of angiogenesis as primary tumors develop

During analyses of the development of primary tumorigenesis using *lacZ*-tagged human neuroblastoma, KLEINMAN et al. (1994) raised the question as to when blood vessels could be detected near or within the developing tumor. To do so, they used cardiac perfusion of fixative to stably fix the red blood cells within blood vessels, making their visualization much more facile. It then became clear that the smallest blood vessels could be seen sprouting toward the tumor within 48 hours. An example is shown in Fig. 4. Within several days one or more of these very small vessels were developing into much larger vessels that eventually became quite large. This important finding indicates that the tumor cells that become established in the subcutis within 24 hours (O'CONNOR and CULP 1994; KLEINMAN et al. 1994) contain information for inducing angiogenesis. These angiogenic events have become central to studies of tumor progression and involve a

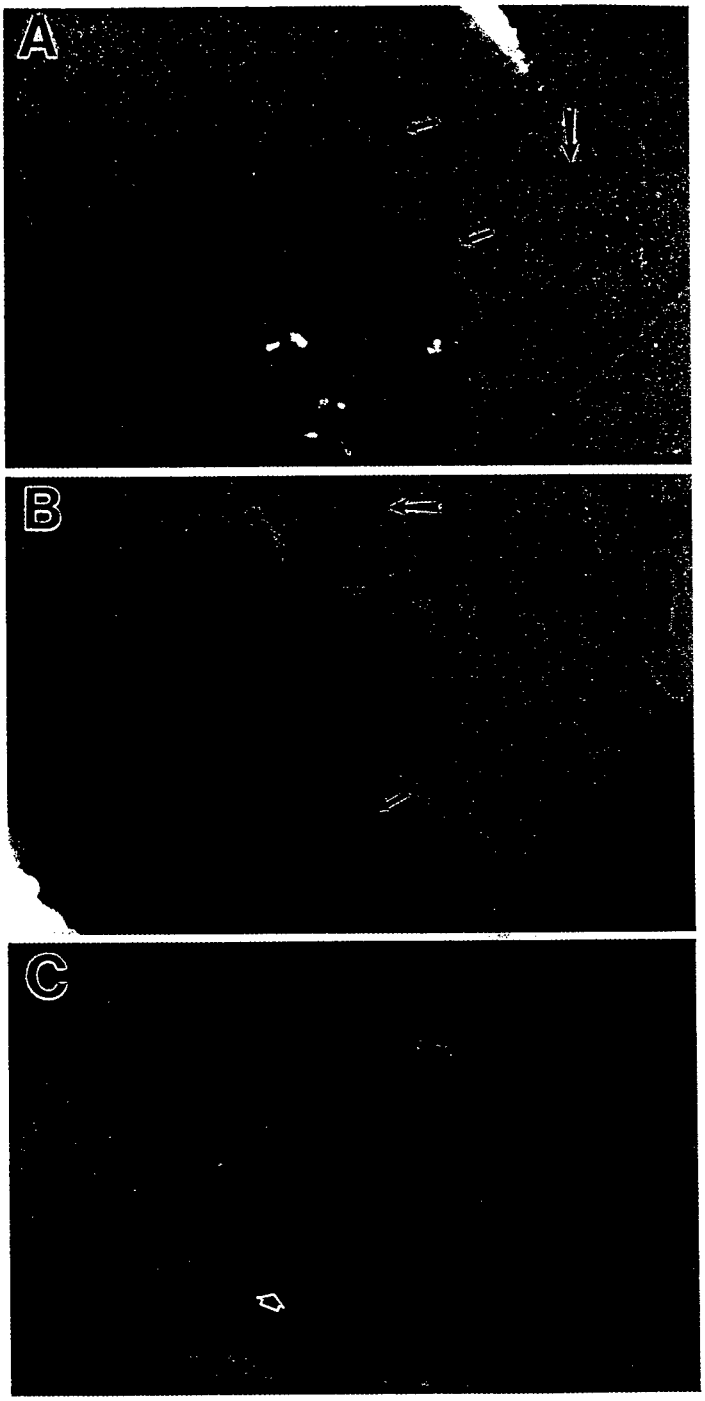
A
B
C

large array of negative and positive chemokine factors (BLOOD and ZETTER 1990; FOLKMAN 1995). Using histochemically-tagged tumor cells, it will now be possible to modulate the activities of specific genes in these cells while in culture and then assay their relative ability or inability to promote blood vessel sprouting at virtually any injection site in the host animal.

3 Human prostate carcinoma cell "tagging" with marker genes

3.1 Selection of cell systems

Progression and metastasis of human prostate carcinoma (PCA) has been a very understudied area of tumor biology, principally because of the paucity of excellent cell systems in culture and suitable animal models (PRETLOW et al. 1994; LALANI et al. 1997). The most commonly used cultured cell systems include PC3, DU145, and LNCaP; however, these were isolated from metastases in human patients and therefore represent highly selected subsets of tumor cells. Greater hope was generated for more and better cultured cell systems with the development of many xenografts of human PCA primary tumors in nude mice by the Pretlows and their collaborators (WAINSTEIN et al. 1994; CHENG et al. 1996; NAGABHUSHAN et al. 1996). They took advantage of the stabilization of transplant of human primary tumor tissue into nude mice co-injected with Matrigel. Three promising cell systems have now evolved from these studies, including CWR21 (androgen-dependent, metastatic), CWR22 (androgen-dependent, nonmetastatic), and a relapsed variant of the latter (CWR22R-androgen-independent, metastatic to lungs of nude mice). CWR22R xenografts have now been adapted to growth in tissue culture by Dr. James Jacobberger and his colleagues at Case Western Reserve University (manuscript submitted for publication) and offer an excellent population of primary PCA tumor cells for study.

Fig. 4. Angiogenesis during primary tumor establishment. *LacZ*-transfected human neuroblastoma tumor cells were injected into the dermis or into the subcutis between two India ink spots on the skin. At the indicated times, animals were sacrificed and fixative solution perfused into the left ventricle of the heart to preserve blood vessel red staining and contrast. The injection sites were then excised, fixed, and stained with X-gal.
A: Tumor cells 48 hours after injection into the dermis. Very small blood vessels are beginning to branch toward the tumor (small arrows) from a major blood vessel (large arrow). × 87.
B: A tumor 2 weeks after dermal injection. A large number of small blood vessels are invading the tumor site (small arrows) and in select cases expanding into a major blood vessel (large arrow). × 87.
C: A tumor 3 weeks after injection into the subcutis. Much of this tumor has lost X-gal-stainability with the exception of one region (open arrow). The tumor is now fed by a major blood vessel (large arrow), many intermediate-sized vessels (small arrow), and very small micro-vessels (black arrowhead). (Taken from KLEINMAN et al. 1994, with permission).

3.2 Major issues to address

Our laboratory has successfully transfected the *lacZ* gene into CWR22R human PCA cells (CAMPERO, HOLLERAN, MILLER, and CULP, unpublished data) and is undertaking a variety of studies with these tagged cells. Of particular note, virtually all experimental human PCA tumor model systems have failed to identify metastasis to the bone and liver which are common sites for the human disease. Metastasis to the lung in these animal models is much more common (PRETLOW et al. 1994; LALANI et al. 1997). *LacZ*-tagged cells should facilitate the detection of tumor cells in liver and bone (see below on this point) and provide opportunity for evaluating the relative significance or insignificance of androgen ablation or supplementation in these processes. Of equal importance is a comparison of ectopic or orthotopic injection sites, since the latter may provide a more accurate pattern of metastatic spread to all three organs (STEPHENSON et al. 1992; FU et al. 1992; SATO et al. 1997).

With regard to acquisition of metastatic competence, we recently reported the plasticity of expression of CD44s during progression and metastasis in the mouse fibrosarcoma system (KOGERMAN et al. 1997a, b, 1998). This isoform of CD44 is the simplist form, is exclusively expressed in fibroblasts, and binds hyaluronan (HA) when "activated" at the cell surface by one of several possible mechanisms (LESLEY et al. 1993; CULP and KOGERMAN 1998). Transfection of an overexpressing human CD44s gene into nonmetastatic *sis*-transformed 3T3 cells converted them into highly metastatic cells (KOGERMAN et al. 1997a). Micrometastatic tumor cells, reisolated from lungs, expressed very high levels of the human antigen while large primary tumors or overt metastases had lost expression of the human gene, demonstrating the plasticity of expression of the transfected human gene in this system. Down-regulation of hCD44s in the large tumors occurred by hypermethylation of its promoter. Furthermore, transfection of the human gene into 3T3 cells made them tumorigenic *and* metastatic (KOGERMAN et al. 1998). These results indicate that the HA-binding and overexpressed human protein (mouse CD44s in these cells does not bind HA) conveyed metastatic competence but was antagonistic for outgrowth of tumors, whether they be primary or secondary.

An experimental metastasis model was then used to explore the mechanism(s) of this conveyance (KOGERMAN et al. 1997b). hCD44s-overexpressing cells colonized and stabilized micrometastases in the lungs 7–10-fold over nonexpressing cells. Furthermore, mixing overexpressing/transfected cells with nonexpressing cells prior to injection into tail veins revealed that the nonexpressing cells do not compete with the overexpressing cells for their more efficient colonization of the lung. These differences were also maintained when comparing primary tumor cell populations that had lost hCD44s overexpression with lung micrometastatic tumor cells that conserved overexpression; the micrometastatic cells were severalfold more effective at stably colonizing the lung. Therefore, the HA-binding and overexpressed hCD44s protein must provide a more effective mechanism of colonizing the lung at the endothelium and/or promote more

effective stabilization of each micrometastasis. It is possible that hCD44s at the tumor cell surface binds to HA on the surface of the endothelium, conveying this competence. In this latter regard, it will be critical to test HA-nonbinding mutants of hCD44s in this system (KOGERMAN et al. 1997b). Clearly, the use of histochemically-tagged cell systems can facilitate these mechanistic studies. We can also transfect an overexpressing CD44 gene into *lac*Z-tagged CWR22R prostate carcinoma cells and evaluate this protein's ability to modulate progression and metastasis of this particular tumor type.

3.3 Bone micrometastasis and overt metastasis

Neuroblastoma tumor cells injected into the subcutis or the dermis failed to metastasize effectively to any organ, even though some of these human neuroblastoma isolates were from metastases in the patient (KLEINMAN et al. 1994; FLICKINGER et al. 1994; JUDWARE et al. 1995). This indicated the difficulty of paralleling the human disease process in an animal model. In contrast, orthotopic injection of these same tumor cells into the adrenal gland produced metastases to the lungs and several other organs of nude mice (FLICKINGER et al. 1994; JUDWARE et al. 1995).

A notable target organ for neuroblastoma metastasis is bone, an organ which is rarely considered or identified as a target in animal models. As shown in Fig. 5, bone metastasis could be readily detected using *lac*Z-tagged neuroblastoma cells after adrenal gland injection while a control mouse not injected with tumor cells failed to yield any X-gal background staining of its vertebrae as expected. These micrometastases occurred at the surface of the bone and in some cases grew out as significant nodules of cancer in this site. These findings raise confidence that bone metastasis using prostate carcinoma models may eventually identify routing of *lac*Z-tagged PCA cells to this important organ in the animal model.

4 Genetic instability in tumor populations deciphered with marker genes

4.1 Mouse fibrosarcoma studies

Histochemical marker genes such as *lac*Z, PAP, and ADH offer no particular selective advantage to cells expressing them. Therefore, they offer an ideal opportunity to evaluate genetic stability or instability of their expression in many independent transfectants of tumor populations (LIN and CULP 1992a). A full spectrum of genetic instabilities have now been documented in our three tumor systems.

Using oncogene-transformed mouse 3T3 cells, different degrees of expression stability were observed with LZEJ or APSI cells (LIN et al. 1992; 1993). LZEJ cells persisted

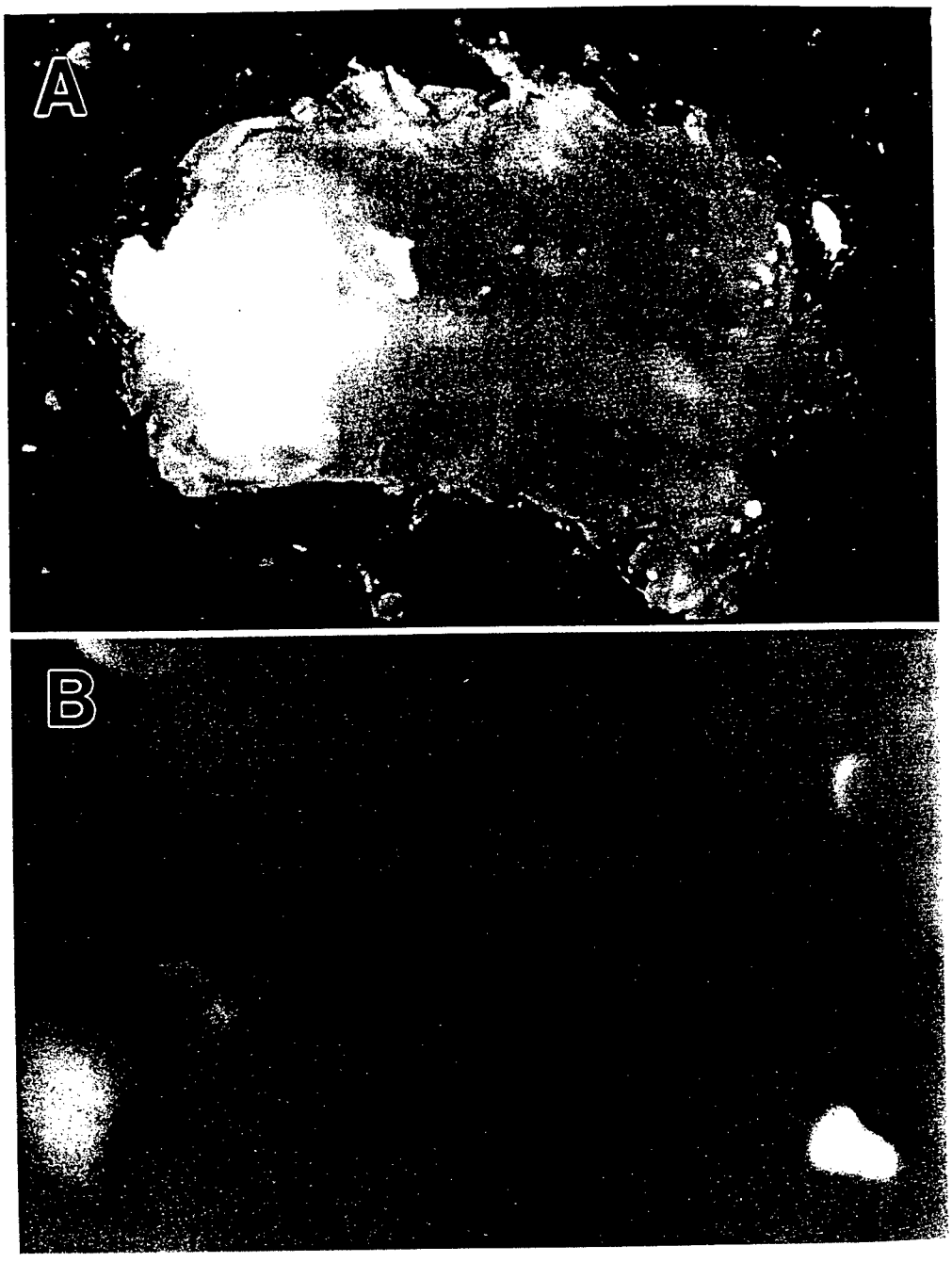
A
B

in their high levels of *lacZ* expression whether grown in culture for 10–15 passages in the absence of selection drug or whether developed into large tumors in nude mice. In contrast, large tumors of APSI frequently had segments that failed to stain for the PAP marker gene, as did cells grown in culture for > 5 passages. Therefore, APSI tumor cells were rapidly losing expressability of the PAP gene for any one of a number of reasons. One possibility is that hypermethylation occurred at the PAP promoter, leading to loss of activity. This was observed for human CD44s gene in our transfected *sis*-transformed cells reported above (KOGERMAN et al. 1997a, 1998). Altered methylation appears to be a much more common pattern of changing gene expression in tumor cells than was originally thought. A second mechanism is a DNA rearrangement in APSI cells leading to truncation, deletion, or interrupted promotion of the PAP gene. A third possibility is loss of the chromosome bearing the integrated PAP gene since most transfectants carry only one copy of the histochemical marker gene. Greater study should be dedicated to the use of histochemical marker genes as tools, to decipher how tumor cells generate their genetic instability, particularly since this instability is essential for generating metastatic variants.

4.2 Human neuroblastoma studies

The same variety of marker gene stability of expression was observed in human neuroblastoma cells tagged with *lacZ* (KLEINMAN et al. 1994). One clone was particularly stable, generating well-staining cells after many passages in culture or growth *in vivo* into very large tumors. A second transfectant displayed an intermediate stability and a third clone was highly unstable, rapidly losing stainability as very small primary tumors.

4.3 Human prostate carcinoma studies

The recent isolation of *lacZ*-transfected CWR22R human prostate carcinoma cells (CAMPERO, HOLLERAN, MILLER, and CULP, unpublished date) has provided opportu-

Fig. 5. Metastasis to bone detected with *lacZ* staining. *LacZ*-transfected human neuroblastoma tumor cells were injected into the adrenal gland, an orthotopic site for this tumor (FLICKINGER et al. 1994; JUDWARE et al. 1995). Animals were euthanized at various time points, various bone structures excised from the animal, and these bones fixed and stained with X-gal to detect micrometastases.
A: A spinal column vertebra from an animal that has not been injected with tumor cells. Note the complete absence of X-gal staining of the bone.
B: X-gal-stainable micrometastases observed in spinal vertebrae from an animal 55 days after adrenal injection. Note the multiplicity of micrometastases in the vertebrae by this time point.

nity to analyze the relative genetic stability of multiple independent clones of PCA. As shown in Fig. 6, X-gal staining of late passage cells, grown in the absence of a selection drug for > 10 passages, demonstrates diversity in stability. Clone IG4-H is very stable in its expression over this lengthy period of time. Clone IG4-B has an intermediate level of stability while clone IG4-D is so unstable that virtually no blue-staining cells could be observed after 10 passages in culture.

These stability comparisons were quantitated by dilution plating of these cells into large tissue culture dishes, their outgrowth as individual colonies, and then enumeration of the percentage of blue-staining colonies (Table 1). Clone IG4-H, after ten passages in culture in the absence of a selecting drug, contains almost 90% of its population as *lacZ*-expressing cells. This confirms a remarkable stability of expression of this particular tumor subpopulation. In contrast, clone IG4-B has lost much of its activity and is reduced to only 27–35% colony staining. Clone IG4-D has lost all stainability. To test whether some of this loss of expression could be due to hypermethylation of the LTR promoter regulating *lacZ* in these transfectant cells (KOGERMAN et al. 1997a), colonies were also grown in the presence of the methylation inhibitor, 2-aza-5'-deoxycytidine to test revertability of expression. As shown also in Table 1, the azadeoxycytidine did not significantly increase the percentage of staining colonies in clones IG4-B or IG4-D (this would not have been expected in the excellent-staining clone H cells). Therefore, promoter hypermethylation is probably not the mechanism of down-regulation of *lacZ* expression in these unstable clones. Colonies were then grown in medium containing the selection drug G418 to test for plasmid persistence. This did not increase the percentage of blue-staining colonies in either clones IG4-B or D (again, no change was expected in the excellent-staining clone H cells) [data not shown]. Other genetic or epigenetic mechanisms must be responsible for this loss of *lacZ* gene activity. These processes can now be compared with those of our fibrosarcoma and neuroblastoma populations to resolve any tumor-specific or commonly-observed mechanisms of gene activity loss.

Fig. 6. Genetic stability of *lacZ* in prostate carcinoma cells. Human prostate carcinoma CWR22R tumor cells, transfected with *lacZ*, were isolated as three separate transfectant clones (IG4-clone B, D, and H). These three clones were then grown in culture for > 10 passages without any selection drug (G418) to test the relative stability of X-gal-stainability of these three clones. Colony analyses and quantitation of *lacZ* stability is provided in Table 1. In this figure, mass cultures of the three clones were stained in the absence of any selection drug.
A: Clone D-note the virtual absence of any staining, except for an isolated single cell (arrow).
B: Clone B-approx – one quarter of these cells have retained *lacZ* expression while the remainder have lost expressability.
C: Clone H-virtually all of these cells have retained stainability, indicating remarkable stability of *lacZ* expression in the absence of any selection pressure to maintain its expression.

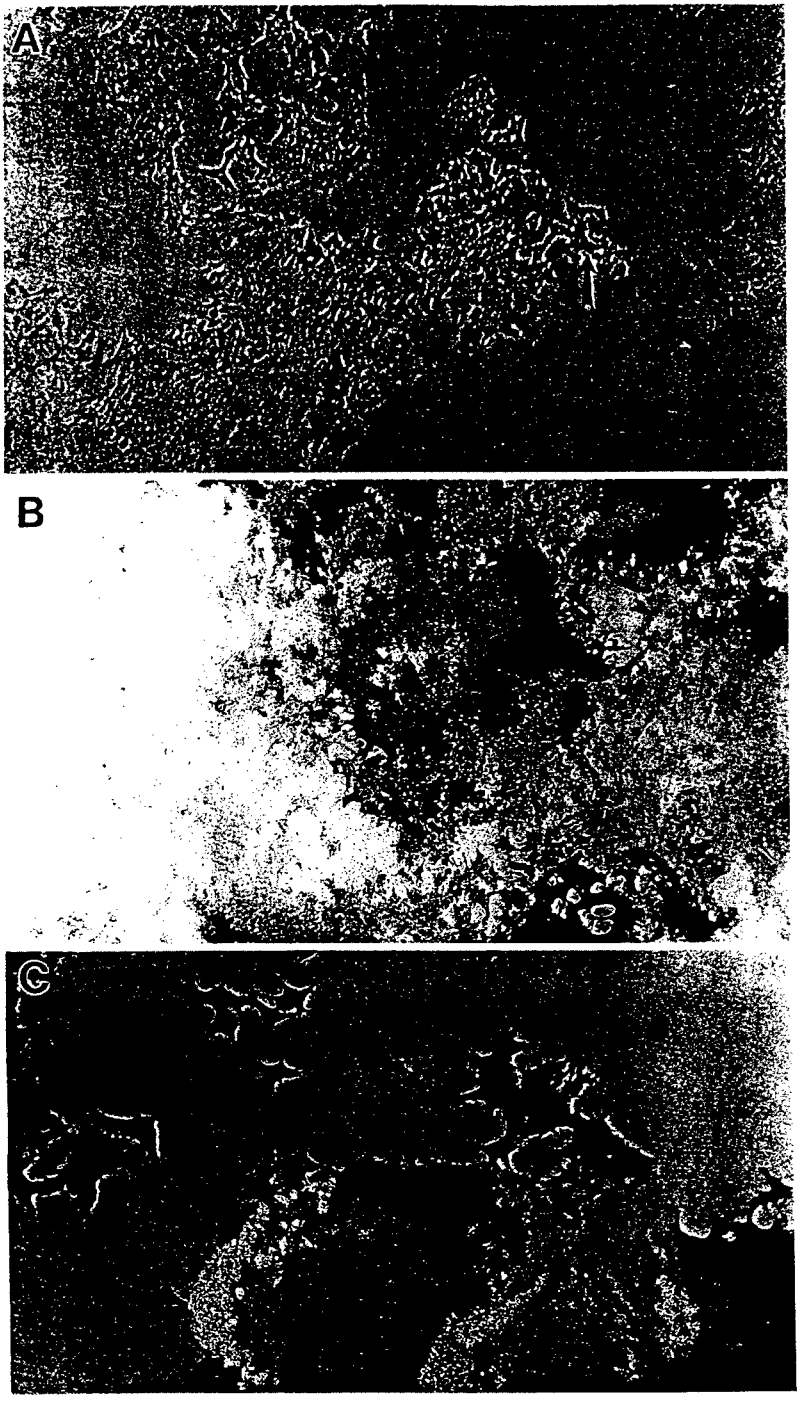
A
B
C

Table 1. Genetic stability of *lacZ* marker gene expression in prostate carcinoma cells.

	Clones[a]	
	IG4-B	IG4-H
Colonies/plate[b] ± (SD)		
– Aza[d]	198.0 colonies ± 35.9	170.3 colonies ± 53.2
+ Aza[e]	203.3 colonies ± 46.6	206.7 colonies ± 67.7
% Blue colonies[c] ± (SD)		
– Aza	27.2% ± 10.4	90.3% ± 1.77
+ Aza	34.5% ± 12.6	87.9% ± 10.9

[a] The prostate carcinoma cell line CWR22R was transfected with the plasmid pRSVlacZII. This plasmid carries bacterial *lacZ* under the control of the RSV LTR promoter as well as a neomycin^R gene. Independent transformation events produced several stably-transformed cell lines, such as IG4-B, IG4-H, and IG4-D, which originally expressed *lacZ* in nearly all cells. Cells used in this study had been grown for 10 passages in the absence of selective media to examine whether known genetic instabilities of carcinoma cells might affect expression of the *lacZ* marker gene. Approximately 5000 cells were plated onto each of twelve 100 mm tissue culture plates and colonies were grown at 37 °C. After 7 or 10 days (lines B and H, respectively), half of the plates were supplemented with 3 μM 2-aza-5'-deoxycytidine. Five days later cells were fixed and stained. Virtually all IG4-D colonies were nonstaining after lengthy growth in nonselective medium, indicating considerable instability of *lacZ* in this particular clone.

[b] There was no significant difference in the number of colonies per plate between clones IG4-B and IG4-H ($p = 0.569$, ANOVA) or among plates with and without 2-aza-5'-deoxycytidine ($p = 0.326$, ANOVA).

[c] There was no significant difference in the percentage of blue colonies between 2-aza-5'-deoxycytidine plus and minus plates ($p = 0.887$, ANOVA). However, IG4-H had a significantly higher percentage of blue colonies than IG4-B ($p < .0001$, ANOVA). A third clone, IG4-D, showed negligible x-gal staining with or without 2-aza-5'-deoxycytidine. Therefore, data from this clone was not included in the table.

[d] – Aza = colonies grown in the absence of 2-aza-5'-deoxycytidine.

[e] + Aza = colonies grown in the presence of 3 μM 2-aza-5'-deoxycytidine.

5 Gene regulation in single tumor cells – importance of *in vivo* analyses

5.1 Two distinct functions for marker genes in vivo – identification and gene instability studies

The studies described above demonstrate how histochemical marker genes can be used in two very different ways. Initially they have been used to locate very small primary tumors and micrometastases at virtually any organ in order to assess these very early

events. This includes quantitation of micrometastases in various target organs. In addition, the ease of identification and quantitation of histochemical marker genes offers ideal opportunity to quantitate and evaluate various mechanisms for genetic instability in select tumor subpopulations. Such information is critical for predicting how rapidly metastatic variants could be generated by this genetic instability. Marker genes can be used in these gene stability studies because they are "irrelevant" to the successful growth and survival of tumor cells – i. e., they do not offer any selective advantages or disadvantages. Combined with laser-capture microdissection (EMMERT-BUCK et al. 1996) and other high-resolution analyses of tumor populations *in vivo*, we can now directly evaluate genetic instability of tumor populations in various tissue sites in the experimental animal. This will allow us to determine whether orthotopic or ectopic sites differ in their conveyance of genetic instability to specific tumor populations. Angiogenesis at the primary tumor site may also be a significant factor in selecting rare tumor cell subsets once genetic instability has generated opportunistic variants in the population. Overall, there has been little study as to the significance of the *in vivo* environment for conveying how rapidly gene stability changes and which subsets competitively overgrow their neighbors.

5.2 Laser-capture microdissection in combination with marker gene studies

Laser-capture microdissection (LCM) is a powerful tool for evaluating gene regulation in single or a few tumor cells in any tissue of the animal (EMMERT-BUCK et al. 1996). Histochemical markers permit us to precisely identify the location of tumor cell subsets whose gene regulation mechanisms may be most important. This may be the subset proximal to small blood vessels during early angiogenesis. The subset proximal to host organ connective tissue may also be of considerable interest because of the speculated synergy between tumor cell gene regulation and factors provided by neighboring host cells. A very important subset to evaluate by LCM includes cells in the act of intravasating into blood vessels, the earliest stage of metastatic migration; section 2.1 demonstrates the feasibility of such a study. Finally, gene regulation in the tumor cell subsets that are extravasating into different organs of the same animal may indicate whether common mechanisms operate in these different organs or whether there are true organ-specific metastatic steps involved.

5.3 Chimeric genes to track functional expression of specific gene classes during progression and metastasis

The active sites for enzyme activities in histochemical marker genes are being reduced to much smaller sequences of protein. Minigenes containing these minimal sequences retaining histochemcal activity can now be fused with the N-terminal or C-terminal

domains of receptors and other molecules of tumor cells felt to be highly significant in metastatic progression. Examples would include CD44s and its variant isoforms, the extracellular matrix receptor integrin subunits, and receptors for growth factors. By transfecting chimeric genes into tumor cells in which the histochemical activity is actually fused to the receptor protein, investigators can localize the optimal functions of these receptors in various topological sites of primary tumors, micrometastases, and overt metastases to test plasticity of expression. This may also be a case where a fluorescent marker, such as luciferase or green fluorescent protein, provides greater resolution in tissue sections than the conventional histochemical markers described above.

An alternative approach can also be used here. A dominant-negative inhibitor of a tumor cell receptor can be fused with the histochemical marker. This chimeric gene, transfected into cells, may demonstrate where and how the dominant-negative regulator of receptor function might modulate tumor growth, progression, and/or metastatic spread.

The methodologies are now available for asking and answering some very important questions at the level of single tumor cells in virtually any tissue site. This also applies to specific gene activities and to their possible modulation during these early events. The next decade should generate some very exciting and important mechanistic information about tumorigenesis and metastasis.

References

BLOOD, C. H., ZETTER, B.: Tumor interactions with the vasculature: angiogenesis and tumor metastasis. – Biochim. biophs. Acta (Amst.) *1032*, 89–118 (1990).

CHENG, L., SUN, J., PRETLOW, T. G., CULP, J., YANG, N.-S.: CWR22 xenograft as an ex vivo human tumor model for prostate cancer gene therapy. – J. natl. Cancer Inst. *88*, 607–11 (1996).

CULP, L. A., BARLETTA, E.: Matrix adhesion of neuroblastoma and related neuronal derivative cells: cell type- verus tumor-specific mechanisms. – Semin. Develop. Biology *1*, 437–452 (1990).

CULP, L. A., KOGERMAN, P.: Plasticity of CD44s expression during progression and metastasis of fibrosarcoma in an animal model system. – In: Frontiers of Bioscience, vol. 3, pp. 672–683 (1998).

EMMERT-BUCK, M. R., BONNER, R. F., SMITH, P. D., CHUAQUI, R. F., ZHUANG, Z., GOLDSTEIN, S. R., WEISS, R. A., LIOTTA, L. A.: Laser capture microdissection. – Science *274*, 998–1001 (1996).

FIDLER, I. J., ELLIS, L. M.: The implications of angiogenesis for the biology and therapy of cancer metastasis. – Cell *79*, 185–188 (1994).

FIDLER, I. J., GERSTEN, D. M., HART, I. R.: The biology of cancer invasion and metastasis. – Adv. Cancer Res. *28*, 149–250 (1978).

FLICKINGER, K. S., JUDWARE, R., LECHNER, R., CARTER, W. G., CULP, L. A.: Integrin expression in human neuroblastoma cells with or without N-*myc* amplification and in ectopic/orthotopic nude mouse tumors. – Exp. Cell Res. *213*, 156–163 (1994).

FOLKMAN, J.: Angiogenesis in cancer, vascular, rheumatoid and other disease. – Nature Med. *1*, 27–31 (1995).

FU, X., HERRERA, H., HOFFMAN, R. M.: Orthotopic growth and metastasis of human prostate carcinoma in nude mice after transplantation of histologically intact tissue. – Int. J. Cancer *52*, 987–990 (1992).

HEPPNER, G. H., MILLER, B. E.: Tumor heterogeneity: biological implications and therapeutic consequences. – Cancer Metastasis Rev. 2, 5–23 (1983).

JUDWARE, R., LECHNER, R., CULP, L. A.: Inverse expressions of the N-*myc* oncogene and β1 integrin in human neuroblastoma: relationships to disease progression in a nude mouse model system. – Clin. exp. Metastasis *13*, 123–133 (1995).

KLEINMAN, N. R., LEWANDOWSKA, K., CULP, L. A.: Tumour progression of human neuroblastoma cells tagged with a *lacZ* marker gene: earliest events at ectopic injection sites. – Brit. Journal Cancer *69*, 670–679 (1994).

KOGERMAN, P., SY, M.-S., CULP, L. A.: Counter-selection for over-expressed human CD44s in primary tumors versus lung metastases in a mouse fibrosarcoma model. – Oncogene *15*, 1407–16 (1997a).

–: Overexpressed human CD44s promotes lung colonization during micrometastasis of murine fibrosarcoma cells: facilitated retention in the lung vasculature. – Proc. natl. Acad. Sci. USA *94*, 13233–8 (1997b).

–: Over-expression of human CD44s in murine 3T3 cells: selection against during primary tumorigenesis and selection for during micrometastasis. – Clin. exp. Metastasis *16*, 83–93 (1998).

LALANI, E.-N., LANAIDO, M. E., ABEL, P. D.: Molecular and cellular biology of prostate cancer. – Cancer Metastasis Rev. *16*, 29–66 (1997).

LESLEY, J., HYMAN, R., KINCADE, P. W.: CD44 and its interaction with extracellular matrix. – Adv. Immunology *54*, 271–335 (1993).

LIN, W.-C., CULP, L. A.: New insights into micrometastasis development using ultrasensitive marker genes. – In: Current Perspective on Molecular and Cellular Oncology, Vol. 1, Part B (SPANDIDOS, D. A., ed.), pp. 261–309. – JAI Press, London 1992a.

–: Altered establishment/clearance mechanisms during experimental micrometastasis with live and/or disabled bacterial *lacZ*-tagged tumor cells. – Invasion & Metastasis *12*, 197–209 (1992b).

LIN, W.-C., O'CONNOR, K. L., CULP, L. A.: Complementation of two related tumour cell classes during experimental metastasis tagged with different histochemical marker genes. – Brit. J. Cancer *67*, 910–921 (1993).

LIN, W.-C., PRETLOW, T. P., PRETLOW, T. G., CULP, L. A.: Bacterial *lacZ* gene as a highly sensitive marker to detect micrometastasis formation during tumor progression. – Cancer Res. *50*, 2808–2817 (1990a).

–: Development of micrometastases: earliest events detected with bacterial *lacZ* gene-tagged tumor cells. – J. natl. Cancer Inst. *82*, 1497–1503 (1990b).

–: High resolution analyses of two different classes of tumor cells *in situ* tagged with alternative histochemical marker genes. – Amer. J. Pathol. *141*, 1331–1342 (1992).

MILLER, B. E., MILLER, F. R., WILBURN, D. J., HEPPNER, G. H.: Analysis of tumor-cell composition in tumors composed of paired mixtures of mammary tumor cell lines. – Brit. J. Cancer *56*, 561–569 (1987).

NAGABHUSHAN, M., MILLER, C. M., PRETLOW, T. P., GIACONIA, J. M., EDGEHOUSE, N. L., SCHWARTZ, S., KUNG, H.-J., DE VERE WHITE, R. W., GUMERLOCK, P. H., RESNICK, M. I., AMINI, S. B., PRETLOW, T. G.: CWR22: the first human prostate cancer xenograft with strongly androgen-dependent and relapsed strains both in vivo and in soft agar. – Cancer Res. *56*, 3042–6 (1996).

NICOLSON, G. L.: Cancer progression and growth: relationship of paracrine and autocrine growth mechanism to organ preference of metastasis. – Exp. Cell Res. *204*, 171–180 (1993).

NOWELL, P. C.: Mechanisms of tumor progression. – Cancer Res. *46*, 2203–2207 (1986).

O'CONNOR, K. L., CULP, L. A.: Topological and quantitative analyses of early events in tumor formation using histochemically-tagged transformed 3T3 cells. – Oncology Rep. *1*, 869–876 (1994).

PRETLOW, T. G., PELLEY, R. J., PRETLOW, T. P.: Biochemistry of prostatic carcinoma. – In: Biochemical and Molecular Aspects of Selected Cancers, Vol. 2 (ed. T. G. PRETLOW and T. P. PRETLOW), pp. 169–237. – Academic Press, San Diego 1994.

RADINSKY, R., KRAEMER, P. M., RAINERS, M. A., KUNG, H.-J., CULP, L. A.: Amplification and rearrangement of the Kirsten *ras* oncogene in virus-transformed Balb/c 3T3 cells during malignant tumor progression. – Proc. natl. Acad. Sc. USA *84*, 5143–5147 (1987).

SANES, J. R., RUBENSTEIN, J. L. R., NICOLAS, J.-F.: Use of a recombinant retrovirus to study post-implantation cell lineages in mouse embryos. – EMBOj *5*, 3133–3142 (1986).

SATO, N., GLEAVE, M. E., BRUCHOVSKY, N., RENNIE, P. S., BERALDI, E., SULLIVAN, L. D.: A metastatic and androgen-sensitive human prostate cancer model using intraprostatic inoculation of LNCaP cells in SCID mice. – Cancer Res. *57*, 1584–9 (1997).

STEPHENSON, R. A., DINNEY, C. P. N., GOHJI, K., ORDONEZ, N. G., KILLION, J. J., FIDLER, I. J.: Metastatic model for human prostate cancer using orthotopic implantation into nude mice. – J. natl. Cancer Inst. *84*, 951–7 (1992).

WAINSTEIN, M. A., HE, F., ROBINSON, D., KUNG, H.-J., SCHWARTZ, S., GIACONIA, J. M., EDGEHOUSE, N. L., PRETLOW, T. P., BODNER, D. R., KURSH, E. D., RESNICK, M. I., SEFTEL, A., PRETLOW, T. G.: CWR22: androgen-dependent xenograft model derived from a primary human prostatic carcinoma. – Cancer Res. *54*, 6049–52 (1994).

Subject index

In: ***TARGETED THERAPY FOR CANCER***
Ed. Konstantinos N. Syrigos & Kevin J. Harrington
Oxford University Press, London, UK, 1999

Targeting the Metastatic Process

Lloyd A. Culp[1], Wen-chang Lin[1,2], Nanette R. Kleinman[1,3], Priit Kogerman[1,4], Raymond Judware[1,5], Carson J. Miller[1], and Julianne L. Holleran[1]

[1]Department of Molecular Biology and Microbiology
Case Western Reserve University
School of Medicine
Cleveland, OH 44106 USA

[2]Current address: Institute of Biomedical Sciences
Academia Sinica and Clinical Cancer Center
National Health Research Institutes
Taipei, Taiwan, Republic of China

[3]Current address: Animal Resource Center
Case Western Reserve University
School of Medicine
Cleveland, OH 44106 USA

[4]Current address: Karolinska Institutet
Department of Biosciences
Novum, S-141 57, Huddinge, Sweden

[5]Current address: Tropix, Inc., Bedford, MA 01730 USA

Key Words: Histochemical marker gene, tumor progression, micrometastasis, angiogenesis, CD44, integrin receptor, N-*myc* oncogene, gene regulation

Running Title: Tracking tumor progression and micrometastasis

Table of Contents

(I) Recent Approaches to Dissect Tumor Progression and Metastasis in Animal Model Systems

Metastasis of a tumor to target organ sites is a very complex series of events (1-7). It must involve highly selected primary tumor subpopulations, blood and/or lymphatic vessels, and specific organs amenable to "receive" the tumor cells. At least six to eight different steps can be envisioned in this migratory sequence, each of which must require specific and specialized gene products to be successful. One of the most impressive aspects of cancer metastasis is the remarkable versatility of tumor cells to generate such sophisticated subpopulations.

Angiogenesis is one critical consideration during metastasis (1,10,11). Not only must metastatic tumor subsets intravasate and extravasate currently-established blood vessels, they must also secrete the critical factors required at their foreign target sites to induce new blood vessel formation if micrometastases are to grow successfully into overt metastases. Since other chapters in this volume deal with angiogenesis regulation specifically, no further comment will be made on the significance of these specialized gene products and their functions in this chapter.

There are analogies between the evolution of metastatic variants in the primary tumor and some complex events that occur during normal embryonic development (12,13). For example, development of the neural crest generates multiple cell subsets that migrate to other "foreign" regions of the embryo where they differentiate into adrenal gland cells, peripheral neurons at many sites,

melanocytes throughout the skin, and some facial bones. Developmental biologists have shown that these complex patterns require a shifting in the expression of many genes, not just one or a few genes (13).

Likewise, metastasis to various target organs from the site of the primary tumor must involve a large array of gene activities. This is evident since the primary tumor is embedded in its "native" cellular environment while all target metastatic sites must be viewed as "highly foreign" to that particular tumor cell (1-6). This complexity is compounded by intravasation/extravasation of blood vessels and/or lymphatic vessels during these events and by the fact that a particular class of primary tumor does not metastasize to only one target site (although one site might be highly preferred during early events) but to multiple sites.

Targeting multiple tissue sites presumably requires different, but overlapping, gene classes in tumor cell subsets. In support of this hypothesis, evidence is mounting for organ-specific regulation of tumor cell genes (7,8; see sections II and III below). Furthermore, these new patterns of gene expression in metastatic tumor subsets are a reflection of the genetic instability of cells in the primary tumor, permitting select subsets to be successful and efficient in the multiple steps involved. Therefore, it is highly unlikely that there is a master "metastasis-control" gene in any tumor type that oversees these complex events (9); rather, it is genetic instability leading to many subsets of tumor cells that guarantees success in metastasis to lung, liver, bone, bone marrow, brain, and other target organs.

Another consideration in these experimental paradigms of tumor progression and metastasis is the pattern(s) by which genes change their expression. It is highly likely that some genes are turned off to generate metastatic variants, while other gene classes are turned on to execute specialized functions. There is also evidence, reviewed in section III, of reversible expression of at least one gene during progression and metastasis, a concept predicted by Nicolson (4) many years ago.

Our studies, summarized in this review, involve three different tumor systems. The first is the mouse fibrosarcoma system in which Balb/c 3T3 cells are transfected with one of three different oncogenes-- the human EJ-H-*ras* oncogene, the mouse Ki-*ras* oncogene, or the human c-*sis* oncogene (14). The second system is human neuroblastoma, with or without N-*myc* oncogene amplification (15). More recently, we have initiated studies of the progression and metastasis of new human prostate carcinoma (PCA) tumor cell systems (16). These PCA studies are particularly significant since so little is known in the human disease and/or model systems regarding its mechanism(s) of metastatic progression. In all cases, <u>in vivo</u> studies have been analyzed in athymic nude mice and compared with phenotypes of respective tissue culture cell subpopulations.

These three tumor systems will be reviewed from three different methodological and gene-regulatory perspectives that bear directly on metastatic mechanisms. First, the use of histochemical marker genes will be reviewed for genetically-tagging tumor cells and following their fate during

metastatic spread in virtually any organ of the experimental animal. Single tumor cells can be followed with relative ease by these approaches. We have now used these marker genes in fibrosarcoma, neuroblastoma, and prostate carcinoma experimental models. Second, we will review evidence that modulation of expression of the CD44 gene is a critical factor in metastatic spread of fibrosarcoma, as well as provide some insight into CD44's mechanism of action. Finally, evidence will be summarized for down-regulation of specific integrin genes by highly-amplified N-*myc* oncogene in the neuroblastoma system. Analyzing these three tumor systems with these and other methodologies will enable us to predict some important advances in metastasis studies during the next decade.

(II) Histochemical Marker Genes to Track Micrometastasis Formation and Subsequent Development into Overt Metastases

(A) Micrometastasis to organs never implicated previously. During early studies of fibrosarcoma and neuroblastoma metastasis in athymic nude mice (14,15), we had been frustrated by our inability to detect the earliest events in primary tumor formation and, more importantly, the earliest events during micrometastasis. Following the precedent set by developmental biologists to study single-cell lineages in embryos (12), we transfected the E. coli *lacZ* gene into fibrosarcoma cells to track these tumor cells. Using the X-gal histochemical staining reaction, single tumor cells could be easily detected in virtually any target organ of the animal (17,18). In later studies (19), we developed the use of Red-gal which stains these cells red, rather than the blue product generated

from X-gal. This approach using histochemical marker genes generated the first studies in any tumor system (17,18). EJ-H-*ras*-transformed Balb/c 3T3 cells were detected undergoing spontaneous metastasis to the lung and liver, as expected from previous low-resolution methods. The sensitivity for detecting tumor cells was so refined that single tumor cells could be detected in sections of lung adherent to the lining of blood vessels, possibly in the act of extravasating; in other cases single tumor cells had already escaped (Fig. 1). Moreover, micrometastases were detectable in the brain and kidney, organs never previously implicated in metastasis of fibrosarcoma tumors (6,17,18). In the case of the brain, these micrometastases were transient and failed to thrive into overt metastases, possibly indicating an environment hostile for fibrosarcoma growth promotion (6).

The versatility of this system was enhanced further by genetically tagging a second fibrosarcoma tumor cell class with the histochemical marker gene, placental alkaline phosphatase (PAP) whose enzyme product remains intercalated in intracellular membranes thereby permitting its enzymatic product to remain intracellular (19,20). The resulting color reflecting PAP enzyme activity could also be manipulated by the chemical nature of the substrate, thereby yielding red, reddish-brown, black, or blue staining cells depending upon which combination of histochemical substrates were used (19). For this system, the PAP gene was transfected into *sis*-transformed 3T3 cells to evaluate their micrometastatic potential from the subcutaneous site (19,21). In contrast to the excellent metastatic potential of the *ras* transformant, virtually no

spontaneous micrometastasis could be detected with the *sis* transformant from the subcutis.

The effectiveness of this approach for evaluating micrometastatic potential in nude mice has been demonstrated for the first time in human prostate carcinoma using PCA cells transfected with *lacZ* (16; C. Miller, J. Holleran, and L. Culp, unpublished data). In the vast majority of animal experimental models of human prostate carcinoma, metastasis can only be observed to the lung and rarely to liver and bone which are high-probability targets of the human disease (22,23). Using the new human PCA cell line, CWR22R (24), generated from a human xenograft in nude mice and transfected with *lacZ*, we have shown that these cells spontaneously metastasize from the subcutaneous site to lung, liver, and brain (J. Holleran, C. Miller and L. Culp, unpublished data). In some of these cases, micrometastases gave rise to well-staining overt metastases. This multiplicity of targets for PCA metastasis should markedly improve our ability to quantitatively and qualitatively evaluate the mechanisms by which difficult-to-study PCA tumor cells undergo metastatic processes.

(B) Micrometastases converted into overt metastases. The ease of detecting *lacZ*-tagged fibrosarcoma cells in micrometastases enabled us to monitor the efficiency with which micrometastases became overt metastases. The lung was the ideal site for such a study since an enormous number of micrometastases could be readily detected in this organ, even with spontaneous metastasis from the subcutis as the site of primary tumor

development (18,19). Many micrometastases persisted in the lung for days and weeks and failed to expand into overt metastases. Others developed slowly into overt metastases while a select few grew very rapidly (within 1 week) into metastases. This phenotypic diversity raises question as to the genetic diversity within the *ras*-transformed 3T3 population responsible for these three subsets of tumor cells. Alternatively, there may be special microenvironments within the lung that permit more successful outgrowth of micrometastases or that may be inhibitory for their outgrowth. These issues require much more detailed molecular biological analyses that histochemically-tagged tumor cells will now permit.

Using the experimental metastasis model provided by tail-vein injections, the ability to detect single fibrosarcoma tumor cells in the lung permitted us to analyze the time course of events for establishment of micrometastases in this target organ (18,25). Within 5 minutes after injection, micrometastases were becoming established in the lung, the quantitation of which revealed maximization in number by 1 hour (Table 1). Within 24 hours, >98% of these foci were "cleared" from the lung while the remaining 1.5% became truly established (18). These results confirm studies from the 1970s of melanoma and other tumor systems for clearance from the lungs of the majority of experimental micrometastases but not all of them (1-4). However, the mechanisms of the selective "clearance" or "resistance" of individual micrometastases remain to be determined in terms of molecular and cellular targeting events.

Lin and Culp (25) took a different approach in addressing micrometastatic mechanisms in the lung. They pretreated their *lacZ*/H-*ras*-transformed 3T3 cells with formaldehyde, ^{60}Co irradiation, or mitomycin C to effect any modulation on micrometastasis size, morphology, or stability. Pre-fixation generated micrometastases that were somewhat larger and more rounded in morphology while the irradiation or mitomycin treatments generated micrometastases that were identical to those of live, untreated cells. However, the irradiated- or mitomycin-treated cells were cleared from the lungs completely and more rapidly than live cells while the fixed cells persisted for much longer periods of time. When untreated cells were mixed with fixed cells and then the mixture injected into the tail vein, all micrometastases were cleared from the lungs, including those containing live cells. These studies indicate the importance of cell surface events (altered by fixation but not by the DNA-directed irradiation or mitomycin treatments) for (a) establishing micrometastases longterm in the lung and (b) guaranteeing their survivability in this organ site (25).

(C) Synergy between two genetic classes during metastasis to the lung. We generated two different oncogene derivatives of Balb/c 3T3 cells--one transformed with EJ-H-*ras* and the other with *sis* (the former is spontaneously-metastatic and the latter nonmetastatic). Tagging these with two different histochemical marker genes (19,21)--the former with *lacZ* and the latter with PAP-- enabled us to evaluate possible synergistic or interferring mechanisms in mixed populations of the two classes. When equal numbers of the two cell

types were mixed and injected into the subcutis (21), primary tumors developed that were regionally concentrated with only one cell type, providing a mosaic of blue-staining or reddish brown staining tumor tissue(16). Sectioning revealed that each region was comprised of only one cell type; there was very little intermixing of the two tumor classes except at the margins of two stained regions. This result for all s.c. primary tumors indicated that clonal dominance of each tumor class must occur to give rise to this regional pattern (16). These studies also indicate that the two oncogenes change the gene expression pattern differently in the same Balb/c 3T3 parent population such that selective growth patterns can be observed in the earliest primary tumors (16).

When mixtures of these two fibrosarcoma classes were injected into tail veins, synergy between the two classes became evident when quantitating sites and qualitatively analyzing cell distributions in the lung (19,21) [Table 1 and Fig. 2]. Most micrometastases were comprised of only the *ras* transformant or the *sis* transformant based on homogeneous staining of blue or red sites (both in whole-organ staining as well as in section staining) (Fig. 2A and B). However, a significant fraction (>7%) of sites that became stably established after 24 hours contained both cell types (Table 1; Fig. 2A and B). When *sis*-transformed cells alone were injected into tail veins, all their micrometastases were cleared from the lungs within a few days, demonstrating the absence of a stabilizing set of conditions for these transformants and contrasting with the stability of *ras*-transformed micrometastases [Table 1]. With mixtures of these two cell classes, the *ras* population provides some unknown stabilizing

influence on the *sis* population such that the latter persist as micrometastases and some develop into overt metastases containing both classes of tumor cells (19,21) (Fig. 2C and D). There is an enrichment of the two-cell-class of metastases indicating the synergy between the two during their outgrowth [Table 1]-- the *ras* transformants must be providing environmental cues to neighboring *sis* transformants for stability and subsequent outgrowth. Whether this synergy is mediated by soluble factors secreted selectively by one of these cell types or by extracellular matrix-mediated events remains to be determined. Having two histochemically-tagged cell types permits us to examine gene regulation events in these earliest mixed-cell micrometastases.

(D) Multiple tumor cells in the earliest micrometastases in lung. Injection of *lacZ*-tagged, *ras*-transformed 3T3 cells into tail veins permitted us to evaluate the number of tumor cells in individual micrometastases (18,25). Sectioning, embedding, and histochemically staining these lungs revealed some surprises (25). Rarely were single cells observed in early micrometastases; the vast majority were comprised of 2-7 cells under conditions where single-cell suspensions were being injected into the tail veins. This indicates that fibrosarcoma cells form micro-aggregates during the first minutes in the animal's circulation or that they aggregate at each site in the smallest blood capillaries of the lung. Cardiac perfusion of fixative during euthanasia also revealed details of the lung's microvessels and demonstrated that micrometastases almost always form in the very smallest capillaries. The same results were observed for *lacZ*-tagged human neuroblastoma cells (26) while

our *lacZ*-tagged prostate carcinoma cells remain to be tested in this paradigm. Could multi-cellularity result from physical entrapment of micro-aggregates in these sites or are these sites preferentially adhesive for tumor cells? Use of histochemically-tagged tumor cells and high-resolution molecular biological approaches (see section V below) should assist better definition of these potential mechanisms.

(E) Angiogenesis during tumor progression. Cardiac perfusion of fixative also permitted us to evaluate the formation of new blood vessels in the vicinity of the developing primary tumor by contrasting red-staining blood vessels with blue-staining tumor cells (26). In the case of *lacZ*-tagged neuroblastoma in the subcutis, staining of the entire subcutaneous site or transverse sections of the primary tumor revealed how quickly angiogenesis is promulgated by tumor cell-secreted factors. New blood vessels were seen developing at the periphery of dense populations of tumor cells within 48-72 hours. Several days post-injection, a few of these micro-vessels had developed into sizable blood vessels. By the time the primary tumor had become palpable, one or more of these larger vessels had become a major vessel feeding the central regions of the tumor.

The rapid induction of new blood vessels by tumor cells indicates that a long period of adaptation in the subcutis by tumor cells to secrete angiogenic factors is unlikely. Rather, the tumor cells may be secreting angiogenic factors (10,11) as cultured populations prior to their injection into the subcutis; alternatively, induction of angiogenesis genes occurs in tumor cells within the

first 24 hours of residence. This system can now be used to assay pro-angiogenic and anti-angiogenic factors in ectopic and orthotopic sites of primary tumor development.

(F) Histochemical markers as indicators of tumor cell genetic instability. Since histochemical marker genes do not provide any selective advantage or disadvantage for tumor cell growth at any site in the experimental animal, their activities can be used quantitatively and qualitatively to monitor the relative genetic instability of tumor cell subsets (6,16). This instability was noted in our very first fibrosarcoma tumor studies (19,21). *LacZ*-transfected, *ras*-transformed 3T3 cells retained excellent stainability in culture for >20 passages and in very large primary tumors grown over a period of weeks in the animal. In contrast, PAP-transfected, *sis*-transformed 3T3 cells began losing stainability within 5-10 passages in culture and virtually all large primary tumors contained regions of non-staining cells (16,19,21).

The same spectrum of stability applied to *lacZ*-transfected human neuroblastoma cells (26). One clone yielded excellent stainability for >15 passages in culture and throughout large primary tumors in the subcutis. A second clone, by contrast, was losing stainability within 5-10 passages and virtually all primary tumors using this clone contained large regions of nonstainable tumor tissue.

Three different *lacZ* transfectants of the human prostate carcinoma cell line, CWR22R, also demonstrate this gradient of genetic instability in expression (16; C. Miller, J. Holleran, and L.Culp, unpublished data). Clone H cells stain

very well for >25 passages in medium without drug selection and produced excellent staining primary tumors after 6-12 weeks in the subcutis of animals. Clone B steadily lost stainability over 10-20 passages in culture without selective media and invariably gave rise to tumors with large regions of nonstainable tissue. Clone D was so unstable that virtually all stainability was lost after 5 passages in culture.

The ease of quantitation of histochemical marker gene expression affords us the opportunity to evaluate the molecular mechanisms of this instability and whether it relates to organ-specific metastasis at all. Several mechanisms for loss of reporter gene expression can be envisioned. First, the marker gene may be deleted from the genome or rearranged in such a way that it has lost integrity. Second, transcriptional down-regulation may occur by induction of a new transcriptional-inhibitory factor (trans-acting) in tumor subpopulations. Third, the marker gene may be transcriptionally down-regulated by a hypermethylation mechanism, which is known to alter regulation of many genes in tumor cells (see section III on this point). Fourth, transcription of the marker gene may be perfectly normal but there may be induction of a factor(s) that inhibits protein enzymatic activity in the cytoplasm of cells. As discussed more fully in section V, there are approaches available now that permit resolution of these various possibilities.

(III) Selection and Counter-selection for CD44 Overexpression During Progression and Metastasis

CD44 is a transmembrane glycoprotein on the surface of many, but not all, cell types in animals (27,28). It harbors several binding domains-- its most external domain binds hyaluronan (HA); a membrane-proximal domain homes lymphocytes; and its cytoplasmic tail binds intracellular cytoskeletal elements. Its pre-mRNA is alternatively spliced into a wide variety of splice products, most of which occur in the membrane-proximal/external portion of the molecule responsible for lymphocyte homing. In contrast to the "standard" isoform (CD44s) which lacks all spliced sequences and is the only identifiable product in lymphoid cells and fibroblasts, its "variant" isoforms (CD44v) frequently do not bind HA, have lost lymphocyte-homing ability, and are observed in cell-type-specific distributions among various epithelial cell types (27,28).

CD44 is a likely gene product with significance for progression and metastasis of some human tumor systems (29). First, many primary tumors of human or experimental animal origin have elevated levels of CD44s or CD44v; in some cases, there are different distributions of CD44v in the tumor population from that of the host tissue (30-33). Second, metastases of tumors express more elevated levels of these CD44 isoforms or a different isoform distribution than that observed in the primary tumor, suggestive of unique functions for the spliced variants (34-37). Third, transfection and overexpression of CD44v (38) induces metastatic potential in normally nonmetastatic carcinoma cells. Transfection/overexpression of CD44s in lymphoma cells (39) also induces

metastatic competence. Finally, CD44s on the surface of lymphoid cells with its ability to bind HA is a critical element in the homing of these cells to adhere to blood vessel endothelial cells and their successful extravasation from vessels (40,41). These processes resemble those undertaken by metastatic tumor cells as they migrate to target organs.

Because of these functional implications for metastasis, we undertook analyses of the significance of CD44s in our fibrosarcoma systems--i.e., Balb/c 3T3 cells transformed with either a *ras* oncogene to make them metastatic or with the *sis* oncogene which does not confer metastatic competence (as described in section II). We also analyzed nontumorigenic revertants (IIIA4 cells) of the *ras* transformants that had lost the transforming *ras* oncogene (14). These studies have revealed a remarkable plasticity of expression of CD44s in these cells during progression and metastasis, as delineated below (42-45).

(A) Oncogene-dependent regulation of mouse CD44s gene expression. FACS (fluorescence-activated cell sorting) analysis of Balb/c 3T3 cells demonstrated that they had modest levels of mouse CD44s (mCD44s) on their surfaces and no detectable CD44v isoforms as expected (42). In contrast, *ras* transformants of these 3T3 cells had very high levels of mCD44s and no CD44v isoforms. *Sis* transformants had levels of mCD44s comparable to those of 3T3 cells while revertant IIIA4 cells had reduced expression levels from the high levels observed in the original *ras*-transformed population. These data indicated correlation of metastatic competence with the elevated levels of mCD44s in the *ras* transformants (42). A second correlation was also made--

the high mCD44s-expressing *ras* transformants could bind exogenously-added HA very well while the *sis* transformants and the revertant cells could bind very little HA in a CD44-dependent manner. When a wide variety of nude mouse primary tumors and lung metastases, derived from the *ras* transformants, were evaluated by FACS and/or Western blotting after transplant back into tissue culture, all demonstrated very high levels of CD44s (42). Therefore, expression of the *ras* oncogene leads to up-regulation in mouse CD44s expression while expression of *sis* is without effect on expression of this gene.

(B) Transfection of human CD44s gene into *sis* transformants--acquisition of metastatic competence and the counter-selection model of progression. We then designed a system to artificially elevate levels of CD44s in transformed cells with a molecule that could be differentiated from the endogenous mouse homolog using specific monoclonal antibodies (43). The human CD44s cDNA gene, under regulation of a very active LTR promoter, was transfected into *sis*-transformed 3T3 cells in an effort to test elevation of cell surface CD44s (either hCD44s or mCD44s). Three independent and stable transfectants were isolated. There was no elevation of mCD44s in any transfectants. In contrast, there were very high levels of hCD44s on these cells. Furthermore, exogeneously-added HA could bind to the hCD44s on the cell surface but not to the mCD44s, providing further functional discrimination between these two classes of molecules (43).

When the hCD44s-overexpressing transfectants were injected into the subcutis of nude mice (43), very aggressive primary tumors formed within 1-2

weeks. Furthermore, these cells were now highly metastatic to the lung, contrasting with the lack of spontaneous metastasis using the original *sis* transformants. When micrometastatic tumor cells from the lung were isolated back into culture, FACS analyses of their CD44s levels revealed the expected levels of mCD44s and very high levels of hCD44s (Fig. 3B and 3D), consistent with the hypothesis that overexpressed levels of hCD44s led directly to acquisition of metastatic competence.

Similarly, primary tumors in this series were isolated into culture and evaluated for their CD44s levels. This led to a very surprising finding (43). All large primary tumors from transfectants had lost expression of hCD44s while retaining the modest levels of mCD44s; this loss was observed in >20 primary tumors examined (Fig. 3A and 3C). These results indicate that overexpression of the human gene may be counter-productive and/or antagonistic for outgrowth of primary tumor in the subcutis. This counter-selection against hCD44s gene expression contrasted with the high-expression levels of this gene product in all lung micrometastatic tumor cells.

This led us to examine a third tumor population. Micrometastases of some hCD44s transfectants in the lung invariably grew into large overt metastases (43). When large metastases were transplanted back into culture and tested by FACS for CD44s levels, they had lost virtually all of their hCD44s while retaining the expected levels of mCD44s. This would indicate that there is not an organ-specific down-regulation of this gene in the two tissue sites. Rather, aggressive outgrowth of tumor, whether it be the primary tumor or

distant metastases, required down-regulation of hCD44s for some inapparent reason, perhaps linked to its HA-binding ability that is defective in mCD44s.

These important studies led us to hypothesize a selection/counter-selection model of tumor progression in this system (43,46). Elevated levels of hCD44s would be critical to get metastatic spread from the subcutis to the lung. Conversely, outgrowth of the primary tumor and any overt metastases required that the gene be turned off in highly selected subpopulations if aggressive cell division was to be successful.

What is the origin of the lung micrometastatic cells with overexpressed hCD44s (43,46)? Two alternative models for the origin of lung metastatic cells could be envisioned. Perhaps these cells migrate from the subcutis to the lung soon after injection and prior to down-regulation of the hCD44s gene. Alternatively, a small subpopulation of hCD44s-overexpressing cells may exist at all times in the primary tumor; it cannot be readily identified by FACS analyses (or by Western blotting for that matter).

As one approach to address these questions, we undertook a second round of tumor analyses (43). In the first case, primary tumor cells that had lost expression of hCD44s were re-injected subcutaneously into a second group of animals. These cells formed excellent primary tumors, all of which failed to express detectable hCD44s. These primary tumors also gave rise to micrometastatic tumor cells in the lungs of these animals. When these micrometastatic tumor cells were explanted into culture and grown out in drug selection medium to eliminate any mouse lung cells, these micrometastatic

tumor populations expressed high levels of hCD44s in all cases. Therefore, metastatic competence correlated again with acquisition of high levels of cell surface hCD44s. In the second case, lung micrometastatic tumor cells from the first round (high hCD44s expressors) were injected into a second group of animals--all s.c. primary tumors had lost hCD44s expression while lung micrometastatic tumor cells retained high levels of this cell surface protein. These experiments demonstrate the remarkable plasticity of hCD44s expression during progression and metastasis with these *sis* transformants of 3T3 cells.

(C) Possible mechanism of modulation of the hCD44s gene. These studies raised the question of how the elevated levels of hCD44s may facilitate metastatic spread while endogenous mCD44s does not convey this competence (46). It appears likely that the ability of the human protein to bind exogenous HA is the critical characteristic that distinguishes hCD44s from the properties of the mouse protein. To prove this, we must test overexpression of a mutant form of hCD44s that is specifically unable to bind HA but is capable of other binding functions. If such a molecule proves incompetent in conveying metastatic competence, then clearly HA binding is a central issue for metastatic spread of fibrosarcoma tumor cells (also will the mutant gene be downregulated in primary tumor cells if it cannot bind HA?). If HA-nonbinding mutants persist in conveying metastatic competence, then there must be some additional and unknown binding activity in this domain of the molecule that is

critical. Further experiments along these lines should prove particularly informative.

Some insight has been provided into the mechanism of modulation of hCD44s expression in these tumor cells (43). Hypermethylation of gene promoter regions has been shown to down-regulate a number of genes in tumor cells (47,48). Testing the hCD44s gene region for sensitivity to digestion with restriction enzymes responding to hypermethylated DNA sequences revealed two very different levels of methylation in or proximal to this gene(43). In the original transfectant cells and lung micrometastatic tumor cells, both of which express considerable hCD44s, there were low levels of methylation in this gene region. In contrast, primary tumor cells and overt metastatic tumor cells that had lost hCD44s protein displayed high levels of DNA methylation in this region. This correlation was further reinforced using aza-deoxycytidine treatment of cells in culture to inhibit DNA methylation (43). This treatment led to high levels of hCD44s in primary tumor cells and only slightly increased the levels in transfectant cells and in lung micrometastatic tumor cells that already had elevated levels. Therefore, it is highly likely that plasticity of expression of this transfected gene in these fibrosarcoma cells is effected by regulation of DNA methylation in this gene's promoter region. To test this hypothesis directly, we can transfect hCD44s gene into these cells under regulation of other active promoters that are much less susceptible to hypermethylation and then test for plasticity of hCD44s expression, aggressiveness of primary tumor development, and acquisition of metastatic competence in this paradigm.

(D) Additional hCD44s expression/plasticity systems. In addition to the *sis* transformants described above, transfection of the hCD44s gene was performed in revertant IIIA4 cells (43). These revertant cells were isolated from a clonal population of K-*ras*-transformed 3T3 cells and were shown to have deleted the *ras* oncogene by some unknown mechanism (14). In doing so, they had lost much of their tumorigenic potential.

Several stable transfectants of IIIA4 cells were isolated after transfecting the hCD44s gene (43). They expressed very high levels of hCD44s protein which was competent for binding exogenous HA. Upon subcutaneous injection into nude mice, they were much more tumorigenic than parental IIIA4 cells. Of particular interest, they had acquired metastatic competence for the lungs of these animals. Lung micrometastatic tumor cells, explanted into culture, expressed high levels of hCD44s while the large primary tumors had lost expression.

This led us to test the third biological system (44). The hCD44s gene was transfected into nontumorigenic Balb/c 3T3 cells to determine if their phenotype was altered in any way. Several stable transfectants were isolated with low, intermediate, or high levels of hCD44s on their surfaces; in all cases, exogenous HA binding was proportional to the amount of cell surface hCD44s and unaffected by mouse CD44s. Of particular note, the highest hCD44s-expressing clone was tumorigenic in the subcutis of nude mice and subpopulations of these cells formed spontaneous micrometastases. In agreement with the other two systems, the primary tumor cells lost expression of

hCD44s while the lung micrometastatic tumor cells retained high levels of hCD44s (44).

This latter 3T3 system was explored further by testing whether these hCD44s levels, observed with tissue cultured populations, could be reflective of tumor populations in vivo (44). Using immunohistochemical approaches, we demonstrated that fixed sections of the primary tumor tissue retained immunohistochemical stainability for mouse CD44s but lacked any significant levels of human CD44s. In contrast, small foci of tumor cells in the lung expressed high levels of hCD44s and low levels of mCD44s (44). These experiments confirmed the results of tissue culture analyses of these various tumor populations and discounted an artifact of altered expression upon tissue culturing of these populations.

(E) Experimental metastasis system to evaluate functional significance of overexpressed hCD44s. The results described above suggest that overexpressed hCD44s facilitated metastatic spread of normally-nonmetastatic *sis* transformants and other cell types to the lung. One approach for testing this hypothesized mechanism involves injection of tumor cells into tail vein blood vessels to evaluate later steps in metastatic spread but not the initiating events. This approach would not be evaluating the intravasation steps into blood vessels at the site of the primary tumor. Since the plasmid used for transfection of the *sis* oncogene into these transformants also harbored the hygromycin B resistance gene, we could quantitate lung colonization by enumerating drug-resistant colonies grown out in culture after harvesting lungs and dispersing

them into single-cell suspensions. This approach yielded some very important mechanistic information for the significance of overexpressed hCD44s in the early events of micrometastatic establishment (45).

Untransfected *sis*-transformed cells generated a low number of micrometastatic foci in lungs at any time point examined after tail vein injection--e.g., 1 hour, 24 hours, and 4 weeks (45) (Fig. 4). In contrast, hCD44s transfectant cells yielded three times that number of foci at 1 hour, more than ten-fold that number at 24 hours, and ten-fold more at 4 weeks (Fig. 4). These results indicate that high hCD44s levels (a) greatly improve initial implantation of micrometastases in the small blood vessels of the lung within the first hour in the circulation and (b) further improve the stabilization of these micrometastases during the clearance mechanisms that operate between 1 and 24 hours. Furthermore, persistence of these micrometastases over the next 4 weeks reveal a lasting effect on their residence in the lungs.

These culture-isolated colonies were also evaluated by FACS for levels of hCD44s and its ability to bind exogenous HA (45). As expected, the lung-colonizing population of transfectant cells had very high levels of hCD44s and excellent ability to bind HA at the 1 and 24 hour time points. In contrast and consistent with plasticity of hCD44s gene expression, the 4 week-harvested cells had lost much of their cell surface hCD44s and their ability to bind HA. These results confirm the importance of cell surface hCD44s in establishing and stabilizing micrometastases but not in promoting their eventual outgrowth in the lung into overt metastases.

The next series of experiments in this paradigm tested the various tumor cell types described in section IIB above and harvested after s.c. injection of hCD44s-overexpressing transfectants (45). hCD44s-negative primary tumor cells, injected into tail veins, gave colony numbers from the lungs that were not statistically different from those of untransfected *sis*-transformed cells. In contrast, hCD44s-overexpressing lung micrometastatic tumor cells, injected into tail veins, gave colony numbers that were 7-10 fold higher than primary tumor cells and comparable to the numbers observed with the original transfectant cells. FACS analyses revealed very high levels of hCD44s on these cells and excellent binding of exogenous HA as well. These results confirm the correlation of high levels of HA-binding hCD44s on cells with their efficiency at colonizing the lung microvasculature (45,46).

In the experimental metastasis assays described above using hCD44s-overexpressed cell classes, a large number of overt metastases grew out within 3-5 weeks (45). Re-isolation of these cells into culture, based on their selection using the drug resistance marker on the transfected plasmid, yielded populations that were depleted of cell surface hCD44s and displayed poor HA binding. These results also confirm those of section IIB and illustrate the selection against high levels of hCD44s when tumor outgrowth becomes aggressive, whether it is the primary tumor in the subcutis or large metastases in the lung (46).

Two general models for these results can be proposed (45,46). First, hCD44s and its ability to bind HA could promote formation of small aggregates

of tumor cells in the circulation that would subsequently be trapped in the microvessels of the lung--i.e., promotion of tumor cell:tumor cell adherence. The second model involves more effective adherence of tumor cells to endothelial cells of these blood vessels by overexpressed hCD44s on the tumor cell surface binding to HA on the surface of the endothelium. Such binding may be relatively weak, as suggested by studies of lymphoid cell homing to sites of inflammation (40,41). Because microvessels do not experience the fluid shear stress that occurs in larger vessels, hCD44s:HA interactions in microvessels may be strong enough to hold tumor cell aggregates to the endothelium. This may explain why tumor cell aggregates are only observed in microvessels of the lung.

To test these alternatives, hCD44s transfectant cells were mixed with untransfected cells in varying ratios. Then the mixtures were injected into tail veins to test the "specific activity" of the overexpressors to colonize lungs in competition with untransfected cells. Hygromycin B was used to select all tumor cell classes in the lung while puromycin (the drug resistance marker on the hCD44s-bearing plasmid) was used to select transfectant cells specifically. Increasing the proportion of untransfected cells had no adverse effect on the much greater efficiency of colonization by the transfected subset. Consistent with this result, the lung tumor populations re-isolated into culture were tested for levels of cell surface hCD44s and were found to be overwhelmingly high expressors. These results would suggest that tumor cell:tumor cell adhesion is not playing a critical role in this mechanism. They are more consistent with the

model of much improved adhesion of transfectant cells to the endothelium, possibly mediated by HA-binding hCD44s (45,46). This would parallel a similar mechanism of lymphoid cell adhesion to the endothelium at sites of inflammation (40,41).

To test this model more directly, we can transfect non-HA-binding mutants of the hCD44s gene into these cells and determine if colonization remains low. We can also test whether other cell surface HA-binding receptors (at overexpressed levels) can facilitate the much improved colonization of these cells and whether HA oligosaccharides, co-injected into the circulation at the same time as tumor cells, can hapten-inhibit colonization.

(IV) N-myc Amplification in Neuroblastoma: Its Regulation of Integrin Receptor Expression

Human neuroblastoma is a tumor arising from the malignant conversion of a neural crest cell in the embryo destined to become an adrenal gland, a melanocyte in the skin, a peripheral neuron, or a facial bone (12,13). It afflicts young children prior to the age of 10 and can arise at many different organ sites (15,49,50). Some neuroblastoma tumor cell lines are neuritogenic in culture and have been studied as models of peripheral neuron differentiation (15).

N-*myc* is a proto-oncogene in the human genome and a member of the *myc* family of proto-oncogenes whose protein products are regulators of transcription of specific genes (51). This proto-oncogene displays a unique correlation with neuroblastoma tumor biology and progression (49,50,51). It becomes highly amplified in aggressive and metastatic neuroblastomas of

stage III or IV, does not display any unique mutations in metastatic tumors, and is not amplified in less-aggressive stage I or II tumors that do not metastasize. In the same tumor populations, the c-*myc* proto-oncogene is unaffected during progression and metastasis, suggesting that N-myc protein is responsible for transcription of genes other than those regulated by c-myc protein and that these N-myc-regulated genes participate in the aggressiveness of this tumor.

Earlier studies had demonstrated that amplification of the N-*myc* oncogene in neuroblastoma cells correlated with down-regulation of the major histocompatability complex class 1 gene, protein kinase C signaling, and the NCAM gene (52-54). Since the class of extracellular matrix receptors, called integrins (55), are critical elements in the altered relationship between tumor cells and their environment (14,15, 55), we sought to more directly test whether metastatic progression of neuroblastoma, mediated by N-*myc* amplification/overexpression, could be based on altered regulation of integrin genes in these tumor populations. Such evidence was obtained.

(A) Integrin expression in naturally-occurring human neuroblastoma cells. Our laboratory undertook analysis of the integrin receptor classes in three human neuroblastoma tumor classes (56,57). Two of these, IMR-32 and LaN1, display amplified N-*myc* oncogene while the third, SK-N-SH, does not. IMR-32 and LaN1 cells do not display significant amounts of any of the common β1 integrin family members. When these cells were injected into the subcutis (an ectopic injection site) or the adrenal gland (an orthotopic injection site for neuroblastoma), all primary tumors conserved this pattern of poor integrin

expression. The rounded, weakly-adherent morphologies of LaN1 and IMR-32 cells in culture were also consistent with poor integrin expression.

In contrast, SK-N-SH cells, harboring a diploid number of N-*myc* genes, expressed significant amounts of $\alpha 2\beta 1$, $\alpha 3\beta 1$, and smaller amounts of $\alpha 1\beta 1$ (56,57). These levels of integrins were conserved in all subcutaneous and adrenal gland primary tumors derived from this cell line. When these populations were analyzed by FACS, approximately one-half of the parental SK-N-SH cells expressed $\alpha 3\beta 1$ on their surfaces while the other half did not. Both s.c. and adrenal primary tumors conserved this dual-expression pattern, indicating that $\alpha 3^+$ or $\alpha 3^-$ cells were not clonally dominant during progression of primary tumors. There was also another distinctive pattern change observed in these studies. The parent SK-N-SH cell line did not express $\alpha v\beta 1$, nor did the adrenal gland primary tumors; in contrast, all s.c. primary tumors expressed $\alpha v\beta 1$, suggesting that upregulation of this integrin may be important in the biology of the primary tumor at this site.

These analyses demonstrate several important findings (56,57). First, integrin expression patterns are generally conserved between the original human tumor population, grown for many passages in culture, and the resultant athymic nude mouse tumors derived from them. Second, this conservation of expression is maintained at both ectopic and orthotopic injection sites. Third, induction of $\alpha v\beta 1$ in the s.c. primary tumors may indicate an important function that is specific to this site, possibly for angiogenesis as suggested from other

αv-expressing tumor populations (26, 58). Finally, clonal heterogeneity for α3β1 expression is conserved in all primary s.c. or adrenal gland tumors, indicating that expression of this integrin is not essential for primary tumor expansion. These studies raise question as to how N-*myc*-amplified tumor cells interact with extracellular matrices, since they lack common fibronectin- and collagen-binding integrins and since these are the more aggressive and metastatic classes of this tumor. The weak adherence of these cells in culture is certainly consistent with this poor integrin expression pattern.

(B) Transfection/overexpression of N-*myc* oncogene in SK-N-SH cells. To test more directly hypotheses relating N-*myc* oncogene overexpression with altered regulation of integrin subunit expression, we transfected an episomal plasmid, pREP4 harboring the human N-*myc* oncogene under regulation of a very active LTR promoter, into SK-N-SH cells which have a diploid number of N-*myc* genes and express a basal level of N-myc protein (59). Using the episomal plasmid for transfection permitted us to raise the concentration of N-*myc* oncogene in these cells by selection with increasing concentrations of hygromycin, the drug-resistance marker on this plasmid (59).

Several notable changes were identified in N-*myc* transfectant cells (59). They displayed an altered morphology in culture from that of well-spread SK-N-SH--they were rounded and easily detachable from the substratum, resembling IMR-32 or LaN1 cells in this regard. Selection with higher concentrations of hygromycin generated a higher precentage of rounded cells and much higher levels of N-myc protein. The levels of N-myc protein in these transfectants was

directly related to the dosage of the N-*myc* oncogene in these cells. Conversely, higher concentrations of hygromycin led to cell populations with greatly decreased amounts of β1 integrin subunit. Plotting the levels of N-myc protein against the levels of β1 integrin subunit in many different transfectants and at many hygromycin selection concentrations demonstrated the inverse relationship between the levels of these two gene products (Fig. 5) (59). Transfection of SK-N-SH cells with an antisense construct of N-*myc* failed to generate these changes. Therefore, these experiments directly relate higher dosages of N-myc protein in neuroblastoma cells to decreasing levels of β1 integrin subunit and are consistent with either direct or indirect regulation of the β1 integrin gene by the N-myc protein.

(C) Two different mechanisms for downregulating integrin expression by N-*myc*. The studies described above left open the issue whether integrin subunits α2 or α3 were also altered in N-*myc* transfectants. This was shown to be the case with the discovery that two different molecular mechanisms are operating (60).

Increasing concentrations of hygromycin, to select for increased levels of N-myc protein, led to cells with decreased levels of both α2 and α3 integrin subunits (60). In contrast, the modest levels of α1 subunit observed in these cells were unaffected by higher N-myc levels, dissociating regulation of this subunit from those of the other two (61). Very little α2β1 or α3β1 were observed

at the cell surface in N-*myc* overexpressors (60) while the levels of cell surface $\alpha1\beta1$ was unaffected (61). Evaluation of the levels of mRNAs for these subunits by RNase protection assay showed that levels of $\alpha2$ and $\alpha3$ mRNAs were greatly reduced (>85%) in N-*myc* overexpressors while the level of $\beta1$ mRNA was reduced only 40-50% (Fig. 6) (60). Of significance as well, the levels of *max* mRNA were unaltered in these cells (Fig. 6), demonstrating that this co-effector of N-myc transcriptional regulation was not being co-regulated by the much higher levels of N-myc protein (Fig. 6). Metabolic radiolabeling of proteins in these cells, in concert with pulse-chase analyses, revealed that the half-life of $\beta1$ was greatly reduced in transfectants while those of the α subunits were unaffected. Therefore, it is likely that the greatly reduced amounts of $\alpha2$ and $\alpha3$ subunits in these cells lead to uncomplexed $\beta1$ which then undergoes degradation (60). The exception to this fate is the modest amount of $\alpha1$ subunit that does complex with small amounts of $\beta1$ and successfully gets to the cell surface (61).

Overall, these studies indicate three different regulatory patterns of integrin genes in neuroblastoma tumor cells with highly overexpressed N-*myc* oncogene. First, there appears to be transcriptional down-regulation of the integrin $\alpha2$ and $\alpha3$ genes by an N-myc protein-dependent pathway; the *max* co-regulator is unaffected in these cells. Second, downregulation of $\beta1$ levels are effected at the post-transcriptional level, probably by protein instability caused

by insufficient amounts of α subunit for complexing. Finally, the expression of the α1 integrin gene is unaffected by N-*myc*, consistent with levels of α1β1 that persist in high-metastatic, N-*myc*-amplified tumor populations. It remains to be seen how tumorigenic and how metastatic the N-*myc* transfectants are in nude mice. Do they display the same progression and metastasis patterns as the naturally-occurring N-*myc*-amplified IMR-32 and LaN-1 tumor cells? Both ectopic and the orthotopic (adrenal gland) injection sites must be tested in these regards (56,57).

(D) Is N-*myc* downregulation of integrins tumor-specific? These analyses questioned whether N-myc protein regulation of integrins was specific to neuroblastoma tumors because one or more unknown factors in these tumor cells conveyed tumor specificity. To address this question, we transfected the same overexpressing episomal plasmid of N-*myc* into human Saos-2 osteosarcoma cells, a tumor cell line whose biology and lineage are very different from that of neuroblastoma having been derived from a connective tissue cell type (62).

Several transfectants of Saos-2 were isolated which had greatly elevated levels of N-myc protein (62). While parental Saos-2 cells were well-spread on the substratum and expressed considerable α2β1 and α3β1 integrins, the transfectant cells displayed very little of these integrins on their surfaces and displayed very rounded, easily-detachable morphologies. When mRNA levels and protein turnover patterns were analyzed, the same changes were found to occur in these cells (62) as shown above for N-*myc*-overexpressing

neuroblastomas (59,60). There was transcriptional downregulation of α2 and α3 genes while β1 transcription was minimally altered. In contrast, β1 protein turned over much more rapidly, probably because of lack of a partners and resulting in much lower basal levels of this subunit (62). *Max* mRNA levels were unaltered in transfectant cells, again casting the regulatory role on excess amounts of the N-myc protein. These results indicate that N-*myc* regulatory mechanisms can apply to a different cell and tumor types and are not neural lineage-specific. However, the osteosarcoma system is artificial in that there is no evidence for N-*myc*-dependent regulation or N-*myc* amplification in this tumor under naturally-occurring conditions.

These analyses of N-*myc*-overexpressing neuroblastoma and osteosarcoma cells prompt more extensive study of the interactions (or lack thereof) of N-myc protein, complexed with max protein, with the promoter regions of these three integrin genes. Unfortunately, these promoters have not been well-studied or their cis- or trans-acting sequences deciphered completely (63). If N-myc protein regulates transcription of specific genes, including α2 and α3 integrin genes, in ways that are independent of c-myc protein, then these N-myc mechanisms may be targetable for interfering with metastatic competence of these tumor cells.

(V) Perspectives on "Regulating" the Metastatic Phenotype

The findings described in the preceding sections, when combined with new high-resolution methodologies, enable us to speculate on future directions

in deciphering and possibly interfering with metastasis. First, we will be able to more precisely define the small cell subpopulations in which metastatic competence is being acquired as a consequence of altered regulation of genes, such as CD44 and integrin receptors. Second, by defining which genes are critical for metastatic competence, clinicians will be afforded much more powerful molecular tools for predicting when and where metastasis occurs. A corollary of this is that we should be able to generate reagents that specifically disrupt the functions of these metastasis-conveying gene products while minimally interfering with their "normal" functions in well-behaved cell populations. Finally, if we are able to define organ-specific regulation of some genes in tumor subpopulations, interference with the functions of these genes may permit us to inhibit metastasis specifically to that organ. Some examples of these approaches are offered below. Angiogenesis may be a particularly important target for antagonizing the metastatic process and other chapters in this volume deal with this issue specifically.

(A) Histochemical marker gene-tagged cells for drug screening studies. As shown in section II above, tumor cells tagged with histochemical marker genes can be easily visualized and quantitated in lung and other organs during experimental metastasis. Coinjection of marker gene-tagged tumor cells and candidate metastasis-inhibiting drugs will facilitate identification of useful drugs in several ways. Many drugs can be screened for metastasis-interfering properties using fewer animals and much shorter assay times. In addition, different routes for introducing these drugs into animals can be monitored for

the potential to interfere with spontaneous metastasis after either ectopic or orthotopic injections of tumor cells.

(B) Laser-capture microdissection--a high-resolution tool to analyze gene expression patterns in single tumor cells. The recent development of laser-capture microdissection (LCM) of tissue sections (64-66) permits investigators to select one or a few tumor cells in a tissue environment to analyze. Gene products may be detected in these select cells by immunohistochemistry or by their specific functions (65,66). Expression of any gene may also be analyzed at the transcriptional level by RT-PCR or in situ hybridization (64,66). Furthermore, use of histochemical marker genes will greatly facilitate the identification of tumor cells, to be selected by LCM, in experimental animal models as discussed in section II above. These markers discriminate the tagged tumor cells from untagged neighboring host-organ cells, whose gene expression pattern must also be considered. Therefore, LCM in combination with histochemical tags should be effective at determining whether "normal" host organ cells, adjacent to the primary tumor or metastatic cells, have altered gene regulation programs from their distant counterparts; conversely, the possible altered regulation of tumor cell genes by neighboring host cells can be addressed.

LacZ- or PAP-tagged tumor cells can be detected in fixed sections by first performing histochemical staining and then identifying the appropriate small subset of cells for subsequent laser capture. When two genetically-different tumor classes are tagged with different marker genes as shown in section II, this

approach becomes particularly beneficial in addressing clonal dominance of one cell type over another in specific regions of the primary tumor and in potential metastatic target sites. These dual approaches should prove particularly effective in deciphering the gene expression patterns in micrometastases as they form.

LCM, in combination with histochemical markers, can be used to determine when and where the CD44 gene is being upregulated (or different isoforms expressed) with RT-PCR and primers recognizing specific CD44 splice products. Does this regulation occur early in primary tumor formation or is it occurring in small subpopulations at later stages of the primary tumor? These approaches will permit us to determine whether selected tumor subpopulations, with altered expression of CD44, occur randomly throughout the primary tumor or only in regions adjacent to larger blood vessels, the latter possibly predicting more effective intravsation into blood vessels for eventual metastatic spread.

As reviewed in section IV, neuroblastoma metastasis correlates with N-*myc* amplification and subsequent downregulation of $\alpha 2\beta 1$ and $\alpha 3\beta 1$ integrin receptors, but not the $\alpha 1\beta 1$ receptor. Using LCM in combination with marker-tagged neuroblastoma cells, we can test a variety of hypotheses relating the absence of the two integrins to acquisition of metastatic competence. As an example, *lacZ*-tagged/N-*myc*-amplified neuroblastoma cells can be mixed with PAP-tagged/N-*myc*-amplified neuroblastoma in which $\alpha 2$ integrin subunit expression is upregulated by transfection with an $\alpha 2$ gene under control of a

very active promoter. Do both cell types contribute to formation of the primary tumor or does one cell type clonally dominate? By LCM and by following the two histochemical tags, we can determine the relative distributions of the two cell types near major blood vessels in the primary tumor and near other host tissue sites that may be synergistic. Do both cell types metastasize to the same or differing organs? These experiments may reveal some level of synergy between two classes of tumor cells. LCM could be used to examine the gene expression patterns in the earliest micrometastases of these different organs.

(C) Interfering with the functions of genes critical for metastasis. The studies of sections III and IV indicate the relative importance of two different gene classes in the progression of two different tumors in apposing regulation schemes--CD44s in the case of fibrosarcoma metastasis and integrin receptors for neuroblastoma metastasis. In the former, overexpression of the CD44s appears important for conveying metastatic competence while for neuroblastoma downregulation of integrin expression appears important. The identification of such genes raises the issue as to whether antagonists can be identified that inhibit metastasis effectively, based on the structure and function of the metastasis-targeting molecule(s). Hopefully, such an antagonist would not inhibit the normal functions of this molecular class in host organ cells.

An early indication of the possible success in this approach was the demonstration of small synthetic peptides, containing the Arg-Gly-Asp-Ser (RGDS) sequence, to effectively inhibit colonization of the lung when they were co-injected with melanoma and other tumor cells injected into the tail veins of

experimental animals (67,68). This approach proved successful because some integrins on tumor cells recognize an RGDS sequence in target extracellular matrix ligands, such as fibronectin, laminin, and certain collagens. These target ligands in the lungs of the animal would be the "natural" adherence site for tumor cells and provide the stabilization mechanism for eventual extravasation into lung tissue to establish micrometastases. Remarkably, there was very little toxicity to other tissues of the animal when high dosages of these synthetic peptides were injected.

Histochemical marker gene-tagged cells will provide much more facile and quantitative approaches for testing inhibition of metastasis by other haptens or antagonists of specific molecular domains. As examples, specific spliced sequences of CD44v on the surface of some carcinoma cells may provide binding sites for as-yet unidentified receptors on the surface of endothelial cells, thereby facilitating development of micrometastases (27-30). Synthetic peptides may be identified which inhibit this specific binding function while leaving the other generic binding functions of CD44v unaffected; these peptides would be ideal candidates for specific inhibition of metastatic spread of some carcinoma tumor types while being minimally toxic to other cell and tissue types.

CD44s is the simplest member of the CD44 family and has been shown important in metastasis of fibrosarcoma as reviewed in section III via improved colonization of the lung once tumor cells entered the circulation. Some monoclonal antibodies to specific epitopes of CD44s may be identified that interfere with metastatic spread while having limited inhibition of normal

lymphocyte or connective cell functions. Alternatively, the hyaluronan-binding function of CD44s appears very important in the lung colonization function of this molecule. Therefore, small oligosaccharides of HA may hapten-inhibit this colonization process and afford a complementary therapeutic approach with other drug modalities. As much more molecular information becomes available on the multiple binding functions of this complex class of cell surface receptors, we may be able to design dominant-negative inhibitors of one or more of these specific functions and greatly improve the tumor-targeting potential of such antagonists.

Molecular biological approaches may also prove useful for interfering with metastatic processes. An antisense gene for CD44s may inhibit metastatic spread of lymphoma (39) or fibrosarcoma (46) if it could be expressed in a retroviral construct that infects tumor cells more effectively than any neighboring host tissue cells. A similar and more specific approach might be considered for CD44v isoforms-- use of antisense constructs with sequences targeting specifically the alternatively-spliced domains to inhibit carcinoma metastasis (46). In the case of integrin receptors where downregulation occurs commensurate with metastatic spread of neuroblastoma, retroviral infection with an $\alpha 2$ or $\alpha 3$ integrin subunit gene, regulated by a high-activity promoter, may improve extracellular matrix adhesion of the primary tumor population and subsequently inhibit any spreading potential of these cells by other adhesion mechanisms. This is comparable to the overexpression of transfected E-

cadherin gene in some carcinoma cells, thereby inhibiting their invasion and metastatic behavior (69,70).

(D) Will genetic instability in tumor populations help or hinder in targeting the metastatic phenotype? It is fair to say that one characteristic of malignant cells is their ability to generate many genetically-different subpopulations as the primary tumor expands, thereby providing the versatility that permits metastatic spread for highly-selected subpopulations (1-5). The small number of these subpopulations may provide greater efficiency at inhibiting their functions but may require weeks or months of patient treatment to do so because metastatic-competent subpopulations may be generated in the primary tumor on a regular basis. If there were some way to specifically kill such subpopulations by inhibiting their metastatic-competence functions, chances for success in treating the patient may be greatly improved. Greater knowledge of apoptotic and other cell death mechanisms in tumor cells, some of which may be tumor- or cell type-specific, may afford the complementary treatment approach that will ultimately prove successful. In response, however, the versatility in generating many different subpopulations may also lead to antagonist-resistant variants within the primary tumor that can overcome the treatment modality and still metastasize to various target organs. In any case, greater knowledge of the various mechanisms for generating genetic instability in tumor populations will be a prerequisite for more effective targeting of the metastatic phenotype.

Acknowledgements

The authors acknowledge partial support for some of these studies from NIH grants to LAC (CA27755 and NS17139), from the Comprehensive Cancer Center of the Ireland Cancer Center at Case Western Reserve University (NCI-supported via P30-CA43703) for pilot studies on prostate carcinoma metastasis, and research grant DAMD17-98-1-8587 from the U.S. Army on prostate carcinoma metastasis (LAC). Athymic nude mouse experiments were conducted in the Athymic Animal Facility (AAALAC-I-approved) of the Case Western Reserve University/Ireland Cancer Center and approved by the Animal Care and Use Committee of this University. One of the authors (NK) was supported by the Animal Resource Center of Case Western Reserve University. The authors thank Drs. Thomas and Theresa Pretlow of the Department of Pathology for assistance with tumor and organ tissue sectioning and immunohistochemistry protocols, as well as pathology consultation. Special gratitude is extended to Dr. James Jacobberger of the Ireland Cancer Center for the donation of tissue culture-adapted CWR22R prostate carcinoma cells.

References

(1) Fidler, IJ and Ellis, LM. The implications of angiogenesis for the biology and therapy of cancer metastasis. Cell 1994, 79, 185-188.

(2) Fidler, IJ, Gersten, DM, and Hart, IR. The biology of cancer invasion and metastasis. Adv Cancer Res 1978, 28, 149-250.

(3) Heppner, GH and Miller, BE. Tumor heterogeneity: biological implications and therapeutic consequences. Cancer Metastasis Rev 1983, 2, 5-23.

(4) Nicolson, GL. Cancer progression and growth: relationship of paracrine and autocrine growth mechanisms to organ preference of metastasis. Exp Cell Res 1993, 204, 171-180.

(5) Nowell, PC. Mechanisms of tumor progression. Cancer Res 1986, 46, 2203-2207.

(6) Lin, W-c and Culp, LA. New insights into micrometastasis development using ultrasensitive marker genes. In Current Perspectives on Molecular and Cellular Oncology, Vol 1, Part B, Spandidos, D.A. (ed), 1992, pp. 261-309. JAI Press: London.

(7) Radinsky, R. Modulation of tumor cell gene expression and phenotype by the organ-specific metastatic environment. Cancer Metastasis Rev 1995, 14, 323-338.

(8) Singh, RK, Tsan, R, and Radinsky, R. Influence of the host microenvironment on the clonal selection of human colon carcinoma cells

during primary tumor growth and metastasis. Clin Exp Metastasis 1997, 15, 140-150.

(9) Fidler, IJ and Radinsky, R. Search for genes that suppress cancer metastasis. J Natl Cancer Inst 1996, 88, 1700-1703.

(10) Blood,CH and Zetter, B. Tumor interactions with the vasculature: angiogenesis and tumor metastasis. Biochim Biophs Acta 1990, 1032, 89-118.

(11) Folkman, J. Angiogenesis in cancer, vascular, rheumatoid and other disease. Nature Med 1995, 1, 27-31.

(12) Sanes, JR, Rubenstein, JLR, and Nicolas, J-F. Use of a recombinant retrovirus to study post-implantation cell lineages in mouse embryos. EMBOj 1986, 5, 3133-3142.

(13) LeDouarin, NM, Teillet, MA, and Catala, M. Neurulation in amniote vertebrates: a novel view deduced from the use of quail-chick chimeras. Int J Dev Biol 1998, 42, 909-916.

(14) Culp, LA, Radinsky, R and Lin, W-c. Extracellular matrix interactions with neoplastic cells: tumor- vs. cell type-specific mechanisms. In Pretlow, T.G. II and Pretlow, T.P., eds, Aspects of the Biochemistry and Molecular Biology of Tumors. Academic Press, Inc., Orlando, FL, 1991, pp. 99-149.

(15) Culp, LA and Barletta, E. Matrix adhesion of neuroblastoma and related neuronal derivative cells: cell type- verus tumor-specific mechanisms. Seminars Developmental Biology 1990, 1, 437-452.

(16) Culp, LA, Lin, W-c, Kleinman, NR, Campero, NM, Miller, CJ and Holleran, JL. Tumor progression, micrometastasis, and genetic instability tracked with

histochemical marker genes. Progress Histochem Cytochem 1998, 33, 329-350.

(17) Lin, W-c, Pretlow, TP, Pretlow, TG, and Culp, LA. Bacterial *lacZ* gene as a highly sensitive marker to detect micrometastasis formation during tumor progression. Cancer Res 1990, 50, 2808-2817.

(18) Lin, W-c, Pretlow, TP, Pretlow, TG, and Culp, LA. Development of micrometastases: earliest events detected with bacterial *lacZ* gene-tagged tumor cells. J Natl Cancer Inst 1990, 82, 1497-1503.

(19) Lin, W-c, Pretlow, TP, Pretlow, TG, and Culp, LA. High resolution analyses of two different classes of tumor cells *in situ* tagged with alternative histochemical marker genes. Am J Pathol 1992, 141, 1331-1342.

(20) Lin, W-c and Culp, LA. Selectable plasmid vectors with alternative and ultrasensitive histochemical marker genes. BioTechniques 1991, 11, 344-351.

(21) Lin, W-c, O'Connor, KL, and Culp, LA. Complementation of two related tumour cell classes during experimental metastasis tagged with different histochemical marker genes. Brit J Cancer 1993, 67, 910-921.

(22) Pretlow, TG, Pelley,RJ, and Pretlow, TP. Biochemistry of prostatic carcinoma. In Pretlow, T.G. II and Pretlow, T.P., eds, Biochemical and Molecular Aspects of Selected Cancers, Vol. 2, Academic Press, Inc., San Diego, CA, 1994, pp. 169-237.

(23) Lalani, E-N, Lanaido, ME, and Abel, PD. Molecular and cellular biology of prostate cancer. Cancer Met Rev 1997, 16, 29-66.

(24) Sramkoski, RM, Pretlow, TG, Giaconia, JM, Pretlow, TP, Schwartz, S, Sy, M-S, Marengo, SR, Zhang, D, and Jacobberger, J. A new human prostate carcinoma cell line, 22Rv1. In vitro 1999, in press.

(25) Lin, W-c and Culp, LA. Altered establishment/clearance mechanisms during experimental micrometastasis with live and/or disabled bacterial *lacZ*-tagged tumor cells. Invasion & Metastasis 1992, 12, 197-209.

(26) Kleinman, NR, Lewandowska, K and Culp, LA. Tumour progression of human neuroblastoma cells tagged with a *lacZ* marker gene: earliest events at ectopic injection sites. Br J Cancer 1994, 69, 670-679.

(27) Lesley, J, Hyman, R and Kincade, PW. CD44 and its interaction with extracellular matrix. Advances in Immunology 1993, 54, 271-335.

(28) Knudson, CB, and Knudson, W. Hyaluronan-binding proteins in development, tissue homeostasis, and disease. FASEB J 1993, 7, 1233-41.

(29) Tarin, D and Matsumura, Y. Deranged activity of the CD44 gene and other loci as biomarkers for progression to metastatic malignancy. J Cellular Biochem 1993, 17G, 173-85.

(30) Matsumura,Y, and Tarin, D. Significance of CD44 gene products for cancer diagnosis and disease evaluation. Lancet 1992, 340, 1053-8.

(31) Heider, K-H, Hofmann, M, Hors, E, van den Berg, F, Ponta, H, Herrlich, P and Pals, S. A human homologue of the rat metastasis-associated variant of CD44 is expressed in colorectal carcinomas and adenomatous polyps. J Cell Biol 1993, 120, 227-33.

(32) Iida,N and Bourguignon, LYW. New CD44 splice variants associated with human breast cancers. J Cellular Physiol 1995, 162, 127-33.

(33) Heider, K-H, Dammrich, J, Skroch-Angel, P, Muller-Hermelink, H-K, Vollmers, HP, Herrlich, P, and Ponta, H. Differential expression of CD44 splice variants in intestinal- and diffuse-type human gastric carcinomas and normal gastric mucosa. Cancer Res 1993, 53, 4197-4203.

(34) Hofmann, M, Rudy, W, Gunthert, U, Zimmer, SG, Zawadzki, V, Zoller, M, Lichtner, RB, Herrlich, P, and Ponta, H. A link between *ras* and metastatic behavior of tumor cells: *ras* induces CD44 promoter activity and leads to low-level expression of metastasis-specific variants of CD44 in CREF cells. Cancer Res 1993, 53, 1516-21.

(35) Jamal, HH, Cano-Gauci, DF, Buick, RN, and Filmus, J. Activated *ras* and *src* induce CD44 overexpression in rat intestinal epithelial cells. Oncogene 1994, 9, 417-23.

(36) Wielenga, VJM, Heider, K-H, Offerhaus, GJA, Adoft, GR, van den Berg, FM, Ponta, H, Herrlich, P, and Pals, ST. Expression of CD44 variant proteins in human colorectal cancer is related to tumor progression. Cancer Res 1993, 53, 4754-56.

(37) Li, H, Hamou, M-F, de Tribolet, N, Jaufeerally, R, Hofmann, M, Diserens, AC, and van Meir, EG. Variant CD44 adhesion molecules are expressed in human brain metastases but not in glioblastomas. Cancer Res 1993, 53, 5345-9.

(38) Gunthert, U, Hofmann, M, Rudy, W, Reber, S, Zoller, M, Haussmann, I, Matzku, S, Wenzel, A, Ponta, H, and Herrlich, P. A new variant glycoprotein CD44 confers metastatic potential to rat carcinoma cells. Cell 1991, 65, 13-24.

(39) Sy, M-S, Guo, YJ, and Stamenkovic,I. Distinct effects of two CD44 isoforms on tumor growth *in vivo*. J Exp Med 1991, 174, 859-66.

(40) DeGrendele, HC, Estess, P, Picker, LJ, and Siegelman, MH. CD44 and its ligand hyaluronate mediate rolling under physiologic flow: a novel lymphocyte-endothelial cell primary adhesion pathway. J Exp Med 1996, 183, 1119-30.

(41) DeGrendele, HC, Estess, P, and Siegelman, MH. Requirement for CD44 in activated T cell extravasation into an inflammatory site. Science 1997, 278, 672-5.

(42) Kogerman, P, Sy, M-S, and Culp, LA. Oncogene-dependent expression of CD44 in Balb/c 3T3 derivatives: correlation with metastatic competence. Clin Exp Metastasis 1996, 14, 73-82.

(43) Kogerman, P, Sy, M-S, and Culp, LA. Counter-selection for over-expressed human CD44s in primary tumors versus lung metastases in a mouse fibrosarcoma model. Oncogene 1997, 15, 1407-16.

(44) Kogerman, P, Sy, M-S, and Culp, LA. Over-expression of human CD44s in murine 3T3 cells: selection against during primary tumorigenesis and selection for during micrometastasis. Clin Exp Metastasis 1998, 16, 83-93.

(45) Kogerman, P, Sy, M-S, and Culp, LA. Overexpressed human CD44s promotes lung colonization during micrometastasis of murine fibrosarcoma

cells: facilitated retention in the lung vasculature. Proc Natl Acad Sci USA 1997, 94, 13233-8.

(46) Culp, LA and Kogerman, P. Plasticity of CD44s expression during progression and metastasis of fibrosarcoma in an animal model system. Frontiers in Bioscience 1998, 3, d672-683.

(47) Lengauer, C, Kinzler, KW, and Vogelstein, B. DNA methylation and genetic instability in colorectal cancer cells. Proc Natl Acad Sci USA 1997, 94, 2545-50.

(48) Smith, SS. Stalling of DNA methyltransferase in chromosome stability and chromosome remodelling. Int. J. Molecular Medicine 1998, 1, 147-56.

(49) Brodeur, GM, Seeger, RC, Barrett, A, et al. International criteria for diagnosis, staging, and response to treatment in patients with neuroblastoma. J Clin Oncol 1988, 6, 1874-1881.

(50) Thiele, CJ. Biology of pediatric peripheral neuroectodermal tumors. Cancer Met Rev 1991, 10, 311-319.

(51) Marcu, KB, Bossone, SA, and Patel, AJ. *myc* function and regulation. Ann Rev Biochem 1992, 61, 809-860.

(52) van't Veer, LJ, Beijersbergen, RL, and Bernards, R. N-*myc* suppresses major histocompatability complex class I gene expression through down-regulation of the p50 subunit of NF-kB. EMBOj 1993, 12, 195-200.

(53) Bernards, R. N-*myc* disrupts protein kinase C-mediated signal transduction in neuroblastoma. EMBOj 1991, 10, 1119-1125.

(54) Akeson, R and Bernards, R. N-*myc* downregulates neural cell adhesion molecule expression in rat neuroblastoma. Molec Cell Biol 1990, 10, 2012-2016.

(55) Albelda, SM. Role of integrins and other cell adhesion molecules in tumor progression and metastasis. Lab Inves 1993, 68, 4-17.

(56) Flickinger, KS, Judware, R, Lechner, R, Carter, WG, and Culp, LA. Integrin expression in human neuroblastoma cells with or without N-*myc* amplification and in ectopic/orthotopic nude mouse tumors. Exp Cell Res 1994, 213, 156-163.

(57) Judware, R, Lechner, R, and Culp, LA. Inverse expressions of the N-*myc* oncogene and β1 integrin in human neuroblastoma: relationships to disease progression in a nude mouse model system. Clin Exp Metastasis 1995, 13, 123-133.

(58) Brooks, PC, Clark, RAF, and Cheresh, DA. Requirement of vascular integrin αvβ3 for angiogenesis. Science 264, 569-571 (1994).

(59) Judware, R and Culp, LA. Over-expression of transfected N-*myc* oncogene in human SKNSH neuroblastoma cells down-regulates expression of β1 integrin subunit. Oncogene 1995, 11, 2599-2607.

(60) Judware, R and Culp, LA. Concomitant down-regulation of expression of integrin subunits by N-*myc* in human neuroblastoma cells: differential regulation of α2, α3, and β1. Oncogene 1997, 14, 1341-1350.

(61) Judware, R and Culp, LA. Persistent a1 integrin subunit expression in human neuroblastoma cell lines which overexpress N-myc and downregulate other integrin subunits. Oncology Rep 1997, 4, 433-437.

(62) Judware, R and Culp, LA. N-*myc* over-expression downregulates $\alpha 3\beta 1$ integrin expression in human Saos-2 osteosarcoma cells. Clin Exp Metastasis 1997, 15, 228-238.

(63) Boudreau, N and Bissell, MJ. Extracellular matrix signaling: integration of form and function in normal and malignant cells. Curr Opin Cell Biol 1998, 10, 640-646.

(64) Emmert-Buck, MR, Bonner, RF, Smith, PD, Chuaqui, RF, Zhuang, Z, Goldstein, SR, Weiss, RA and Liotta, LA. Laser capture microdissection. Science 1996, 274, 998-1001.

(65) Schutze, K and Lahr, G. Identification of expressed genes by laser-mediated manipulation of single cells. Nature Biotechnology 1998, 16, 737-742.

(66) Simone, NL, Bonner, RF, Gillespie, JW, Emmert-Buck, MR, and Liotta, LA. Laser-capture microdissection: opening the microscopic frontier to molecular analysis. Trends in Genetics 1998, 14, 272-276.

(67) Humphries, MJ, Yamada, KM, and Olden, K. Investigation of the biological effects of anti-cell adhesive synthetic peptides that inhibit experimental metastasis of B16-F10 murine melanoma cells. J Clin Invest 1988, 81, 782-790.

(68) Saiki, I, Iida, J, Murata, J, Ogawa, R, Nishi, N, Sugimura, K, Tokura, S, and Azuma, I. Inhibition of the metastasis of murine malignant melanoma by synthetic polymeric peptides containing core sequences of cell-adhesive molecules. Cancer Res 1989, 49, 3815-3822.

(69) Frixen, UH, Behrens, J, Sachs, M, Eberle, G, Voss, B, Warda, A, Lochner, D, and Birchmeier, W. E-cadherin-mediated cell-cell adhesion prevents invasiveness of human carcinoma cells. J Cell Biol 1991, 113, 173-185.

(70) Vleminckx, K, Vakaet, J, Mareel, M, Fiers, W, and van Roy, F. Genetic manipulation of e-cadherin expression by epithelial tumor cells reveals an invasion suppressor role. Cell 1991, 66, 107-119.

Table I Quantitation of pulmonary micrometastases/nodules[a]

	APSI injected singly			*APSI Co-injected with LZEJ*				
Time of sacrifice	*Micro-metastases*[b]	*Staining nodules*[c]	*Non-staining nodules*[c]	*Double staining foci*[d]	*LZEJ nodules*[c]	*APSI nodules*[c]	*Non-staining nodules*[c]	*Double staining nodules*[c]
1 h	2,500-3,000 (100)	0	0	500 (100)	0	0	0	0
6 h	700 (28-23)	0	0	122 (24)	0	0	0	0
24 h	104 (4.2-3.5)	0	0	24 (5)	0	0	0	0
3 weeks	38 (1.5-1.3)	10	0	3 (0.6)	26	20	7	3
5 weeks	37 (1.5-1.2)	54	17	ND[e]	ND[e]	ND[e]	ND[e]	ND[e]
7 weeks	8 (0.3)	10	5	ND[e]	ND[e]	ND[e]	ND[e]	ND[e]

[a]Mice (24 for two separate experiments) were given i.v. injections of $1x10^5$ APSI cells alone or as a mixture with $1x10^5$ LZEJ cells as indicated. At various times post-injection, mice were sacrificed; whole lungs removed, rinsed with PBS and stained with X-phosphate (or sequentially with X-gal and then with X-phosphate/NBT in the case of co-injections of LZEJ and APSI cells). These values for $1x10^5$ LZEJ cells injected alone have been published previously (18). [b]Values = Number of micrometastases determined with the use of a dissecting microscope. Values in parentheses represent the number of foci remaining in the lung as a per cent of the 1 h value. [c]Denotes nodules of considerable size (>100 cells). Nodules which were heterogeneous in their staining of the histochemical marker genes are referred to as non-staining nodules. [d]These are the number of micrometastases containing both LZEJ and APSI cells in co-localized foci. Values in parentheses represent the number of foci remaining in the lung as a per cent of the 1 h value. The maximal number of foci of all cell classes (LZEJ-only plus APSI-only plus co-localized foci) observed at any time point was 6-7,000. [e]Not determined. [Taken from Lin *et al.* (21) with permission]

Figure Legends

Fig. 1. Tumor cell adherence and extravasation in a lung blood vessel. *Ras*-transformed, *lacZ*-tagged 3T3 cells (17,18) were injected into tail veins of athymic nude mice. Thirty minutes post-injection, an animal was sacrificed and the lung was excised, fixed, and embedded in methyacrylate for cutting into 4 μm thin sections after X-gal staining (6). X-gal-staining tumor cells can be observed after escape from blood vessels in the lung tissue (e.g., small arrow). Blood vessels are detectable as red staining (staining red at broad arrow) with alkaline phosphatase reagent while tumor cells are detectable as small clusters of blue staining within the blood vessel (open arrow). X400.

Fig. 2. Two genetically-different classes of tumor cells establish multiple classes of micrometastases and overt metastases in lung. *Ras*-transformed, *lacZ*-tagged 3T3 cells (LZEJ) were mixed with *sis*-transformed, PAP-tagged 3T3 cells (APSI) after detachment from their respective tissue culture dishes. The equal-number mixture was injected into the tail veins of nude mice and at the specified times animals were sacrificed. Lungs were excised, fixed, and in some cases stained as whole organs or in other cases embedded in methyacrylate and sectioned after dual staining--first for β-galactosidase (red staining using Red-gal) and then for placental alkaline phosphatase activity (blue staining using X-phosphate substrate). Homogeneous micrometastases of LZEJ cells are denoted with small arrows; homogeneous micrometastases of APSI with arrowheads; and micrometastases containing both cell types with broad-open arrow. **[A]** 1 hour after tail vein co-injection. This is a section of

lung in which all three classes of micrometastases could be readily identified, with a sizable fraction containing both cell types. These are quantitated in Table 1. **[B]** 5 hours after co-injection; whole-organ staining. Note that all three classes of micrometastases persist, as detected with whole-organ staining. **[C]** 3 weeks after co-injection; whole-organ staining. Some micrometastases persisted at this late time point (LZEJ cells at small arrow) while others were growing into overt metastases(APSI cells at large arrowhead). **[D]** 3 weeks after co-injection; whole-organ staining. An overt metastasis is shown with both cell types (large-open arrow), demonstrating that these two genetically-related cell types can contribute to the same overt metastasis. LZEJ micrometastases are also evident (small arrow). All magnifications, X220.

Fig. 3. Selection for or against overexpressed hCD44s in tumors from two different transfectants. *Sis*-transformed 3T3 cells were transfected with a cDNA form of hCD44s, regulated by an LTR promoter, on a eucaryotic expression plasmid. Several stable transfectants, expressing high levels of hCD44s were isolated, two of which are analyzed here. Transfectants HUSI-hCD44.5 or HUSI-hCD44.6 were then injected into the subcutis of nude mice. After two weeks, animals were sacrificed and the primary tumor cells grown out in culture, along with lung micrometastatic tumor cells selected in culture based on their drug resistance. These culture populations were then analyzed by FACS for expression of mouse CD44s (using monoclonal antibody KM81) or human CD44s (using monoclonal antibodies GKWA3 or 7.10). **[A]** Subcutaneous tumor after injection of transfectant 5 cells. There has been loss

of expression of hCD44s while mCD44s continues to be expressed at the expected levels. **[B]** Lung micrometastatic cells from the same animal as in [A]. These cells retain high-level expression of hCD44s. **[C]** Subcutaneous tumor after injection of transfectant 6 cells. Again, hCD44s but not mCD44s has been lost from the surface of these cells. **[D]** Lung micrometastatic cells from the animal in [C]. High levels of hCD44s persist in these cells. [Taken from Kogerman et al (43) with permission]

Fig. 4. hCD44s promotes the earliest stages of micrometastasis establishment in the lung. Untransfected or hCD44s-transfectant clone 5 or 6 cells were injected into tail vein blood vessels (experimental metastasis assay with three mice per datum point). At the indicated times, mice were sacrificed, their lungs dispersed into culture, and tumor cell colonies were quantitated in a colony growth assay based on their resistance to hygromycin B killing. Colonies were visualized with Coomassie blue staining **[A]** and enumerated **[B]**. *, $P<0.05$; **, $P<0.005$. [Taken from Kogerman et al (45) with permission]

Fig. 5. Quantitation of relationships between increased hygromycin B selection with N-myc and β1 integrin subunit levels. **[A]** SKMYC2 transfectant cells (59) were grown in the indicated concentrations of hygromycin B and the resultant attached (A) or loosely-adherent (L) populations isolated. N-myc and β1 integrin proteins were quantitated by fluorography and scanning densitiometry. The inset is a log:log plot of the same data showing inverse relationships between the levels of the two proteins. **[B]** Five independent

experiments were quantitated as described in **[A].** [Taken from ref. 59 with permission]

Fig. 6. RNase protection assay for levels of various mRNAs in several neuroblastoma cell lines. SK-N-SH, IMR-32, transfectant SKMYC2, and antisense transfectant SKMYCAS (60) cells were grown in culture and total cellular RNAs prepared. Five micrograms of RNA from each sample were analyzed by RNase protection. In **[A],** probe sequences analyzed levels of α2, α3, and β1 integrins, as well as β-actin as a control. In **[B],** probes included those for max, N-*myc*, and β-actin genes. Migration positions of protected fragments are shown on the right of the panels and their sizes (nucleotides) are shown on the left of these autoradiograms. **[C]** and **[D]** display quantitation of these autoradiograms from several experiments by scanning densitometry. 18s rRNA is included as an internal control for RNA levels. [Taken from ref. 60 with permission]

Fig. 7. Model for regulation of integrin expression by N-*myc* amplification in neuroblastoma tumors. The various levels of regulation of three different integrin subunit genes--α2, α3, and β1--are shown, as well as their decreased amounts when high levels of N-myc protein are observed in both naturally-occurring tumors with N-*myc* amplification, as well as in transfectant populations where N-myc protein is elevated artificially (59, 60). Transcription of integrin subunit genes produces mRNA which is translated into immature proteins. Immature α's and β1 then associate, mature, and translocate to the cell surface.

While β1 mRNA levels are reduced approximately twofold in high-N-myc cells, α2 is reduced to less than 20% and α3 to less than 6% of levels observed in the absence of N-myc protein. While very little (ND) α2 or α3 protein are detectable in these cells, the reduced amount of β1 protein produced is incapable of maturation and appearance at the cell surface, undoubtedly because of its inability to partner with an α subunit. Therefore, only approx. 10% of β1 produced actually shows up at the cell surface, partnered with small amounts of α1 subunit produced in these cells and whose production is unaffected by N-myc protein (61). [Taken from ref. 60 by permission]

FIGURE 1

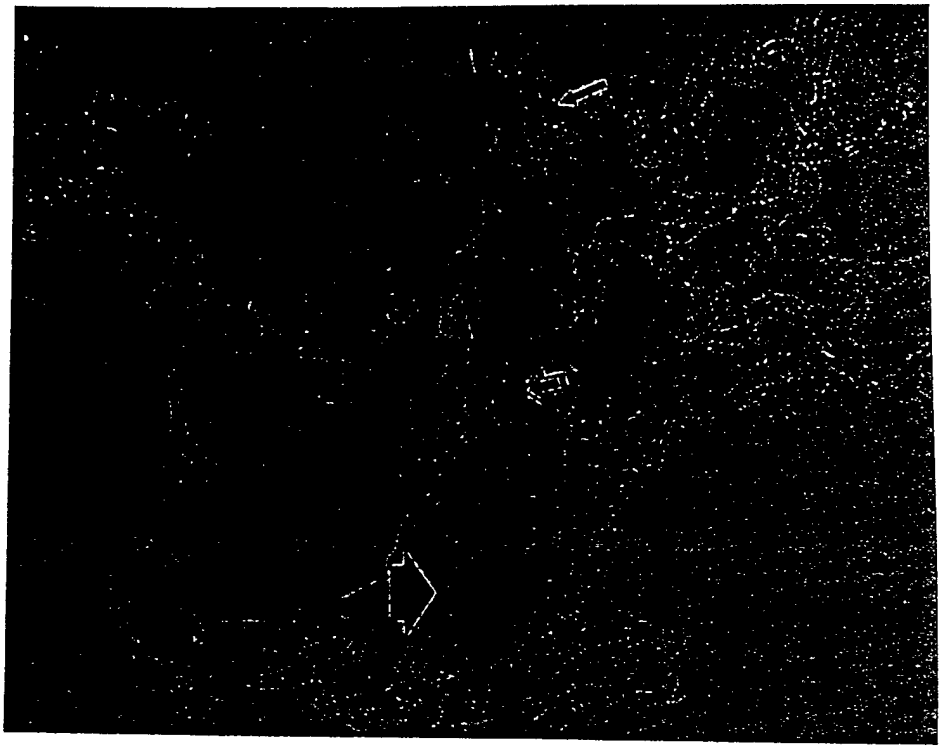

FIGURE 2

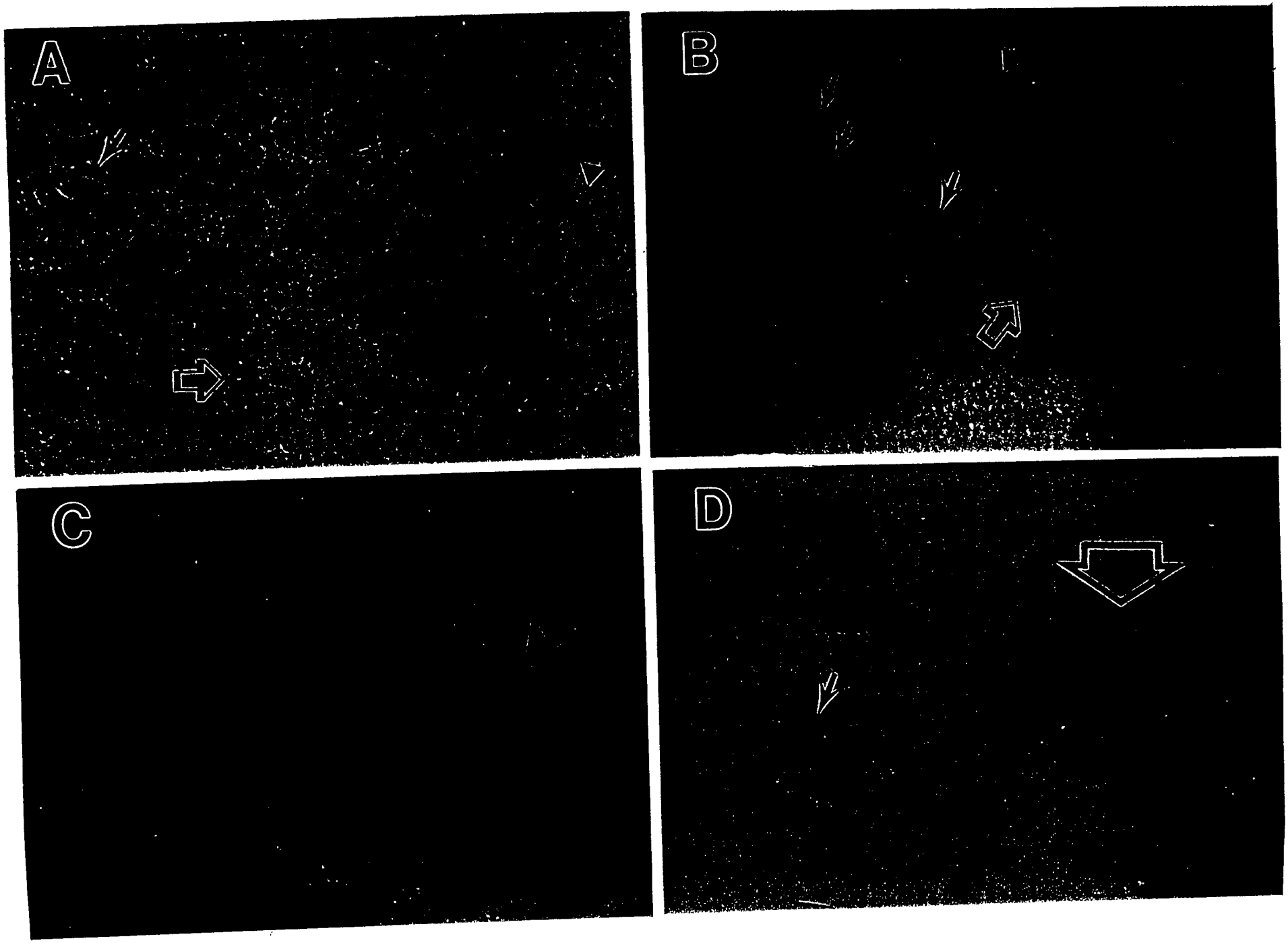

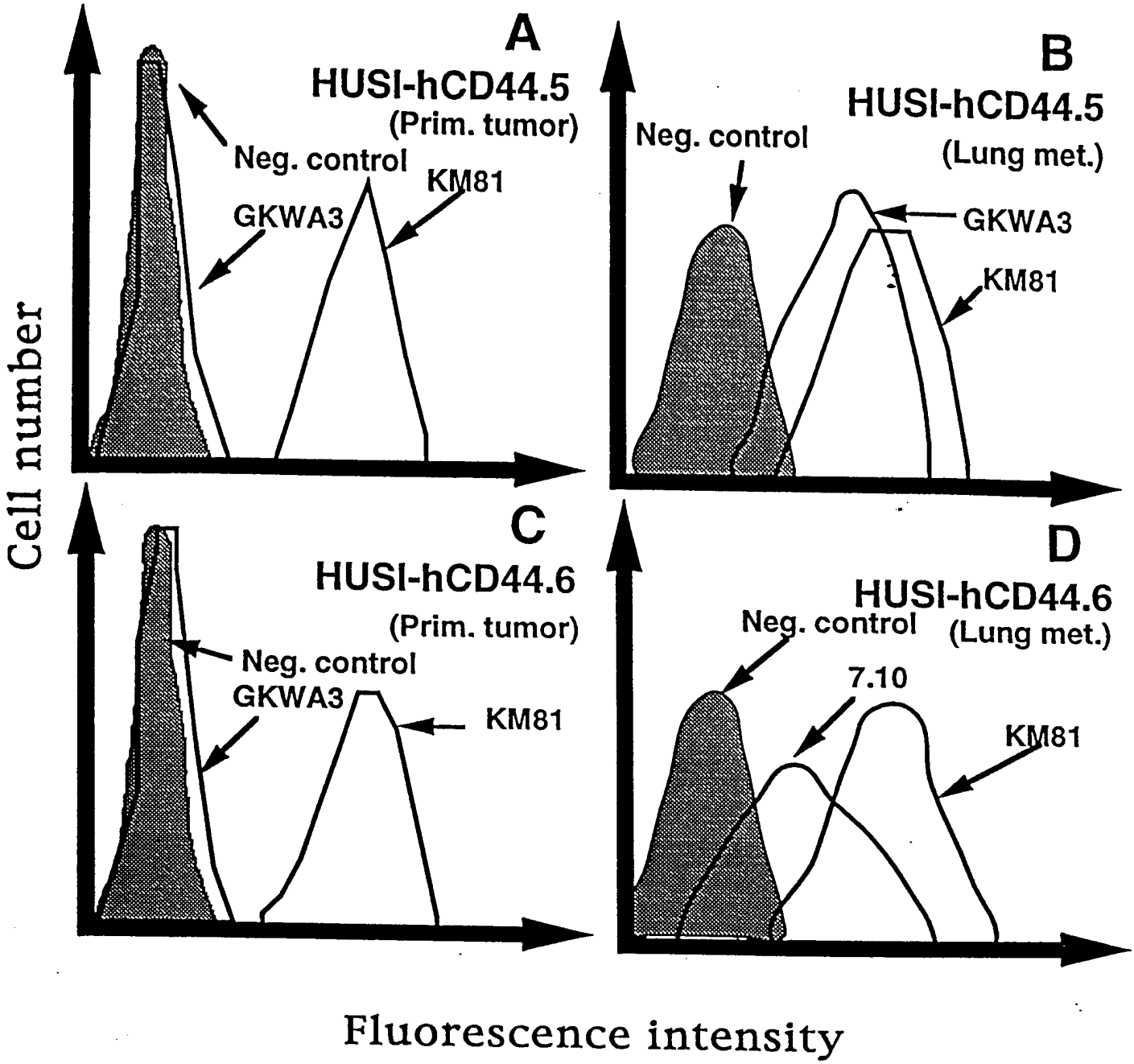
A
HUSI-hCD44.5
(Prim. tumor)
Neg. control
KM81
GKWA3
B
HUSI-hCD44.5
(Lung met.)
Neg. control
GKWA3
KM81
C
HUSI-hCD44.6
(Prim. tumor)
Neg. control
GKWA3
KM81
D
HUSI-hCD44.6
(Lung met.)
Neg. control
7.10
KM81
Cell number
Fluorescence intensity

FIGURE 3

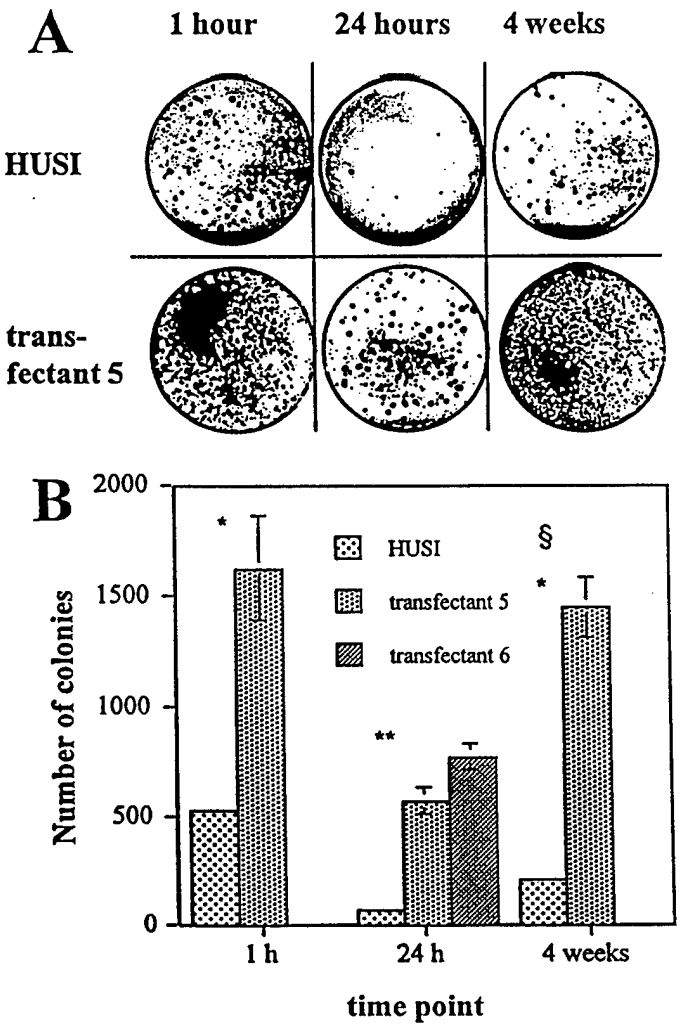
A
1 hour
24 hours
4 weeks
HUSI
trans-
fectant 5
B
2000
1500
1000
500
0
Number of colonies
HUSI
transfectant 5
transfectant 6
*
**
§
*
1 h
24 h
4 weeks
time point

FIGURE 4

FIGURE 5

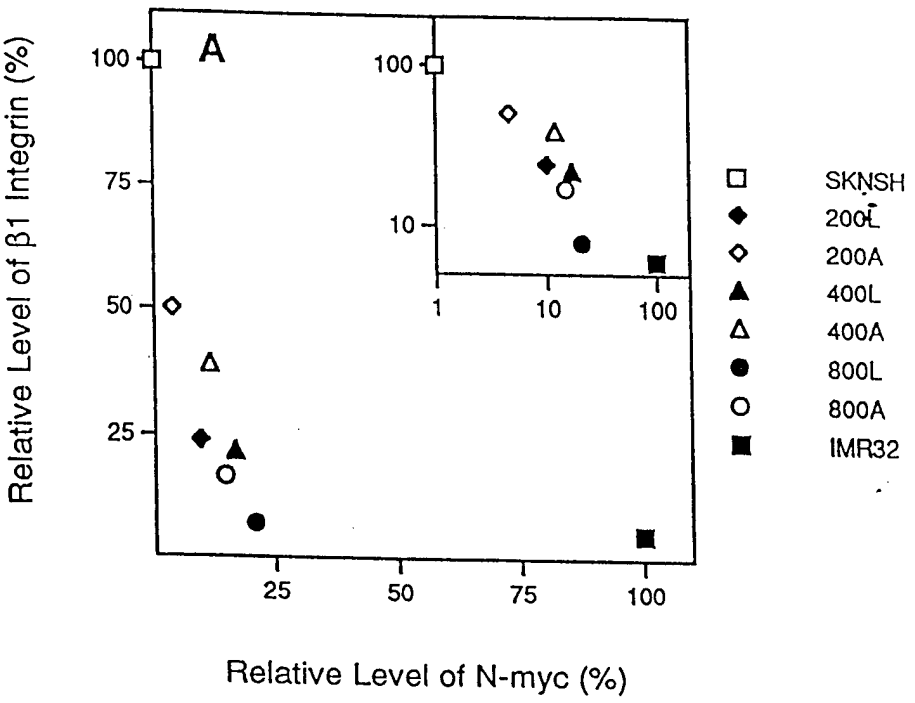
A
Relative Level of β1 Integrin (%)
Relative Level of N-myc (%)
100
75
50
25
10
1
SKNSH
200L
200A
400L
400A
800L
800A
IMR32

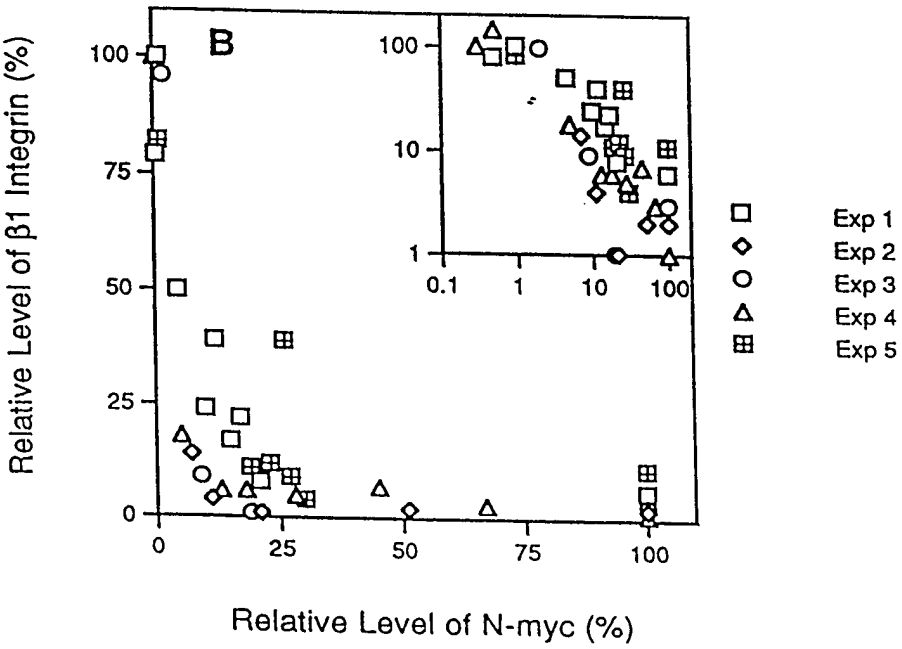
B
Relative Level of β1 Integrin (%)
Relative Level of N-myc (%)
100
75
50
25
0
10
1
0.1
Exp 1
Exp 2
Exp 3
Exp 4
Exp 5

FIGURE 6 A and B TOP

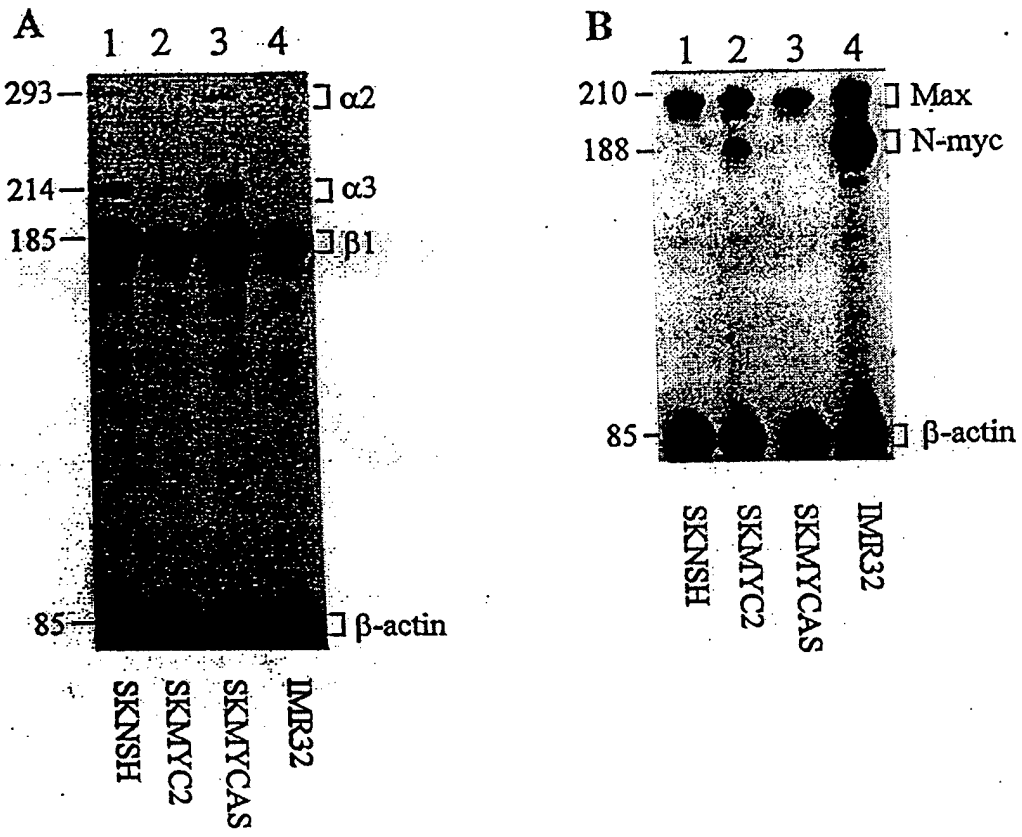

FIGURE 6 C and D TOP

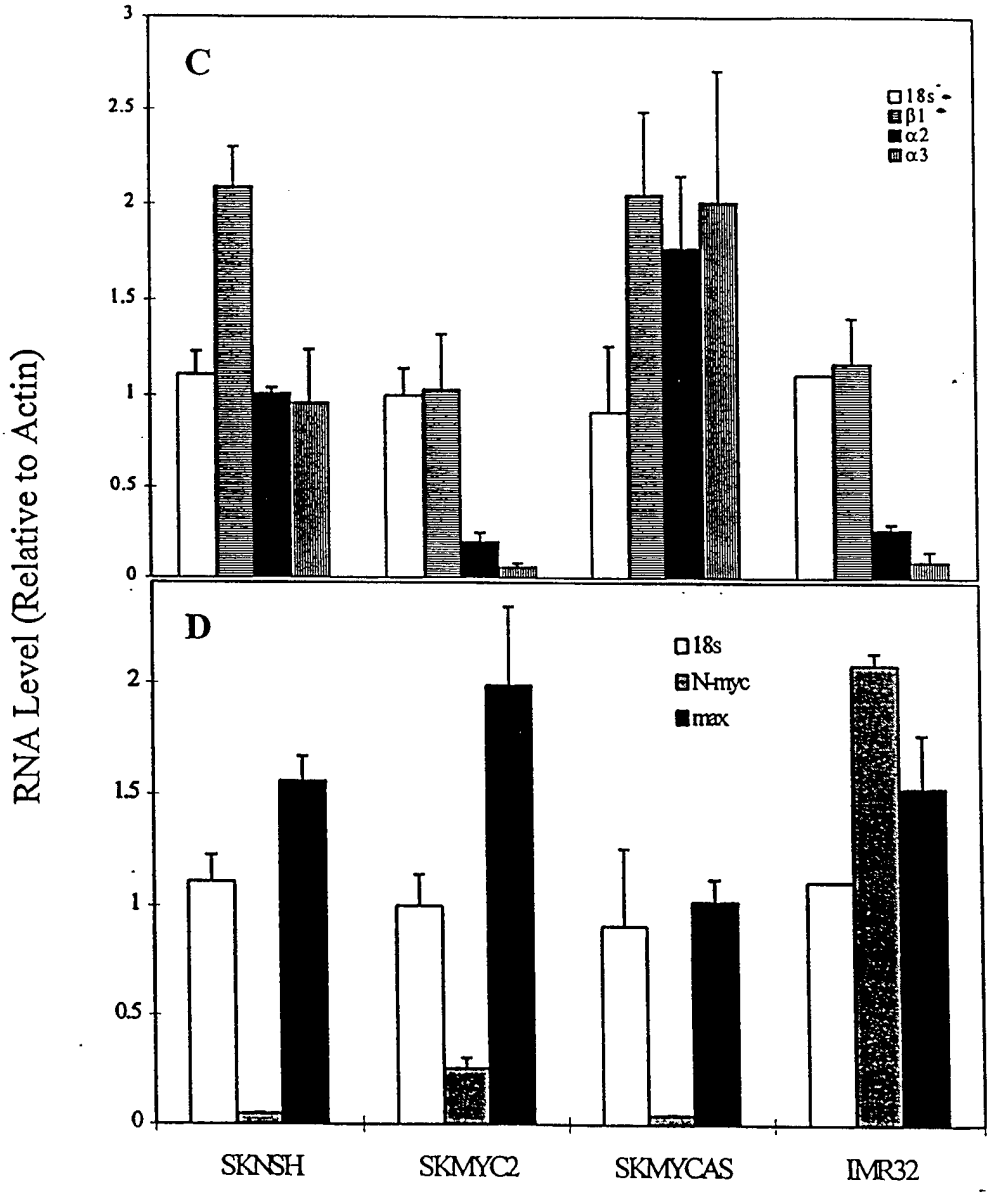

FIGURE 7 Top

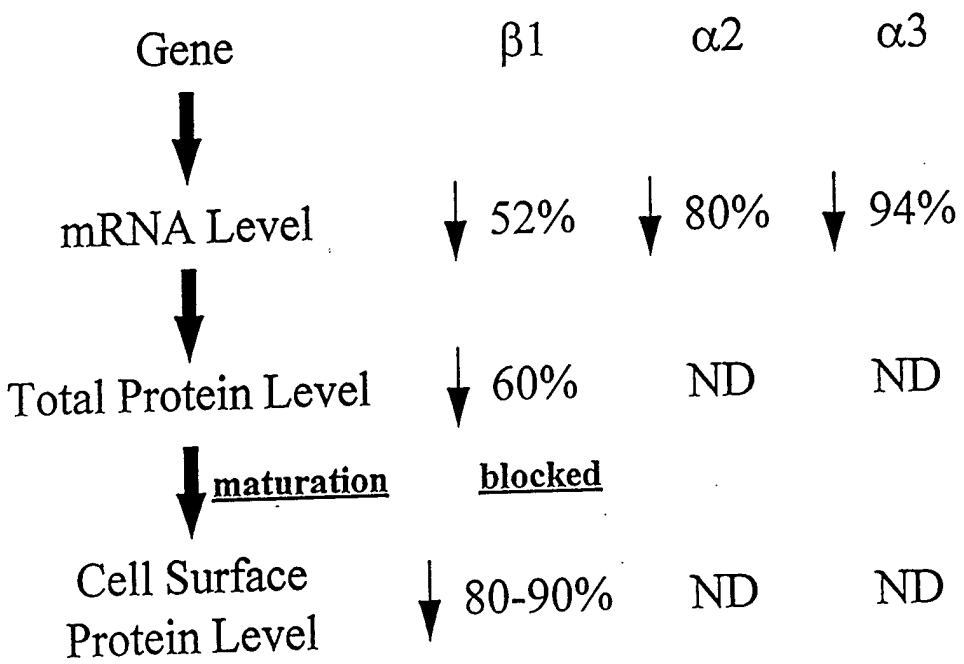
Gene
β1
α2
α3
mRNA Level
52%
80%
94%
Total Protein Level
60%
ND
ND
maturation
blocked
Cell Surface Protein Level
80-90%
ND
ND

Volume 48(5): 643–651, 2000
The Journal of Histochemistry & Cytochemistry
http://www.jhc.org

ARTICLE

Tracking Micrometastasis to Multiple Organs with *lacZ*-tagged CWR22R Prostate Carcinoma Cells

Julianne L. Holleran, Carson J. Miller, and Lloyd A. Culp

Department of Molecular Biology and Microbiology, Case Western Reserve University, School of Medicine, Cleveland, Ohio

SUMMARY Metastasis to organs other than lung is rarely observed in animal model systems of human prostate carcinoma (PCA), with the exception of already metastatic isolates of human PCA cultured for long periods of time. To analyze more directly the evolution of metastatic variants from primary PCA tumor isolates, the *lacZ* histochemical marker gene was transfected into the CWR22Rv1 cell line isolated from the CWR22R xenograft (primary tumor). Three clones of varying *lacZ*-expression stability were analyzed for tumorigenicity and progression in athymic nude mice. Clones B and D were highly tumorigenic in the subcutis; however, *lacZ* expression was highly unstable. In contrast, clone H demonstrated highly stable *lacZ* expression for >25 passages in culture or in animals. Clone H, injected sc in a PBS vehicle, gave a 15–40% tumorigenic take. All primary tumor-bearing animals exhibited micrometastases in lung and other organs. Clone H injected in a Matrigel vehicle gave 100% tumorigenicity, with all animals displaying micrometastases in lung, liver, and/or bone (lower frequency in brain and kidney). Overall, the relative frequency of micrometastasis to multiple organs was lung>liver=bone>>brain>kidney. Overt metastases were never observed in the lung or bone but were occasionally found in liver. *lacZ*-transfected clone H CWR22Rv1 cells represent a much more accurate model of metastasis of PCA to the organs normally involved in progression of the human disease. Use of marker gene-tagged cells and other high-resolution molecular techniques will now permit analyses of the earliest events in PCA progression and micrometastasis. **(J Histochem Cytochem 48:643–651, 2000)**

KEY WORDS
histochemical marker gene
prostate carcinoma
micrometastasis
target organs

STUDIES OF HUMAN PROSTATE CARCINOMA (PCA) in animal model systems have been hampered by the paucity of human PCA cells available in tissue culture (Pretlow et al. 1994; Lalani et al. 1997). Most studies of progression and metastasis have relied on already metastatic human PCA isolates from various target organs that have been cultured for long periods of time, e.g., DU145, PC3, and LNCaP (Pretlow et al. 1994; Zhau et al. 1996; Lalani et al. 1997; Rubio et al. 1998; Yang et al. 1999). Human PCA primary tumors, isolated from patients and carried in athymic nude or SCID mice as xenografts (Pretlow et al. 1994; van Weerden et al. 1996), offer the opportunity to isolate PCA primary tumor cell lines that would be valuable for analyzing progression of this disease. More effective molecular and cellular analyses of progression mechanisms require isolates of such primary tumors of human PCA (Pretlow et al. 1994).

The xenograft approach for isolating human PCA tissue and its passage in nude mice offers an intermediate stage in the development of new cell systems (van Steenbrugge et al. 1994; van Weerden et al. 1996). The Pretlows and their colleagues have made significant advances in isolation and characterization of many independent isolates of PCA primary tumors from patients. These are maintained as xenografts in athymic nude mice (Pretlow et al. 1993; Wainstein et al. 1994; Cheng et al. 1996). This includes the CWR22 xenograft that was not metastatic in nude mice (Wainstein et al. 1994). They reported subsequent isolation of a "relapsed" variant of this xenograft (CWR22R), which was androgen-independent and metastatic to lungs of nude mice (Nagabhushan et al. 1996). A subline of the CWR22R xenograft (Pretlow xenograft

Correspondence to: Lloyd A. Culp, Dept. of Molecular Biology and Microbiology, Case Western Reserve U., School of Medicine, Cleveland, OH 44106.

Received for publication September 29, 1999; accepted January 9, 2000 (9A5088).

0022-1554/00/$3.30

#2152; Nagabhushan et al. 1996) was used by Jacobberger and colleagues to isolate and characterize a tissue-cultured cell line, CWR22Rv1 (Sramkoski et al. 1999). These cells display a karyotype similar to that of the original CWR22 xenograft (approximately 50 chromosomes), secrete prostate-specific antigen (PSA), display a specific point mutation in one exon of the androgen receptor gene (Tan et al. 1997), and generate primary tumors in the subcutis of nude mice pathologically characteristic of prostate carcinomas (Sramkoski et al. 1999).

CWR22Rv1 cells therefore offer an excellent opportunity to test possible metastatic spread to multiple organs from a cell population originally isolated from a human primary tumor and not from already metastatic subpopulations. If metastasis is observed with these cells to organs that are normally involved in the human disease, then we have a more relevant model system for evaluating mechanisms for PCA progression and metastasis.

Our laboratory has maximized sensitivity of progression and metastasis studies in animal models of tumor systems by transfecting a histochemical marker gene (e.g., bacterial *lacZ* or human placental alkaline phosphatase gene) into tumor cells, isolating relatively stable-expressing *lacZ* or PAP transfectants and testing for micrometastases in many target organs of athymic nude mice using ultrasensitive histochemical staining (Lin et al. 1990a,b; Kleinman et al. 1994). Use of histochemical markers permits ready visualization of both tagged tumor cells and neighboring host organ cells in the same field of vision. This is not possible with the use of fluorescent tags for tumor cells, such as luciferase or green-fluorescent protein (Rubio et al. 1998; Yang et al. 1999). These approaches with histochemical marker genes have been previously reviewed by us (Lin and Culp 1992; Culp et al. 1998a,b) and others (Kruger et al. 1999). They demonstrate our ability to detect single tumor cells in the vasculature and in target organs leading to micrometastases (Lin and Culp 1992; Lin et al. 1992; Culp et al. 1998a,b). They also enable us to evaluate relationships between neighboring tumor cells and host connective tissue cells at the highest resolution (Chang and Chung 1989; Culp et al. 1998a,b).

In the analyses reported here, the *lacZ* gene was transfected into cultured CWR22Rv1 cells, three clones were isolated, and the tumorigenic progression and metastasis of these clones were evaluated. These analyses identify one transfectant clone, referred to as LZ-CWR22R-H, that closely mimics metastatic progression normally observed in the human disease to lung, liver, and bone with a reasonable frequency. They also demonstrate remarkable stability of micrometastases in the lung and bone, as well as overt metastasis in the livers of this experimental animal system.

Materials and Methods

Isolation of *lacZ*-transfected CWR22R Cells

Early-passage CWR22Rv1 cells (Sramkoski et al. 1999), free of *Mycoplasma*, were obtained from Dr. James Jacobberger of this institution. This cell line (Sramkoski et al. 1999) was generated on an irradiated bed of STO mouse fibroblasts from the #2152 xenograft subline of CWR22R carried in nude mice by Dr. Thomas Pretlow and colleagues (Nagabhushan et al. 1996). Cells were grown in RPMI 1640 medium supplemented with 10% FCS and with penicillin and streptomycin. The bacterial *lacZ* gene, under regulation of the Rous sarcoma virus LTR on a bacterial plasmid carrying the neo^R gene used for G418 selection (400 μg/ml), was transfected into CWR22R cells. Three clones (B, D, and H) were isolated as described previously (Lin et al. 1990a,b; Kleinman et al. 1994). These will be referred to as LZ-CWR22R-B, -D, or -H cells, respectively. The stability of *lacZ* expression during long-term culturing of these three clones, with or without selection drug, has been described previously (Culp et al. 1998a). Briefly, Clone D is highly unstable in the absence of selection drug, with most cells losing X-gal stainability within 7–10 passages; Clone B displays intermediate stability; and Clone H is highly stable for *lacZ* expression for >25 passages, even in the absence of selection drug.

Tumorigenicity Studies

Athymic nude mice (HSD nu/nu) were bred and housed in the Athymic Animal Facility of the CWRU/Ireland Cancer Center under AAALAC-I approval. All procedures were executed under supervision of the Animal Care and Use Committee of Case Western Reserve University. Nude mice (4–6-week-old males) received two sets of India ink tattoos on each side of their hind flanks, between which cells were injected into the subcutis (Kleinman et al. 1994). The indicated number of *lacZ*-transfected CWR22R cells, dispersed from cultures by trypsinization, were then injected SC and animals monitored daily for evolution of primary tumors. In some cases, cells (0.1 ml) were injected in a PBS vehicle, and in other cases they were injected in a Matrigel suspension (Pretlow et al. 1991). In all cases, the cultured population of Clone H cells stained with X-gal to >90% of the cells, indicating the excellent stability of expression of the *lacZ* gene in this particular clone.

Tissue Isolation and Histochemical Staining

Primary tumors were isolated from sacrificed animals when they were generally >4 mm in their shortest dimension and <10 mm in their longest. In most cases, the entire primary tumor and the surrounding normal mouse tissues were isolated as a unit for X-gal staining. In select cases, the primary tumor was isolated, bisected with a scalpel, and then the halves fixed and X-gal-stained. Lungs and other organs were isolated intact from sacrificed animals as described previously (Lin et al. 1990a,b; Kleinman et al. 1994). Fixation was performed at 4C for 1 hr with 2% (v/v) formaldehyde in PBS.

X-gal staining was executed on fixed tissues as described previously at pH 7.4 (overnight at room temperature) to minimize background tissue staining (Lin et al. 1990a,b; Lin

and Culp 1992; Kleinman et al. 1994; Culp et al. 1998b). X-gal staining was also performed on tissues from animals not injected with tumor cells to evaluate possible background staining of tissues. This was particularly important in bone, in which some background staining is observed in the growth regions at the ends of long bones of the animal. X-gal-stained primary tumors, overt metastases, and micrometastases were photographed on a Nikon SMZU Dissecting Microscope with Kodak 160T film.

Materials

Matrigel was obtained from Collaborative Research (Bedford, MA), X-gal from Research Organics (Cleveland, OH), G418 and RPMI 1640 medium from Gibco (Grand Island, NY), potassium ferricyanide, potassium ferrocyanide, and formaldehyde from Sigma Biochemicals (St Louis, MO), tissue culture plastic ware from Becton-Dickinson Labware (Oxnard, CA), and fetal calf serum and RPMI 1640 medium from Irvine Scientific (Santa Ana, CA).

Results

Primary Tumor Development

When LZ-CWR22R Clone B, D, or H was injected into the subcutis of nude mice in a PBS vehicle, there were differences in the tumorigenicity of the three clones. Clone B yielded tumors in all animals (Table 1). However, the vast majority of these tumors failed to give uniform X-gal stainability. For example, Figure 1A illustrates a tumor with only a minor fraction retaining expression of *lacZ*. In the case of Clone D, many animals yielded tumors when injected with $>1 \times 10^6$ cells, but none of these tumors displayed any staining (not shown), consistent with the considerable instability of *lacZ* expression in cultured populations of Clone D. Because of this rapid loss of X-gal stainability by Clones B and D, they could not be studied any further to test for development of micrometastasis in various organs.

Results for Clone H were very different. Only 15–40% of the animals injected with either 1×10^6 or 5×10^6 cells in a PBS vehicle developed tumors, even as long as 6 months post injection (Table 1). However, all these primary tumors in the subcutis were uniformly stainable with X-gal (Figure 1B), demonstrating the persistent expression of *lacZ* in this particular clone. Figure 1B shows a sizeable and highly stained primary tumor surrounded by fascia that is not X-gal-stainable. When any of these Clone H primary tumors were first sliced into halves with a scalpel and then fixed for X-gal staining, the uniformity of the stainability was again evident (Figure 1C). This shows that non-expressing variants of the tumor cells do not arise at later time points of primary tumor development (e.g., at the most interior regions of the primary tumor). The extensive vasculature of the primary tumor is also evident at these later times [red-staining blood vessels against the intense blue background (Figure 1C)].

In contrast to the relatively low tumorigenicity of Clone H when injected in PBS, the same cells injected in Matrigel were 100% tumorigenic when $1–5 \times 10^6$ cells were used (Table 1). These Matrigel-borne primary tumors developed identically to PBS-borne tumors when pathological parameters were considered (not shown).

Micrometastasis to Multiple Organs of PBS-injected Cells

With PBS-injected Clone H cells, there was little evidence of overt metastases developing in most organs (except for liver; see below). However, *lacZ* stainability enables us to detect the very smallest of micrometastases. Micrometastases were observed in the lung for most mice with large tumors when PBS was used as the injection vehicle (Table 2). An example of one lung micrometastasis is shown in Figure 2A. With lower frequency, micrometastases were observed in other organs as well (Table 2). Figure 2B shows a micrometastasis that has established itself reasonably close to a blood vessel in the liver. Figure 2C shows micrometastases close to a blood vessel in the brain. The relative distribution of micrometastases in animals bearing primary tumors and using PBS-injected

Table 1 Tumorigenic competence of two independent *lacZ* transfectants of CWR22R cells[a]

Clone	Passage #	Cells/Site	Vehicle	Number of mice injected	Number of mice with tumors
B	19	1×10^6	PBS	5	5
H	18	1×10^6	PBS[b]	5	2
	24	1×10^6	PBS[b]	5	1
	24	5×10^6	PBS[b]	5	2
	8	5×10^6	PBS[c]	10	4
	8	5×10^6	Matrigel[c]	10	10

[a]The indicated number of cells were injected, either in PBS or Matrigel as indicated, into the subcutis of the hind flanks of nude mice. Injection sites were identified with tattoos. The indicated number of mice developed primary tumors at the injection site within 8 weeks and animals with tumors were harvested 17–153 days post injection, although animals were examined for at least 6 months to test for any tumorigenic potential.
[b]These were separate experiments.
[c]Very early-passage Clone H cells compared in the same experiment.

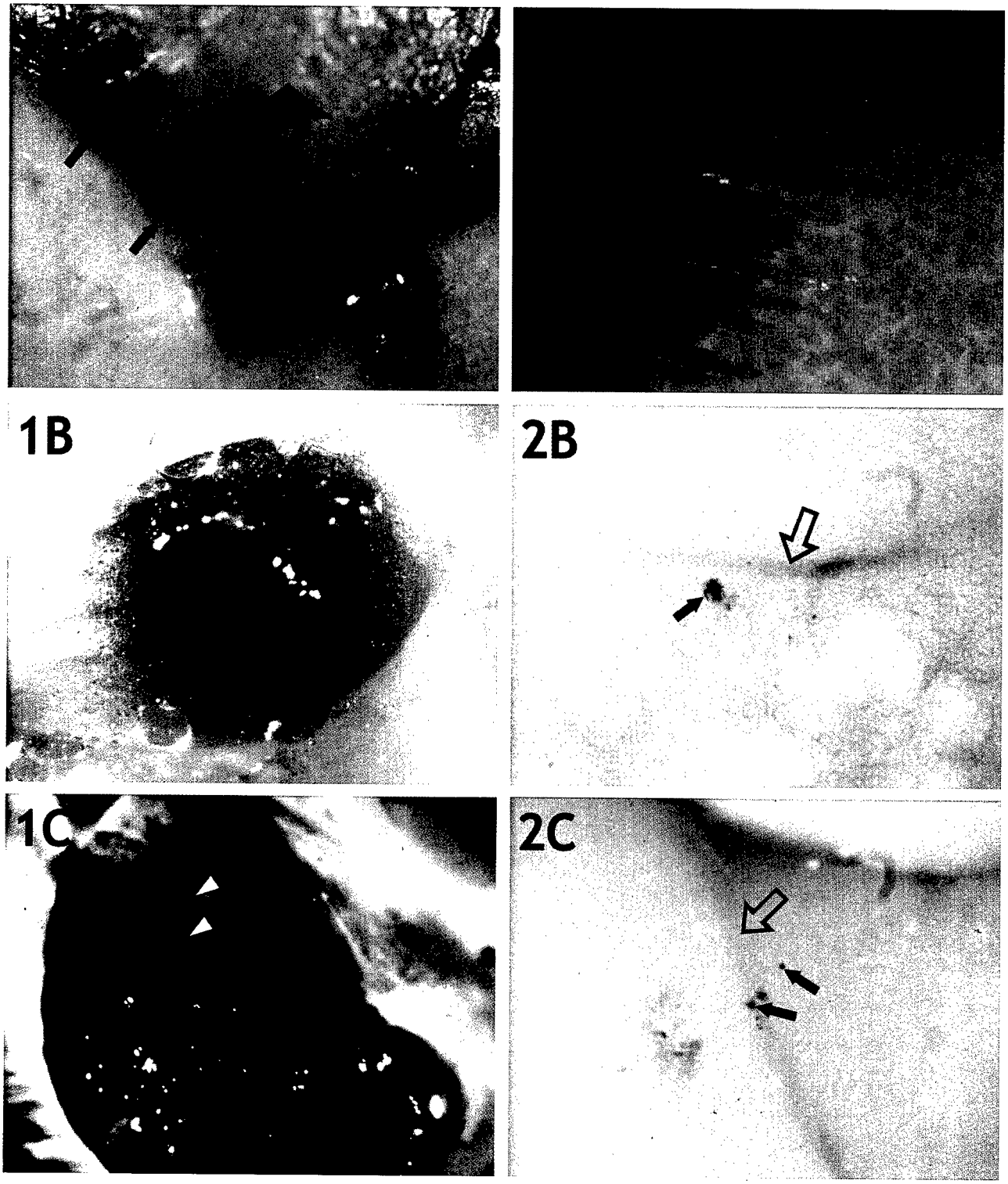

Figure 1 Primary tumors of *lacZ* transfectants. LZ-CWR22R Clone B or H cells (1×10^6) were injected into the subcutis of athymic nude mice. At the indicated times when the primary tumor had become large (>5 mm in the smallest dimension), animals were sacrificed and the region of the primary tumor excised from the surface of the animal. This region was then fixed and X-gal-stained as described in Materials and Methods. **(A)** Clone B primary tumor at 23 days post injection in a PBS vehicle. Most of this tumor does not stain for *lacZ* expression (large arrow), but a few small foci at the edge of the tumor do stain (e.g., small arrows). **(B)** Clone H primary tumor at 17 days post injection in a PBS vehicle. The entire primary tumor stains uniformly blue on X-gal staining. Original magnifications × 17. **(C)** Clone H primary tumor at 44 days post injection in Matrigel. In this case, the primary tumor was bisected with a scalpel before fixation and X-gal staining. Note the uniform staining throughout the cut interface of the tumor. Blood vessels (e.g., white arrowheads) are evident throughout the interior of this large tumor. Original magnification × 13.

Table 2 Tumor size and metastatic potential of Clone H cells[a]

Vehicle	Days Post injection	Tumor Size (mm)		Micrometastases
		Right	Left	
PBS	17	2 × 2	—	2 lung
	65	—	1.5 × 2	1 lung, 1 liver
	83	13 × 7 × 5	5 × 5 × 1	4 lung, 1 liver, 2 brain
	125	11 × 11 × 6	12 × 10 × 4	14 lung, 1 liver
	113	11 × 7 × 4	16 × 13 × 8	1 lung, 2 bone
	153	—	9 × 5 × 3	6 kidney
	56	—	10 × 7 × 4	4 lung
Matrigel	44	13 × 10 × 7	—	2 lung, 17 bone
	56	18 × 8 × 6	13 × 8 × 6	21 lung, 1 liver, 1 bone
	44	10 × 8 × 5	14 × 8 × 4	3 lung, 2 kidney, 15 bone
	79	11 × 8 × 3	9 × 7 × 4	1 lung
	44	8 × 7 × 4	7 × 6 × 5	1 lung
	29	11 × 7 × 5	12 × 8 × 5	>100 lung
	44	13 × 6 × 5	7 × 6 × 3, 5 × 5 × 3	8 lung, 3 kidney, 2 bone
	72	4 × 4 × 2	10 × 8 × 6	1 lung, 5 liver
	79	10 × 6 × 4	14 × 6 × 4	1 lung, 1 bone

[a]Clone H cells (1×10^6 or 5×10^6) were injected bilaterally into the subcutis of nude mice, either in PBS or Matrigel. At the indicated sizes of primary tumors (on the right and/or left sides of the animal), animals were sacrificed from 17 to 153 days post injection as indicated. Primary tumors stained uniformly blue with X-gal. Many organs of all animals were tested for micrometastases, as described in Materials and Methods. As shown, micrometastases were observed in multiple organs.

cells was lung (>90%) >liver=bone (50%) >>kidney=brain.

Micrometastasis to Multiple Organs of Matrigel-injected Cells

When Matrigel was the vehicle, Clone H primary tumors yielded micrometastases in the lungs of all animals examined (Table 2). A lung micrometastasis is shown in Figure 3A, a liver micrometastasis in Figure 3B, and kidney micrometastases in Figure 3C. Micrometastasis frequency for all tumor-bearing animals was as follows: lung (100%) >bone (60%) >liver (20%) >>kidney or brain.

Several precautions were taken in these studies to guarantee that blue-staining foci truly contain tumor cells. First, a clonal population of CWR22Rv1 cells, shown to be tumorigenic in nude mice, was used for transfection of the *lacZ* gene. This obviates any possibility for another cell type from the original xenograft to be transfected with this gene. Second, a chromosome-integrating plasmid was used in these studies to obviate any episomal plasmid being expressed and possibly being transmitted to neighboring host tissue cells (Culp et al. 1998a,b). Third, as shown by our laboratory for tumor cells (Lin and Culp 1992) and many other labs using transgenic animals (Kruger et al. 1999), the polymerized blue product of X-gal digestion cannot be transmitted to neighboring host cells. Finally, the conditions used for fixation and X-gal staining of mouse tissues were developed to avoid any artifactual staining of tissue cell types (Lin and Culp 1992; Culp et al. 1998a,b). By comparing X-gal staining of whole organs with serial sections of X-gal-stained foci, we previously determined that single tumor cells could be detected by our Nikon SMZU dissecting microscope. Therefore, these foci are truly micrometastases of prostate carcinoma cells.

Micrometastasis to Bone

Bone has been the most difficult and elusive target for PCA metastasis studies in animal model systems (Pretlow et al. 1994; Lalani et al. 1997; Wu et al. 1998; Yang et al. 1999). However, this is a very important aspect of the progression of the human disease. Therefore, *lacZ* stainability affords us maximal sensitivity for detecting micrometastases in the various bone systems of the nude mouse. Bone micrometastases were very evident with Matrigel-injected cells (Table 2). An

Figure 2 Micrometastasis to multiple target organs when Clone H cells were injected in a PBS vehicle. PBS-suspended Clone H cells were injected sc into nude mice. When the primary tumors had become large, the animals were sacrificed. Many internal organs were excised, fixed, and X-gal-stained to evaluate possible development of micrometastases. (**A**) A lung micrometastasis (small arrow) at 17 days post injection. Original magnification × 68. (**B**) A liver micrometastasis (small arrow) at 83 days post inection. Note the blood vessel adjacent to the micrometastasis (open arrow). Original magnification × 59. (**C**) Micrometastases in the brain (e.g., small arrows) at 80 days post injection. Note the blood vessel proximal to these micrometastases (open arrow). Original magnification × 68.

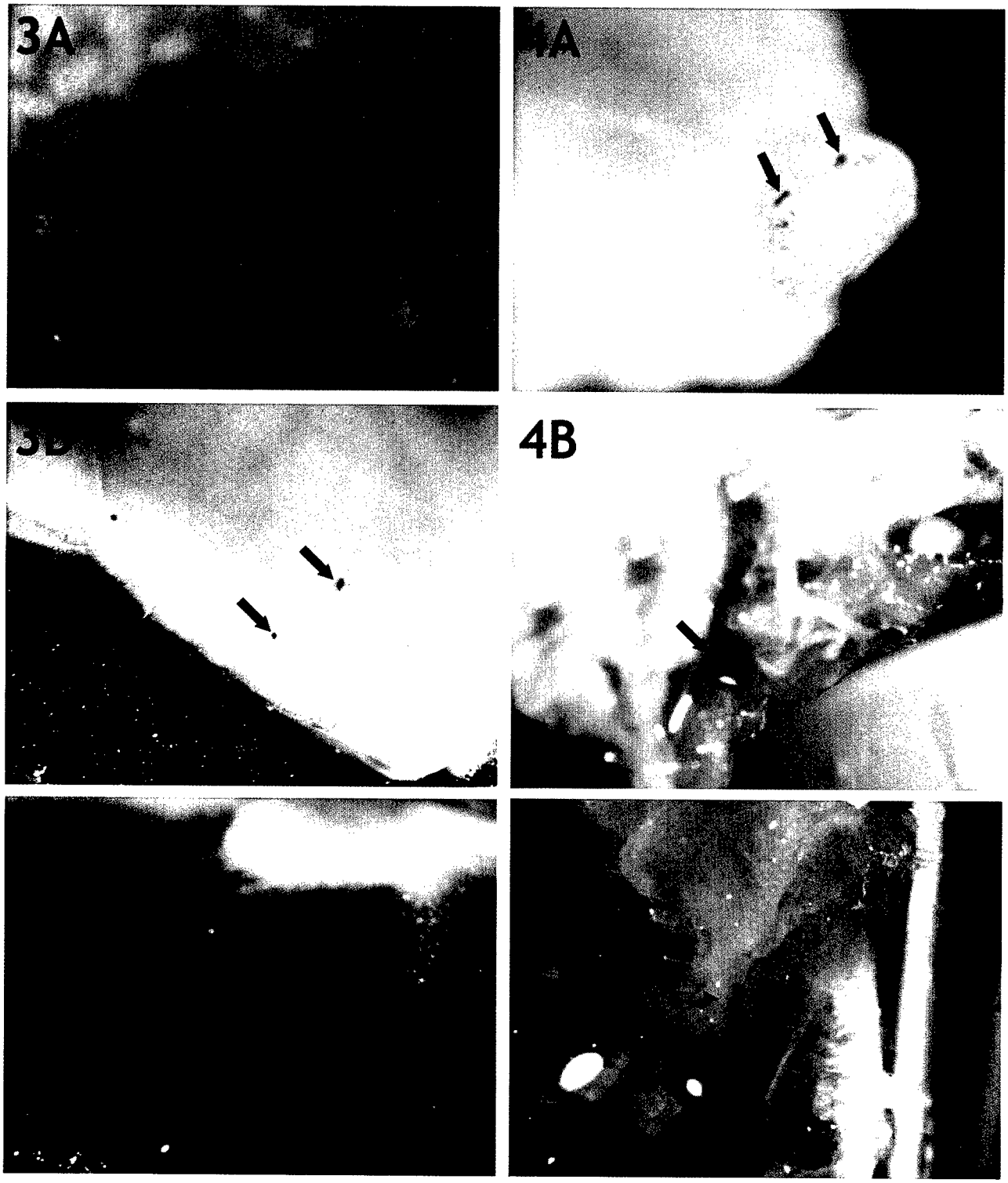

Figure 3 Micrometastasis when Clone H cells were injected in a Matrigel vehicle. Matrigel-suspended Clone H cells were injected sc into nude mice. When the primary tumors had become large, the animals were sacrificed. Many internal organs were excised, fixed, and X-gal-stained to evaluate development of micrometastases. (**A**) A lung micrometastasis (small arrow) at 44 days post injection. Original magnification × 102. (**B**) Liver micrometastases (e.g., small arrows) at 72 days post injection. Original magnification × 34. (**C**) Kidney micrometastases (e.g., small arrows) at 44 days post injection. Original magnification × 17.

Figure 4 Micrometastasis to bone. Clone H cells were injected sc in either PBS or Matrigel vehicles. When primary tumors had become large, the animals were sacrificed for excision of many bones, followed by bone fixation and X-gal staining. (**A**) Micrometastases (small ar-

example of micrometastases along the long bone of the animal is shown in Figure 4A for PBS-injected cells. In PBS-injected cells, micrometastases to spinal column were also occasionally observed (Figure 4B). Figure 4C shows micrometastases along the spine after Matrigel injection.

Micrometastasis Outgrowth into Overt Metastases

The question arises of whether micrometastases in this LZ-CWR22R-H cell system can give rise to overt metastases. In none of the animals examined in this study were overt metastases ever observed in the lungs (not shown). This is a remarkable finding in light of the several hundred micrometastases that were scored in animals with very large primary tumors and in light of all animals that yielded lung micrometastases when primary tumors had developed. The same applied to bone micrometastases.

In contrast, overt metastases were observed in the livers of some animals. An example from a PBS-injected population is shown in Figure 5. Because micrometastases were much less common in the liver than in the lung and because comparable long time periods were involved, it is unlikely that insufficient time is the basis for poor outgrowth of overt metastases in the lung or bones. Apparently, there are environmental cues in the liver that permit effective outgrowth in the liver of Clone H cells, and these cues are missing in lung and in bone.

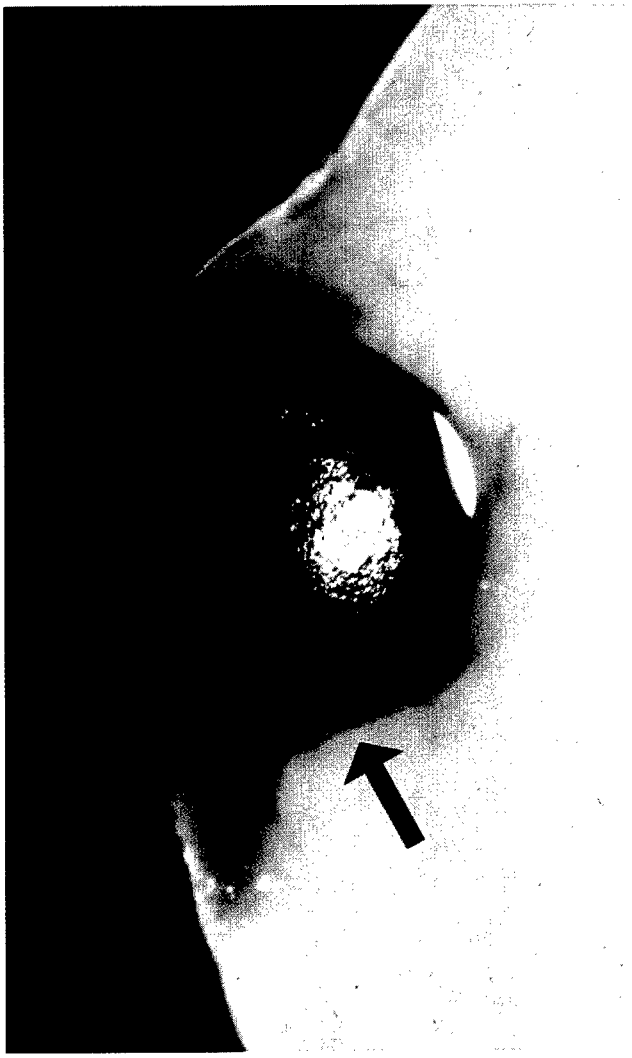

Figure 5 Overt metastasis in the liver. Clone H cells were injected sc in PBS. When primary tumors had become large (65 days post injection), animals were sacrificed for excision of many internal organs, followed by their fixation and X-gal staining. A large liver metastasis (large arow) was developing in the liver; it stained for *lacZ* expression throughout. Original magnification × 13.

Discussion

These studies have identified a highly stable *lacZ* transfectant of a new human PCA cell line isolated from a primary tumor population, CWR22Rv1 (Sramkoski et al. 1999). This LZ-CWR22R-H cell line yields progression and metastatic competence that parallels the targets of the human disease, i.e., to lung, bone, and liver (Pretlow et al. 1994; Lalani et al. 1997). This is an important finding because animal model systems of PCA have not been very successful in documenting metastasis to liver and bone unless already metastatic human PCA isolates were used as the starting material (Wu et al. 1998; Yang et al. 1999). This progression pattern was evident without the need to introduce androgen into young nude mice, indicating the possible androgen-independence of these progression patterns.

Tumorigenesis of LZ-CWR22R-H cells was limited to 15–40% of animals injected when cells were injected sc in a PBS vehicle. However, all tumor-bearing animals yielded micrometastases in their lungs and in some cases in liver and bone, with brain and kidney micrometastases the most infrequent. The relative distribution of micrometastases with PBS-injected cells was lung (>90%) >liver=bone (50%) >>kidney= brain. The reasonably high level of progression of these cells into liver and bone offers optimism that this is a more accurate model of the human disease from

rowheads) in the long bone of the leg 17 days post PBS injection. Original magnification × 42. (**B**) Micrometastases (e.g., small arrow) along the spinal column 113 days post PBS injection. Original magnification × 13. (**C**) Micrometastases (small arrows) along the spinal column 44 days post Matrigel injection. Original magnification × 34.

an unselected primary tumor population of cells (Pretlow et al. 1994; Lalani et al. 1997).

When Matrigel, a now commonly used vehicle for PCA cells (Pretlow et al. 1991), was used as the injection vehicle for LZ-CWR22R-H cells, the pattern of tumor progression changed significantly. First, all animals that received bilateral injections developed primary tumors, many with tumors on both sides of the animal. Second, the pattern of metastasis changed quantitatively but not qualitatively. Micrometastasis frequency was as follows: lung (100%) >bone (60%) >liver (20%) >>kidney or brain. That progression to bone should be increased and that to liver decreased when Matrigel is used (compared to PBS injection) raises some interesting hypotheses that could be tested in future experiments. Matrigel may permit more facile selection and expansion of variants that are effective colonizers of bones. In contrast, there may be less effective expansion of variants that target the liver. Alternatively, Matrigel may permit many more cells to colonize the subcutis and thereby permit more rapid evolution of variants competent for migrating to bone structures. In any case, this system will be an effective model system for analyzing the molecular events that lead to evolution of bone and liver metastatic variants from a population of human PCA cells from a primary tumor of a human patient (Wainstein et al. 1994; Cheng et al. 1996).

A notable surprise in our analyses was the divergence in competence for forming overt metastases. With PBS- or Matrigel-injected cells, overt metastases were never observed in the lung or bone but were occasionally observed in the liver. That the liver received fewer tumor cells than either the lung or bones suggests that time or cell dosage was not a critical element in determining overt metastasis. Perhaps outgrowth in the lung and the bones is retarded by organ-specific environmental cues that are not present in the liver (Nicolson 1993; Radinsky 1995; Singh et al. 1997). It will be important to use orthotopic injection of LZ-CWR22R-H cells into the prostate gland to determine if these progression and overt metastasis patterns differ from those of subcutis-derived tumors (Fu et al. 1992; Stephenson et al. 1992; Sato et al. 1997).

This study is not the first to use a marker gene to track PCA cells in an animal model system. Rubio et al. (1998) evaluated PC-3 cells tagged with luciferase to develop lymph node micrometastases after IM injection and by highly sensitive detection of fluorescence. They provided evidence that the lymphatic system was the preferred route of migration for these cells. Similarly, Yang et al. (1999) tagged PC-3 cells with green-fluorescent protein (GFP) and tracked micrometastasis to many bones of the animal by taking advantage of the ultrasensitive fluorescence of the GFP tag after sc or orthotopic injection. Both these studies used PC-3 cells derived from a bone metastasis from a human patient. However, use of a fluorescent tag (e.g., luciferase or GFP) obviates any evaluation of the tagged tumor cells with neighboring host tissue cells (Chang and Chung 1989). Tumor cells tagged with histochemical marker genes can be readily evaluated at the single-cell level in any tissue in terms of their relationships with other cell types of the target organ, blood vessels, and other organ substructures (Lin et al. 1990a,b; 1992; Kleinman et al. 1994; Culp et al. 1998a,b).

The *lacZ*-tagged CWR22R tumor cells described here provide a valuable system for evaluating gene regulation at the level of single tumor cells. The ability to identify X-gal-stained single tumor cells in any tissue, combined with laser-capture microdissection (Emmert–Buck et al. 1996; Schutze and Lahr 1998; Simone et al. 1998) to target small groups of tumor cells, will enable us to test the levels of genes and their expression levels for possible relevance for metastatic progression of PCA. In addition, tagging of two genetically or phenotypically different CWR22R tumor derivatives with different histochemical marker genes (Lin et al. 1992) will provide a powerful paradigm, when combined with laser-capture microdissection, to evaluate the interrelationships of two different tumor subpopulations in different sites of the animal.

Acknowledgments

Some of these studies were supported in part by the Comprehensive Cancer Center of the Ireland Cancer Center at Case Western Reserve University (NCI-supported via P30-CA43703) for pilot studies on PCA metastasis. More extensive support was provided by research grant DAMD17-98-1-8587 from the US Army on PCA metastasis.

Athymic nude mouse experiments were conducted in the Athymic Animal Facility (AAALAC-I-approved) of the Case Western Reserve University/Ireland Cancer Center and were approved by the Animal Care and Use Committee of this University. The assistance of Pamela Steele and Kathy Pustai of this facility is greatly appreciated. Special gratitude is extended to Drs Thomas and Theresa Pretlow, as well as Joseph Giaconia of their laboratory, for conveying their extensive knowledge of PCA xenograft biology to the authors during the execution of these studies. Special gratitude is extended to Dr James Jacobberger of the Ireland Cancer Center for the donation of tissue culture-adapted CWR22Rv1 PCA cells.

Literature Cited

Chang C-M, Chung LWK (1989) Interaction between prostatic fibroblast and epithelial cells in culture: role of androgen. Endocrinology 125:2719–2727

Cheng L, Sun J, Pretlow TG, Culp J, Yang N-S (1996) CWR22 xenograft as an ex vivo human tumor model for prostate cancer gene therapy. J Natl Cancer Inst 88:607–611

Culp LA, Lin W-c, Kleinman NR, Campero NM, Miller CJ, Holleran JL (1998a) Tumor progression, micrometastasis, and genetic

instability tracked with histochemical marker genes. Prog Histochem Cytochem 33:329–350

Culp LA, Lin W-c, Kleinman NR, O'Connor KL, Lechner R (1998b) Earliest steps in primary tumor formation and micrometastasis resolved with histochemical markers of gene-tagged tumor cells. J Histochem Cytochem 46:557–567

Emmert–Buck MR, Bonner RF, Smith PD, Chuaqui RF, Zhuang Z, Goldstein SR, Weiss RA, Liotta LA (1996) Laser capture microdissection. Science 274:998–1001

Fu X, Herrera H, Hoffman RM (1992) Orthotopic growth and metastasis of human prostate carcinoma in nude mice after transplantation of histologically intact tissue. Int J Cancer 52:987–990

Kleinman NR, Lewandowska K, Culp LA (1994) Tumour progression of human neuroblastoma cells tagged with a *lacZ* marker gene: earliest events at ectopic injection sites. Br J Cancer 69:670–679

Kruger A, Schirrmacher V, Khokha R (1999) The bacterial *lacZ* gene: an important tool for metastasis research and evaluation of new cancer therapies. Cancer Metast Rev 17:285–294

Lalani E-N, Lanaido ME, Abel PD (1997) Molecular and cellular biology of prostate cancer. Cancer Metast Rev 16:29–66

Lin W-c, Culp LA (1992) New insights into micrometastasis development using ultrasensitive marker genes. In Spandidos DA, ed. Current Perspectives on Molecular and Cellular Oncology. Vol 1. Part B. London, JAI Press, 261–309

Lin W-c, Pretlow TP, Pretlow TG, Culp LA (1990a) Bacterial *lacZ* gene as a highly sensitive marker to detect micrometastasis formation during tumor progression. Cancer Res 50:2808–2817

Lin W-c, Pretlow TP, Pretlow TG, Culp LA (1990b) Development of micrometastases: earliest events detected with bacterial *lacZ* gene-tagged tumor cells. J Natl Cancer Inst 82:1497–1503

Lin W-c, Pretlow TP, Pretlow TG, Culp LA (1992) High resolution analyses of two different classes of tumor cells *in situ* tagged with alternative histochemical marker genes. Am J Pathol 141:1331–1342

Nagabhushan M, Miller CM, Pretlow TP, Giaconia JM, Edgehouse NL, Schwartz S, Kung H-J, de Vere White RW, Gumerlock PH, Resnick MI, Amini SB, Pretlow TG (1996) CWR22: the first human prostate cancer xenograft with strongly androgen-dependent and relapsed strains both *in vivo* and in soft agar. Cancer Res 56:3042–3046

Nicolson GL (1993) Cancer progression and growth: relationship of paracrine and autocrine growth mechanisms to organ preference of metastasis. Exp Cell Res 204:171–180

Pretlow TG, Delmoro CM, Dilley GG, Spadafora CG, Pretlow TP (1991) Transplantation of human prostatic carcinoma into nude mice in Matrigel. Cancer Res 51:3814–3817

Pretlow TG, Pelley RJ, Pretlow TP (1994) Biochemistry of prostatic carcinoma. In Pretlow TG II, Pretlow TP, eds. Biochemical and Molecular Aspects of Selected Cancers. Vol 2. San Diego, Academic Press, 169–237

Pretlow TG, Wolman SR, Micale MA, Pelley RJ, Kursh ED, Resnick MI, Bodner DR, Jacobberger JW, Delmoro CM, Giaconia JM, Pretlow TP (1993) Xenografts of primary human prostatic carcinoma. J Natl Cancer Inst 85:394–398

Radinsky R (1995) Modulation of tumor cell gene expression and phenotype by the organ-specific metastatic environment. Cancer Metast Rev 14:323–338

Rubio N, Villacampa MM, Blanco J (1998) Traffic to lymph nodes of PC-3 prostate tumor cells in nude mice visualized using the luciferase gene as a tumor cell marker. Lab Invest 78:1315–1325

Sato H, Gleave ME, Bruchovsky N, Rennie PS, Beraldi E, Sullivan LD (1997) A metastatic and androgen-sensitive human prostate cancer model using intraprostatic inoculation of LNCaP cells in SCID mice. Cancer Res 57:1584–1589

Schutze K, Lahr G (1998) Identification of expressed genes by laser-mediated manipulation of single cells. Nature Biotechnol 16:737–742

Simone NL, Bonner RF, Gillespie JW, Emmert–Buck MR, Liotta LA (1998) Laser-capture microdissection: opening the microscopic frontier to molecular analysis. Trends Genet 14:272–276

Singh RK, Tsan R, Radinsky R (1997) Influence of the host microenvironment on the clonal selection of human colon carcinoma cells during primary tumor growth and metastasis. Clin Exp Metast 15:140–150

Sramkoski RM, Pretlow TG, Giaconia JM, Pretlow TP, Schwartz S, Sy M-S, Marengo SR, Rhim JS, Zhang D, Jacobberger J (1999) A new human prostate carcinoma cell line, 22Rv1. In Vitro 35:403–409

Stephenson RA, Dinney CPN, Gohji K, Ordonez NG, Killion JJ, Fidler IJ (1992) Metastatic model for human prostate cancer using orthotopic implantation in nude mice. J Natl Cancer Inst 84:951–957

Tan J-a, Sharief Y, Hamil KG, Gregory CW, Zang D-Y, Sar M, Gumerlock PH, deVere White RW, Pretlow TG, Harris SE, Wilson EM, Mohler JL, French FS (1997) Dehydroepiandrosterone activates mutant androgen receptors expressed in the androgen-dependent human prostate cancer xenograft CWR22 and LNCaP cells. Mol Endocrinol 11:450–459

van Steenbrugge GJ, van Weerden WM, de Ridder CMA, van der Kwast ThH, Schroder FH (1994) Development and application of prostatic xenograft models for the study of human prostate cancer. In Motta M, Serio M, eds. Sex Hormones and Antihormones in Endocrine Dependent Pathology: Basic and Clinical Aspects. Amsterdam, Elsevier Science, 11–22

van Weerden WM, de Ridder CMA, Verdaaskonk CL, Romijn JC, van der Kwast TH, Schroder FH, van Steenbrugge GJ (1996) Development of seven new human prostate tumor xenograft models and their histopathological characterization. Am J Pathol 149:1055–1062

Wainstein MA, He F, Robinson D, Kung H-J, Schwartz S, Giaconia JM, Edgehouse NL, Pretlow TP, Bodner DR, Kursh ED, Resnick MI, Seftel A, Pretlow TG (1994) CWR22: androgen-dependent xenograft model derived from a primary human prostatic carcinoma. Cancer Res 54:6049–6052

Wu TT, Sikes RA, Cui Q, Thalmann GN, Kao C, Murphy CF, Yang H, Zhau HE, Balian G, Chung LWK (1998) Establishing human prostate cancer cell xenografts in bone: induction of osteoblastic reaction by prostate-specific antigen-producing tumors in athymic and SCID/bg mice using LNCaP and lineage-derived metastatic sublines. Int J Cancer 77:887–894

Yang M, Jiang P, Sun F-X, Hasegawa S, Baranov E, Chishima T, Shimada H, Moossa AR, Hoffman RM (1999) A fluorescent orthotopic bone metastasis model of human prostate cancer. Cancer Res 59:781–786

Zhau H YE, Chang S-M, Chen B-Q, Wang Y, Zhang H, Kao C, Sang QA, Pathak SJ, Chung LWK (1996) Androgen-repressed phenotype in human prostate cancer. Proc Natl Acad Sci USA 93:15152–15157

Differential Experimental Micrometastasis to Lung, Liver, and Bone with *lacZ*-tagged CWR22R Prostate Carcinoma Cells

Julianne L. Holleran[1], Carson J. Miller[1], Nancy L. Edgehouse[2], Theresa P. Pretlow[2], and Lloyd A. Culp[1,3]

[1]Department of Molecular Biology and Microbiology
and [2]Department of Pathology
Case Western Reserve University
School of Medicine
Cleveland, OH 44106 USA

[3]To whom correspondence should be addressed.

Key Words: Histochemical marker gene, prostate carcinoma, micrometastasis, target organs

Running Title: Experimental micrometastasis to multiple organs

Summary

LacZ-tagged human prostate carcinoma CWR22R cells metastasize spontaneously to lung, liver, and bone from subcutaneous primary tumors in athymic nude mice, reflecting metastasis of the human cancer to all three organs (Holleran et al, J. Histochem Cytochem 48: 643-651 [2000]). To evaluate the mechanism(s) of metastasis to these organs, an experimental metastasis model was developed taking advantage of the ultrasensitive detection of the *lacZ* marker gene. Within 15-30 minutes after tail vein injection, micrometastases could be detected in lung, liver, bone, kidney, and brain with very different quantitative levels. The kinetics of loss of unstable micrometastases and retention of stable ones were also very different in these organs. Both whole-organ and serial-section staining with X-gal revealed considerable heterogeneity in cell number of individual lung micrometastases while micrometastases in liver contained only 1 or 2 cells. The size of individual bone micrometastases also suggested only 1 or 2 cells. In rare instances, tumor cells could be detected in the small blood vessels of the lung within minutes after injection. These studies indicate that *lacZ*-tagged CWR22R cells after tissue culture contain subsets of cells capable of establishing micrometastases in lung, liver, and bone after direct injection into the animal's circulation and independently of any selection occurring during development of the primary tumor. Moreover, the quantitative and qualitative properties of the micrometastases in the three organs differ significantly, suggesting different mechanisms for stabilization and fates of micrometastases in these organs.

Introduction

Studies of progression and metastasis of human prostate carcinoma in animal models have usually relied on already-metastatic human PCA isolates from various target organs and tissue cultured for long periods of time--e.g., DU145, PC3, and LNCaP (Pretlow et al. 1994; Zhau et al. 1996; Lalani et al. 1997; Rubio et al. 1998; Wu et al 1998; Yang et al. 1999). It would be far more informative to study progression and metastasis from primary tumors of human prostate carcinoma in animal model systems. This became possible with a series of important experiments. First, human prostate carcinomas as primary tumor populations directly from patients were developed as xenografts in athymic nude mice (Pretlow et al. 1993; Wainstein et al. 1994; Cheng et al. 1996), including the CWR22 xenograft (Wainstein et al. 1994). The nonmetatastatic CWR22 xenograft eventually gave rise to "relapsed" variants, CWR22R, some of which are metastatic to the lungs of animals (Nagabhushan et al. 1996). Furthermore, Sramkoski et al (1999) isolated CWR22Rv1 cells that are grown serially in culture and display excellent tumor-forming competence in nude mice.

Our laboratory then exploited this tissue culture line of primary tumor-derived prostate cancer cells, CWR22Rv1, by transfecting them with the *lacZ* histochemical marker gene and evaluating the competence of these cells to metastasize to any organ of the animal (Holleran et al 2000). Use of histochemical marker genes has been reviewed by us (Lin and Culp 1992a; Culp et al. 1998a & b) and others (Kruger et al. 1999) to detect single tumor

cells in the vasculature and in target organs leading to development of micrometastases. This allows us to evaluate relationships between neighboring tumor cells and host tissue cells at the highest resolution (Culp et al. 1998a & b; Chang and Chung 1989).

Within 2 weeks after subcutaneous injection of *lacZ*-tagged CWR22R cells, micrometastases were detectable in lung, liver, and bone with occasional micrometastases also observed in kidney and brain (Holleran et al 2000). The liver micrometastases also had a greater propensity for developing into overt metastases than those in other organs, although micrometastases in these other organs persisted for long periods of time. Therefore, this model system reflects more accurately the progression characteristics of human prostate cancer and offers an ideal model to dissect mechanisms of progression and metastasis of this disease (Holleran et al 2000).

To analyze further the mechanism(s) of metastasis of *lacZ*-tagged CWR22R clone H cells (Holleran et al 2000), we have now analyzed an experimental metastasis model in athymic nude mice via tail vein injection. This deciphers whether the cultured cell population harbors cell subsets competent to colonize one or more organs, their potential pluripotency in developing micrometastases in multiple organs, and the quantitative and qualitative relationships of these micrometastases. Indeed, colonization of multiple organs was observed with significant quantitative and qualitative differences among these micrometastatic classes. These results differ in many ways from previous experimental metastasis models of melanoma and fibrosarcoma in nude mice.

Materials and Methods

LZ-CWR22R-clone H Isolation and Cell Culture

The generation of LZ-CWR22R-clone H was described previously (Holleran et al 2000). Briefly, CWR22Rv1 cells (Sramkoski et al. 1999) were transfected with the bacterial *lacZ* gene under RSV LTR regulation. Stably-expressing clones were isolated as described previously (Holleran et al 2000). LZ-CWR22R-clone H is highly stable in *lacZ* expression for more than 25 passages in drug-selection-free medium (Culp et al. 1998a). Cells were grown in RPMI 1640 medium supplemented with penicillin, streptomycin, and 10% fetal calf serum.

Nude Mouse Use

Athymic nude mouse (HSD nu/nu) studies were approved by the Animal Care and Use Committee of Case Western Reserve University and conducted in the AAALAC-I accredited Athymic Animal Facility of the CWRU/Ireland Cancer Center. A single-cell suspension of LZ-CWR22R-H cells ($1x10^5$) in 0.1 ml phosphate-buffered saline (PBS) was injected into the tail vein of 8 week old male mice (Lin et al 1990; Lin and Culp 1992b). At the same time, 200 cells were inoculated into 100 mm tissue culture dishes to verify that a single-cell suspension with excellent cell viability had been injected into animals; in all cases reported in this study, this was the case. At the indicated time points, mice were euthanized and formaldehyde was perfused through the circulatory system to preserve the vascular system of organs as described previously (Kleinman et al. 1994).

X-gal Staining

Whole organs were excised from animals immediately after euthanasia and fixed with 2% (w/v) formaldehyde in PBS for 1 hr at 4°C. Tissues were X-gal stained overnight at room temperature as described previously (Lin et al. 1990; Lin and Culp 1992b; Kleinman et al. 1994; Culp et al. 1998b). X-gal staining was also performed on tissues from animals not injected with tumor cells in order to evaluate possible background staining of tissues (particularly important for bone where some background staining is observed in the growth regions at the ends of long bones of the animal). Micrometastases were enumerated that were visible to the eye under the dissecting microscope (magnifications from 10-80X) at the surface of intact organs. Intact issues were also photographed on a Nikon SMZU Dissecting Microscope with a Microflex UFX camera system using Kodak 160T film.

Embedding and Sectioning

Tissues harboring X-gal-stained micrometastases were fixed for an additional 3 hours with 10% (w/v) formalin at 4°C and embedded in paraffin. Sections (5 μm thick) were then counterstained with neutral red and photographed on a Nikon Diaphot-TMD Microscope with a Microflex AFX camera system using Kodak T160 film.

Materials

X-gal was obtained from Research Organics (Cleveland, OH); G418 from Gibco (Grand Island, NY); RPMI 1640 from Mediatech, Inc. (Herndon, VA); glass slides and formalin from Fisher Scientific (Pittsburgh, PA); potassium

ferricyanide, potassium ferrocyanide, and formaldehyde solution from Sigma Biochemicals (St Louis, MO); neutral red counterstain from Harleco (Philadelphia, PA); paraffin from Oxford Labware (St Louis, MO); Biomount from BB International (Fort Washington, PA); tissue culture plasticware from Becton-Dickinson Labware (Oxnard, CA); and fetal calf serum from Irvine Scientific (Santa Ana, CA).

Results

Micrometastases in Multiple Organs

After tail vein injection of LZ-CWR22R clone H cells, many micrometastases could be visualized in the lungs by 15 minutes (Fig. 1A). While the distribution of these micrometastases occurred throughout the surfaces of lung tissue, it was clear that the sizes of these sites were highly heterogeneous. Because of their ready visibility at the surface of the lung under the dissecting microscope, it was relatively easy to quantitate the number of micrometastases throughout the lung as a function of time (Table 1). Micrometastases were very plentiful during the first 1-2 hours but then rapidly disappeared such that none could be detected by 6-24 hours. These results were analyzed with several animals at each time point .

Micrometastases were also detected in the liver (Fig. 1B) and the long bones (femurs) of the leg (Fig. 1C). The sizes of these micrometastases were more homogeneous than those in lung and were comparable to the smaller micrometastases observed in lung (higher magnifications of Fig. 1B & C compared to Fig. 1A). The number of these foci in liver and bone was much

lower than those in lung, particularly during the first hour after injection at which times these numbers maximized (Table 1). However, micrometastases in liver and bone persisted for as long as 4-7 days in contrast to the rapid disappearance of lung sites. Their sizes remained comparable to those at earlier time points (e.g., 24 hours for a bone micrometastasis in Fig. 2A and 96 hours for a liver site in Fig. 2B). Similarly, fewer micrometastases were observed in kidney and brain and these persisted for longer periods of time as well (Table 1). No micrometastases were found in any other organ examined in these animals.

Cellular Complexity of Micrometastases in Serial Sections

To more carefully evaluate the number of tumor cells in individual micrometastases and their topologies in each organ, serial sectioning was performed on lung and liver. Table 2 presents data for 22 different micrometastases that were analyzed in these serial sections of lung for the 15 minute time point; these were chosen randomly. Individual micrometastases comprising single tumor cells could be identified in many cases and were identified in single sections of this organ. In other cases, as many as 10 sections were required to include the entire cell number of more complex micrometastases--e.g., micrometastasis #2 contained 19 cells while #14 comprised 11 cells. These data reveal considerable heterogeneity in the number of tumor cells in individual micrometastases under conditions where a single-cell suspension of tumor cells was being inoculated into tail veins (verified by parallel inoculation into tissue culture dishes and analyses of their

distribution 2-4 hours later). However, the majority of micrometastases were comprised of 5 or fewer cells per site.

Two individual micrometastases are shown in the serial sections of lung in Fig. 3. One is comprised of five cells (small arrows in this figure) and extends across all five sections. The second is comprised of two cells and was localized to two sections (broad arrows in Fig. 3D&E). It was also clear from these analyses that these micrometastases had escaped the small blood vessels of the lung and were occupying lung tissue sites (see below as well on this point).

In rare sections, both tissue-"established" micrometatases could be visualized as well as tumor cells still bound to the endothelium of blood vessels. Examples are provided in Fig. 4 where a 4-cell micrometastasis is identifiable in all three sections at a specific tissue site (narrow arrows in A, B, and C) and a tumor cell still bound to the endothelial lining of a blood vessel could also be identified (broad arrow in C).

These analyses led us to plot the number of cells in individual micrometastases against the number of foci scored with that number of cells. Fig. 5 further illustrates the microheterogeneity in cell number of lung micrometastases. Most tended to contain 1-5 cells; however, a significant number contained many more cells.

Relative Homogeneity of Liver Micrometastases

We performed similar quantitative analyses on liver micrometastases. However, because of their paucity it was prohibitively expensive to examine as many examples as shown above for lung. However, extensive sectioning and

microscopic analyses led to identification of 8 individual micormetastases in liver. Three of these are shown in Fig. 6. Single-cell micrometastases were most common (e.g., Fig. 6A, B, & C). In a couple of cases, two tumor cells could be identified (Fig. 6D). In no case could more than 2 cells per micrometastasis be identified. These results indicate greater simplicity in cell number for individual liver micrometastases than those observed for lung.

Discussion

The ability to detect single tumor cells in nude mouse tissues, tagged with the *lacZ* marker gene, has permitted us to make several important conclusions from these experimental metastasis studies. Their significance is reinforced by the fact that the LZ-CWR22Rv1 clone H cell system was derived from a xenograft of a primary tumor from a prostate cancer patient (Nagabhushan et al 1996) ; therefore, it is not an already-selected set of metastatic tumor cells (Holleran et al 2000). First, experimental micrometastases could be detected readily in lung, liver, and bone which are targets of natural progression of the human disease (Pretlow et al 1994; Fu et al 1992; Lalani et al 1997; Culp et al 1998b). Micrometastases were also observed in kidney and brain at a lower frequency. This is the same pattern of progression as observed in spontaneous metastasis from subcutaneous primary tumors using LZ-CWR22R cells (Holleran et al 2000). Therefore, the *lacZ*-transfected population of CWR22R cells contains subsets that are already competent for establishing micrometastases in multiple organs of nude mice and do not necessarily require extensive selection during primary tumor

formation. However, these experimental micrometastases, by avoiding the first steps in the metastatic cascade from a primary tumor, may differ in their gene expression and tumor-progressing characteristics from those micrometastases in these organs generated by spontaneous events during development of the primary tumor at the subcutis or in the prostate gland (Chang and Chung 1989; Fu et al 1992; Nicolson 1993; Sato et al 1997; Stephenson et al 1992). Additional experiments will be required to determine if the metastatic subsets in this experimental metastasis model have the same cellular and molecular properties as micrometastases in these multiple organs when generated spontaneously from growing primary tumors.

Second, lung micrometastases in this experimental metastasis model of LZ-CWR22R were very heterogeneous in cell number, with 1 to as many as 20 cells per site, while those in liver and bone were far more homogeneous (1 or 2 cells only). This was verified in lung and liver by detailed serial-section analyses of many individual sites. In bone, this conclusion is inferred by comparison of the size of X-gal-stainable foci after whole-organ staining with those in liver since methods for serial sectioning of X-gal-stained bone have not been completely resolved. Since single-cell suspensions with excellent viability were used for injection, these results would suggest either that aggregation of tumor cells occurs within the first several minutes in the circulation of the animal and/or that selected sites in the small blood vessels of the lung permit multiple tumor cells to aggregate and to follow "pioneering" tumor cells into tissue sites as they extravasate blood vessels. Why this does

not occur in liver and bone suggests that either (a) cellular aggregates are "cleared" in the lung and are no longer available for establishing micrometastases in other organs or (b) the microvasculature of other organs does not permit the same intercellular events as occur in the lung. Clearly, much more detailed and complex experiments will be required to distinguish amongst various possibilities.

Third, serial sections of lung at the earliest times after tail vein injection revealed prostate tumor cells bound to the endothelium of the smallest blood vessels in the lung. This highly-selected subpopulation of tumor cells could also be detected with *lacZ*-tagged fibrosarcoma cells (Culp et al 1998a & 1998b), indicating the wider generality of these findings. It will now be important to utilize the laser-capture microdissection method, with its ability to recover single or a few tumor cells from any tissue (Emmert-Buck et al 1996; Schutze and Lahr 1998; Simone et al 1998), to evaluate gene expression differences in the endothelium-bound subpopulation of tumor cells and the "established-but-earliest" micrometastases that escape blood vessels in tissue sites.

Finally, the kinetics of clearance of micrometastases in these organs was quite different. Lung micrometastases were cleared within several hours, with the earliest and most numerous sites at 15 minutes post-injection. This indicates the rapid and facile development of lung micrometastases by escape from the smallest blood vessels of the lung. While a few micrometastases could be detected at the earliest time points in other organs (particularly liver), they

became much more numerous in these other organs at 1 to 24 hours after injection. They also persisted for many days in contrast to their rapid disappearance from the lung. This indicates differences in environmental cues that permit tumor cells to become "comfortable" in these tissues and/or differential attack by natural killer cells (or other immuno-modulatory mechanisms) in athymic nude mice depending upon which tissue site is being considered (Fisher and Fisher 1967; Fidler 1970; Tarin and Price 1981; Fidler and Hart 1982; Weiss et al 1985; Kawaguchi and Nakamura 1986; Fornabaio et al 1988; Nicolson 1993). In this regard, two different immuno-modulatory mechanisms have been invoked for clearing tumor cells in the lung at early or at late time points (Aslakson et al 1991; Glaves 1980; Ramani and Balkwill 1988; Barlozzari et al 1983). The ease of detection of these earliest micrometastases should permit us to evaluate more effectively the molecular and cellular mechanisms of their differential stability.

These results using LZ-CWR22R cells differ in several regards from results using *lacZ*-tagged fibrosarcoma tumor cells in an experimental metastasis model in the same nude mice (Lin et al 1990; Lin and Culp 1992). Both classes of tumor cells established micrometastases in lung within 15 minutes after injection and they both displayed size heterogeneity in the lung under conditions where single-cell populations were being injected. They differ in other regards. First, unstable micrometastases were cleared from the lung over a 24 hour period with fibrosarcoma (Lin et al 1990; Lin and Culp 1992) and 1-1.5% of them persisted for >7 days. In the case of this prostate carcinoma

model, lung clearance was complete within several hours after injection and micrometastases were rare beyond several days. This may be consistent with two different immuno-modulatory mechanisms of clearance of tumor cells from lungs at early or late times (Aslakson et al 1991). Second, fibrosarcoma cells never established micrometastases in any other organ of the nude mouse (Lin et al 1990; Lin and Culp 1992) while prostate carcinoma cells established micrometastases in several other organs that persisted for many days. This suggests some tumor-type specificity to these events, although this conclusion can only be drawn when other examples of fibrosarcoma and prostate carcinoma are tested. Third, the number of lung micormetastases at all time points using fibrosarcoma was several-fold higher than the numbers using prostate carcinoma when the same number of cells were injected into tail veins. This also suggests some quantitative tumor-type specificity in these two systems as well.

Overall, the studies reported herein indicate that the LZ-CWR22R cell system will be particularly valuable for dissecting mechanisms of progression and metastasis in multiple organs of nude mice. They also provide the degree of resolution at the single-cell level that will allow laser-capture microdissection and other powerful molecular analyses to be undertaken to identify critical genes involved in organ specificity of metastasis.

Acknowledgements

The authors acknowledge partial support from the Comprehensive Cancer Center of the Ireland Cancer Center at Case Western Reserve University (NCI-supported via P30-CA43703) for pilot studies on prostate carcinoma metastasis. More extensive support was provided by research grant DAMD17-98-1-8587 from the U.S. Army on prostate carcinoma metastasis. Athymic nude mouse experiments were conducted in the Athymic Animal Facility (AAALAC-I-approved) of the Case Western Reserve University/Ireland Cancer Center and approved by the Animal Care and Use Committee of this University; the assistance of Pamela Steele and Kathy Pustai of this facility has been greatly appreciated.

References

Aslakson CJ, McEachern D, Conaway DH, Miller FR. (1991) Inhibition of lung colonization at two different steps in the metastatic sequence. Clin Exp Metastasis 9: 139-150.

Barlozzari T, Reynolds CW, Herberman RB. (1983) In vivo role of natural killer cells: involvement of large granular lymphocytes in the clearance of tumor cells in anti-asialo GM1-treated rats. J Immunol 131: 1024-1027.

Chang C-M, Chung LWK. (1989) Interaction between prostatic fibroblast and epithelial cells in culture: role of androgen. Endocrinology 125: 2719-2727.

Cheng L, Sun J, Pretlow TG, Culp J, Yang N-S. (1996) CWR22 xenograft as an ex vivo human tumor model for prostate cancer gene therapy. J Natl Cancer Inst 88: 607-611.

Culp LA, Lin W-c, Kleinman NR, O'Connor KL, Lechner R. (1998a) Earliest steps in primary tumor formation and micrometastasis resolved with histochemical markers of gene-tagged tumor cells. J. Histochem. & Cytochem 46: 557-567.

Culp LA, Lin W-c, Kleinman NR, Campero NM, Miller CJ, Holleran JL. (1998b) Tumor progression, micrometastasis, and genetic instability tracked with histochemical marker genes. Progress Histochem Cytochem 33: 329-350.

Emmert-Buck MR, Bonner RF, Smith PD, Chuaqui RF, Zhuang Z, Goldstein SR, Weiss RA, Liotta LA. (1996) Laser capture microdissection. Science 274: 998-1001.

Fidler IJ. (1970) Metastasis: quantitative analysis of distribution and fate of tumor emboli labeled with ^{125}I-5-iodo-2'-deoxyuridine. J Natl Cancer Inst 45: 773-782.

Fidler IJ, Hart IR. (1982) Biological diversity in metastatic neoplasms: origins and implications. Science 217:998-1003.

Fisher B, Fisher ER. (1967) The organ distribution of disseminated ^{51}Cr-labeled tumor cells. Cancer Res 27: 412-420.

Fornabaio DM, Alterman AL, Stackpole CW. (1988) Metastatic dissemination of B16 melanoma: evidence that metastases can result from nonspecific trapping of disseminated tumor cells. Invasion Metastasis 8: 1-16.

Fu X, Herrera H, Hoffman RM. (1992) Orthotopic growth and metastasis of human prostate carcinoma in nude mice after transplantation of histologically intact tissue. Int J Cancer 52: 987-990.

Glaves D. (1980) Metastasis: reticuloendothelial system and organ retention of disseminated malignant cells. Int J Cancer 26: 115-122.

Holleran JL, Miller CJ, Culp LA. (2000) Tracking micrometastasis to multiple organs with *lacZ*-tagged CWR22R prostate carcinoma cells. J Histochem Cytochem 48: 643-651.

Kawaguchi T, Nakamura K. (1986) Analysis of the lodgement and extravasation of tumor cells in experimental models of hematogeneous metastasis. Cancer Metastasis Rev 5: 77-94.

Kleinman NR, Lewandowska K, Culp LA. (1994) Tumour progression of human neuroblastoma cells tagged with a *lacZ* marker gene: earliest events at ectopic injection sites. Br J Cancer 69: 670-679.

Kruger A, Schirrmacher V, Khokha R. (1999) The bacterial *lacZ* gene: an important tool for metastasis research and evaluation of new cancer therapies. Cancer Met Rev 17: 285-294.

Lalani E-N, Lanaido ME, Abel PD. (1997) Molecular and cellular biology of prostate cancer. Cancer Met Rev 16: 29-66.

Lin W-c, Culp LA. (1992a) New insights into micrometastasis development using ultrasensitive marker genes. In Current Perspectives on Molecular and Cellular Oncology, Vol 1, Part B, Spandidos, D.A. (ed), pp. 261-309. JAI Press: London.

Lin W-c, Culp LA. (1992b) Altered establishment/clearance mechanisms during experimental micrometastasis with live and/or disabled bacterial *lacZ*-tagged tumor cells. Invasion and Metastasis 12: 197-209.

Lin W-c, Pretlow TP, Pretlow TG, Culp LA. (1990) Development of micrometastases: earliest events detected with bacterial *lacZ* gene-tagged tumor cells. J Natl Cancer Inst 82: 1497-1503.

Nagabhushan M, Miller CM, Pretlow TP, Giaconia JM, Edgehouse NL, Schwartz S, Kung H-J, de Vere White RW, Gumerlock PH, Resnick MI, Amini SB, Pretlow TG. (1996) CWR22: the first human prostate cancer xenograft with strongly androgen-dependent and relapsed strains both *in vivo* and in soft agar. Cancer Res 56: 3042-3046.

Nicolson GL. Cancer progression and growth: relationship of paracrine and autocrine growth mechanisms to organ preference of metastasis. (1993) Exp Cell Res 204: 171-180.

Pretlow TG, Wolman SR, Micale MA, Pelley RJ, Kursh ED, Resnick MI, Bodner DR, Jacobberger JW, Delmoro CM, Giaconia JM, Pretlow TP. (1993) Xenografts of primary human prostatic carcinoma. J Natl Cancer Inst 85: 394-398.

Pretlow TG, Pelley RJ, Pretlow TP. (1994) Biochemistry of prostatic carcinoma. In Pretlow, T.G. II and Pretlow, T.P., eds, Biochemical and Molecular Aspects of Selected Cancers, Vol. 2, Academic Press, Inc., San Diego, CA, pp. 169-237.

Ramani P, Blackwill FR. (1988) Human interferons inhibit experimental metastases of a human melanoma cell line in nude mice. Br J Cancer 58: 350-354.

Rubio N, Villacampa MM, Blanco J. (1998) Traffic to lymph nodes of PC-3 prostate tumor cells in nude mice visualized using the luciferase gene as a tumor cell marker. Laboratory Invest 78: 1315-1325.

Sato H, Gleave ME, Bruchovsky N, Rennie PS, Beraldi E, Sullivan LD. (1997) A metastatic and androgen-sensitive human prostate cancer model using intraprostatic inoculation of LNCaP cells in SCID mice. Cancer Res 57: 1584-1589.

Schutze K, Lahr G. (1998) Identification of expressed genes by laser-mediated manipulation of single cells. Nature Biotechnology 16: 737-742.

Simone NL, Bonner RF, Gillespie JW, Emmert-Buck MR, Liotta LA. (1998) Laser-capture microdissection: opening the microscopic frontier to molecular analysis. Trends in Genetics 14: 272-276.

Sramkoski RM, Pretlow TG, Giaconia JM, Pretlow TP, Schwartz S, Sy M-S, Marengo SR, Rhim JS, Zhang D, Jacobberger J. (1999) A new human prostate carcinoma cell line, 22Rv1. In vitro 35: 403-409.

Stephenson RA, Dinney CPN, Gohji K, Ordonez NG, Killion JJ, Fidler IJ. (1992) Metastatic model for human prostate cancer using orthotopic implantation in nude mice. J Natl Cancer Inst 84: 951-957.

Tarin D, Price JE. (1981) Influence of microenvironment and vascular anatomy on "metastatic" colonization potential of mammary tumors. Cancer Res 41: 3604-3609.

Wainstein MA, He F, Robinson D, Kung H-J, Schwartz S, Giaconia JM, Edgehouse NL, Pretlow TP, Bodner DR, Kursh ED, Resnick MI, Seftel A, Pretlow TG. (1994) CWR22: androgen-dependent xenograft model derived from a primary human prostatic carcinoma. Cancer Res 54: 6049-6052.

Weiss L, Dimitrov DS, Angelova M. (1985) The hemodynamic destruction of intravascular cancer cells in relation to myocardial metastasis. Proc Natl Acad Sci USA 82: 5737-5741.

Wu TT, Sikes RA, Cui Q, Thalmann GN, Kao C, Murphy CF, Yang H, Zhau HE, Balian G, Chung LWK. (1998) Establishing human prostate cancer cell xenografts in bone: induction of osteoblastic reaction by prostate-specific

antigen-producing tumors in athymic and SCID/bg mice using LNCaP and lineage-derived metastatic sublines. Int J Cancer 77: 887-894.

Yang M, Jiang P, Sun F-X, Hasegawa S, Baranov E, Chishima T, Shimada H, Moossa AR, Hoffman RM. (1999) A fluorescent orthotopic bone metastasis model of human prostate cancer. Cancer Res 59: 781-786.

Zhau H YE, Chang S-M, Chen B-Q, Wang Y, Zhang H, Kao C, Sang QA, Pathak SJ, Chung LWK. (1996) Androgen-repressed phenotype in human prostate cancer. Proc Natl Acad Sci USA 93: 15152-15157.

Figure Legends

Fig. 1. Earliest micrometastases in lung, liver, and bone. LZ-CWR22R cells were injected into the tail veins of athymic nude mice. As detailed in Materials and Methods, mice were euthanized at the indicated times and organs excised for fixation and X-gal staining. Whole-organ staining is shown in all cases. **[A]** Lung at 15 minutes post-injection. Many micrometastases are shown at lower magnification in one lobe of the lung; considerable heterogeneity in size is evident for these micrometastases. Two smaller ones are shown at the arrow. Magnification, X10.1. **[B]** A liver micrometastasis is shown at higher magnification (at the arrow). Magnification, X67. **[C]** A leg bone (femur) micrometastasis is shown at the arrow. Magnification, X67. Note that the sizes of the liver and bone micrometastases are very comparable.

Fig. 2. Micrometastases at later times. Animals were injected and euthanized as described in the legend to Fig. 1. Whole-organ staining with X-gal is shown in both cases. **[A]** A leg bone (femur) micrometastasis (at the arrow) that persists at 24 hours after injection. Magnification, X43.6. **[B]** A liver micrometastasis (at the arrow) 96 hours after injection. Magnification, X54.5.

Fig. 3. Serial sections harboring two lung micrometastases. Animals were injected and euthanized as described in Fig. 1. At the 15 minute time point, a lung was removed, fixed, X-gal-stained, embedded, serially sectioned, and neutral red-counterstained as described in Materials and Methods. These five contiguous sections revealed two micrometastases while the adjoining several sections failed to reveal any tumor cells. One micrometastasis at the

narrow arrow in panels **A**, **B**, **C**, **D**, and **E** contained five cells while the second (at the broad arrow) in panels **C**, **D**, and **E** contained only 2 cells. Magnification, 51X.

Fig. 4. A lung micrometastasis in serial sections with a tumor cell evident in an adjoining blood vessel. Animals were injected and harvested at 15 minutes as described in Materials and Methods and the legend to Fig. 1. Serial sections of X-gal-stained/neutral red counter-stained lung revealed a micrometastasis with 4 cells (at the narrow arrow) in panels **A**, **B**, and **C** and a tumor cell bound to the endothelium of a blood vessel in panel **C** (at the broad arrow). Sections neighboring these failed to revealed any tumor cells. Magnification, X65.

Fig. 5. Quantitation of cell number in individual lung micrometastases. Animals were used as described in the legend to Table 2. Lungs at 15 minutes post-injection were harvested, X-gal stained, and serially-section. Many micrometastases were then scored for the number of tumor cells in each and this number plotted against the number of micrometastases containing that particular number of cells. As shown, micrometastases containing 1 to as many as 5 cells were very common; subsets of micrometastases also contained as many as 20 cells per site.

Fig. 6. Micrometastases in the liver. Animals were injected and harvested at 1 hour as described in Materials and Methods and the legend to Fig. 1. Serial sections of X-gal-stained/neutral red counter-stained liver

revealed micrometastases with only 1 cell (as examples, **A**, **B**, and **C**) or in some cases 2 cells (**D**) in all cases. Magnification in all cases, 53.6X.

Table 1 Experimental Micrometastases in Multiple Organs[a]

Time point	Number of mice examined	Mean number of micrometastases (SE)				
		Lung	Liver	Kidney	Leg	Brain
15 minutes	4	1404 (218.42)	22 (4.71)	8.75 (3.6)	1 (1)	3.5 (0.67)
1 hour	4	826 (343.69)	12 (4.55)	12.5 (4.5)	4.5 (3.30)	7.0 (7.0)
6 hours	2	0	2.5 (2.5)	32.5 (10.5)	2.5 (0.5)	9.5 (7.5)
24 hours	4	0	3.25 (1.97)	35 (27.3)	1.5 (1.19)	7.8 (4.7)
96 hours	2	0	1 (1)	2 (1)	9 (6)	2.5 (0.50)
1 week	4	0	0	0.5 (0.29)	1.75 (0.75)	1.3 (0.75)

[a] LZ-CWR22R clone H cells were injected ($1x10^5$ cells) into tail veins of nude mice. At the indicated time points, the indicated number of mice were euthanized; many organs were excised and X-gal stained. All organs were surveyed under the Nikon SMZU dissecting microscope and X-gal-stained micrometastases enumerated. The mean number of micrometastases are provided with the standard error of the mean across multiple animals and/or organs shown in parentheses.

Table 2 Properties of Individual Lung Micrometastases[a]

Micrometastasis ID #	Total # Sections[b]	Total Depth (μm)[c]	Cell #[d]
1	3	15	2
2	10	50	19
3	2	10	2
4	5	25	5
5	4	20	5
6	6	30	5
7	1	5	1
8	3	15	2
9	4	20	4
10	3	15	2
11	1	5	1
12	1	5	1
13	3	15	5
14	4	20	11
15	3	15	4
16	4	20	4
17	2	10	1
18	5	25	5
19	5	25	8
20	1	5	1
21	3	15	2
22	3	15	3

[a] LZ-CWR22R clone H cells were injected into tail veins of nude mice. At 15 minutes post-injection, animals were euthanized and lungs harvested for fixation and X-gal staining per Materials and Methods. Lungs were serially sectioned and all adjacent sections were scored for each individual micrometastasis whose position in the section was defined by X- and Y-axis coordinates.

[b] These are the number of 5-μm-thick sections in which X-gal-stained tumor cells could be identified for each micrometastasis. Sections adjacent to these failed to reveal any stained cells at these coordinates.

[c] This is the total depth (or maximum dimension) of each micrometastasis estimated in microns.

[d] These are the number of cells enumerated in each micrometastasis by visualizing X-gal-stained nuclei tumor cells.

FIGURE 1

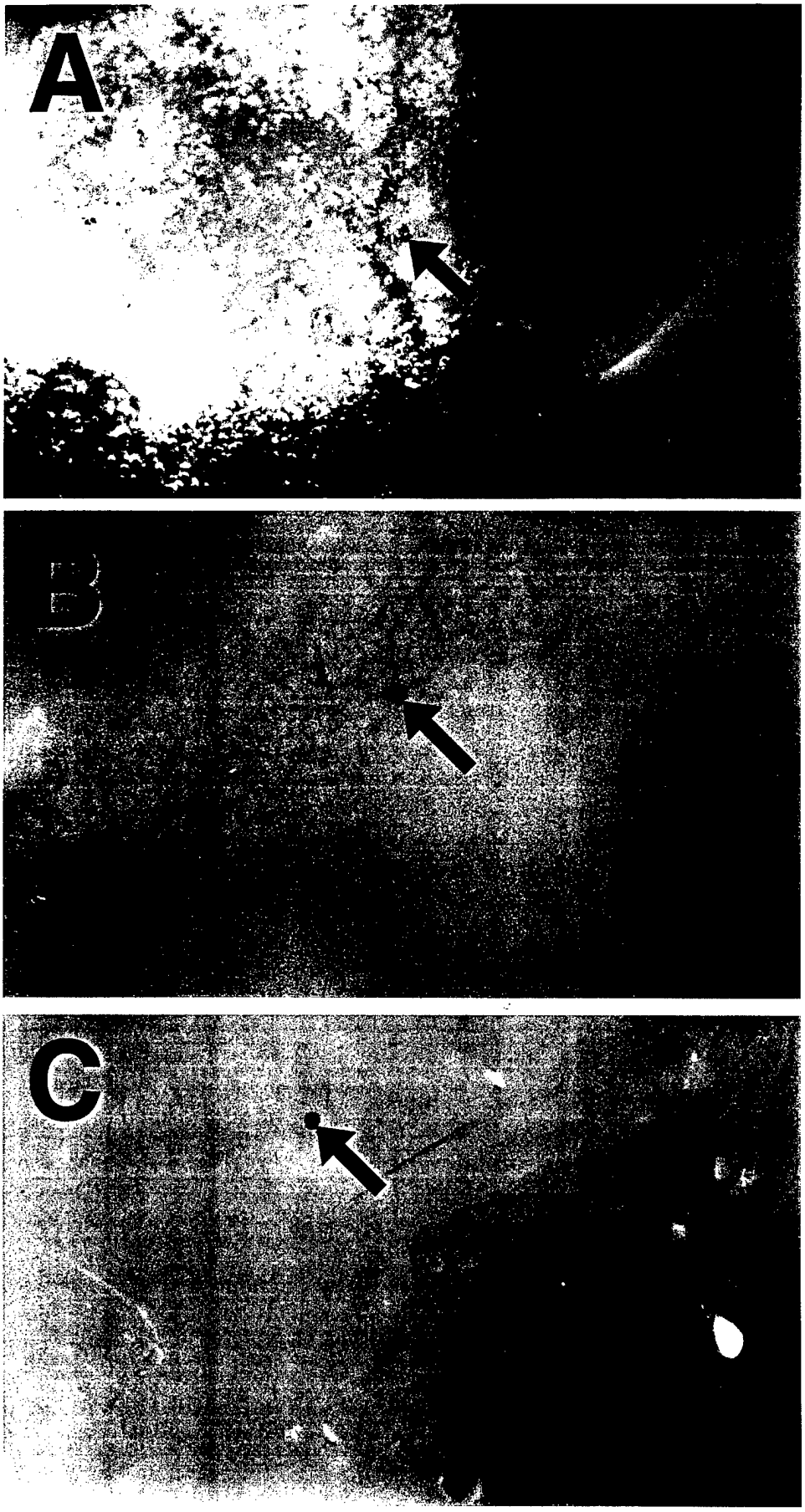

FIGURE 2

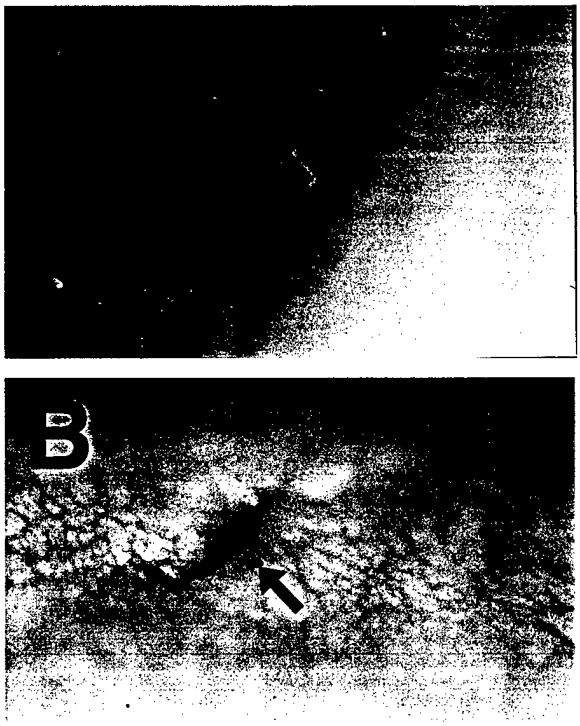

FIGURE 3

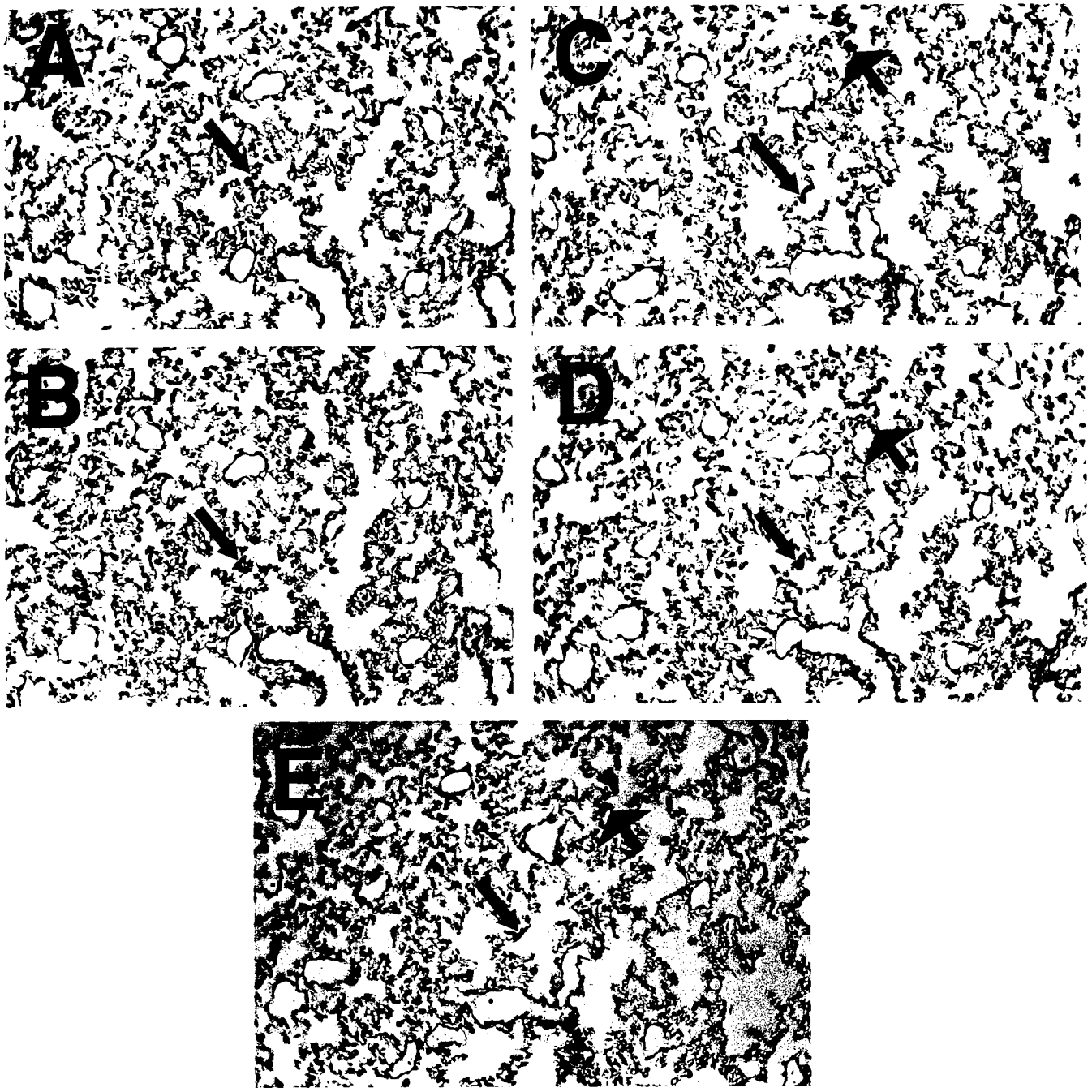

FIGURE 4

FIGURE 5

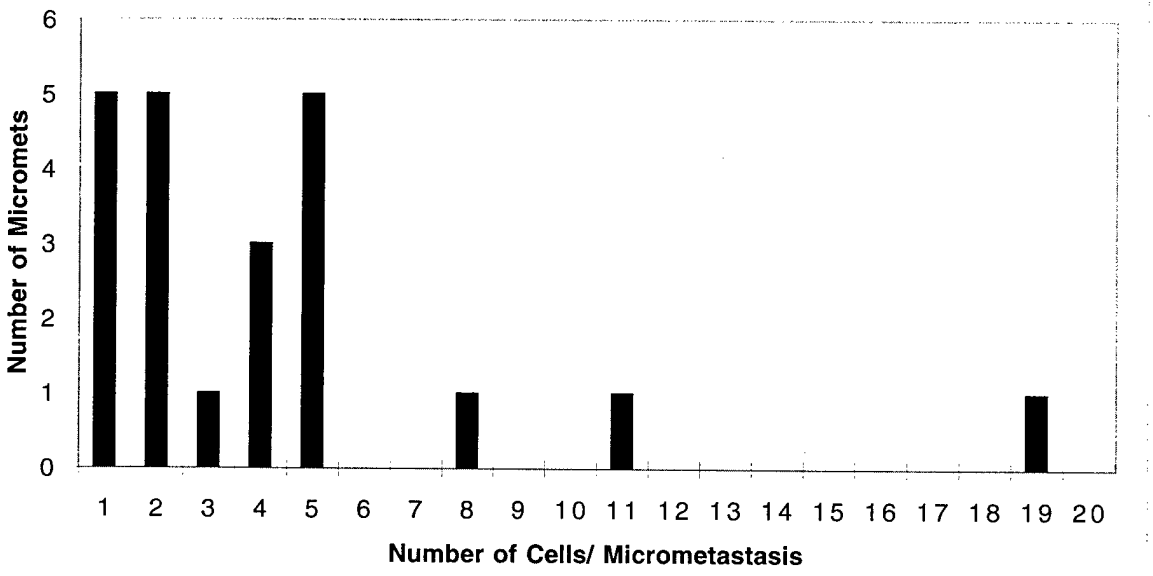
Number of Micromets
0
1
2
3
4
5
6
1 2 3 4 5 6 7 8 9 10 11 12 13 14 15 16 17 18 19 20
Number of Cells/ Micrometastasis

FIGURE 6